

Analyzing the Effect of an Externally Applied Force on the Electrode-Skin Impedance

By

Anas Albulbul, B.Sc., (Hons)

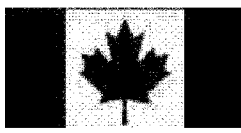
A thesis submitted to the Faculty of Graduate and Postdoctoral Affairs in partial fulfillment of the requirements for the degree of

Master of Applied Science
in
Biomedical Engineering

Ottawa-Carleton Institute for Biomedical Engineering

Department of Systems and Computer Engineering
Carleton University
Ottawa, Ontario, Canada
May 2013

Copyright © Anas Albulbul, 2013



Library and Archives
Canada

Published Heritage
Branch

395 Wellington Street
Ottawa ON K1A 0N4
Canada

Bibliothèque et
Archives Canada

Direction du
Patrimoine de l'édition

395, rue Wellington
Ottawa ON K1A 0N4
Canada

Your file Votre référence
ISBN: 978-0-494-94659-6

Our file Notre référence
ISBN: 978-0-494-94659-6

NOTICE:

The author has granted a non-exclusive license allowing Library and Archives Canada to reproduce, publish, archive, preserve, conserve, communicate to the public by telecommunication or on the Internet, loan, distribute and sell theses worldwide, for commercial or non-commercial purposes, in microform, paper, electronic and/or any other formats.

The author retains copyright ownership and moral rights in this thesis. Neither the thesis nor substantial extracts from it may be printed or otherwise reproduced without the author's permission.

In compliance with the Canadian Privacy Act some supporting forms may have been removed from this thesis.

While these forms may be included in the document page count, their removal does not represent any loss of content from the thesis.

AVIS:

L'auteur a accordé une licence non exclusive permettant à la Bibliothèque et Archives Canada de reproduire, publier, archiver, sauvegarder, conserver, transmettre au public par télécommunication ou par l'Internet, prêter, distribuer et vendre des thèses partout dans le monde, à des fins commerciales ou autres, sur support microforme, papier, électronique et/ou autres formats.

L'auteur conserve la propriété du droit d'auteur et des droits moraux qui protège cette thèse. Ni la thèse ni des extraits substantiels de celle-ci ne doivent être imprimés ou autrement reproduits sans son autorisation.

Conformément à la loi canadienne sur la protection de la vie privée, quelques formulaires secondaires ont été enlevés de cette thèse.

Bien que ces formulaires aient inclus dans la pagination, il n'y aura aucun contenu manquant.

Canada

Abstract

In this study, the impact of force on electrode-skin impedance is examined; electrode-skin impedance can impact the quality of the recorded biological signals. Surface biopotential electrodes experience different levels of applied force during biological signal measurements, especially with wearable biomedical sensor systems. The analysis was based on applying different force levels (0 N, 8.9 N and 22.2 N) on different types of surface biopotential electrodes: 1) Ag/AgCl electrodes, 2) Stainless steel electrodes, 3) Orbital electrodes and on determining the effect of removing the applied force from the electrodes sites on electrode-skin impedance. Electrode-skin impedance was sharply decreased when the first force level was applied on dry electrodes and in the absence of electrolyte gel in the case of Ag/AgCl electrodes. Applying electrolyte gel to Ag/AgCl electrodes made inconsistent results among the subjects under high force level. Performing skin preparation caused the electrode-skin impedance to be sensitive to repeated application of loading/unloading of fixed low force level (5 N). The hysteresis effect was experienced in most of the measurements when force was removed from electrodes sites. An electrical circuit (RC) was used to model the electrode-skin interface. Increasing the applied force level on the electrodes sites resulted in an increase in capacitance (C_d) values and a decrease in resistance (R_d and R_s) values of the electrical circuit model components for the electrode-skin interface.

Decreasing the electrode-skin impedance by the force technique would be beneficial for improving the biological signal quality and improving the performance of modern wearable physiological monitoring system.

Acknowledgements

First and foremost, I would like to express my sincere appreciation to Prof. Adrian Chan for his supervision, assistance, patience, insight, and constructive comments during my study.

I would like to extend my sincere gratitude to Prof. James Green, the Department of Systems and Computer Engineering, and the faculty of Graduate Studies and Research, for their support.

I am thankful to Mr. Terry Flaherty (School of Industrial Design, Carleton University) for his assistance in constructing the custom's clamp device.

I am grateful to all the volunteers who participated in this study and offered their services with patience and interest.

Many thanks to my friends and colleagues for their support.

Special and heartfelt thanks to my family for their help and inspiration.

Table of Contents

Abstract	iii
Acknowledgements	iv
Table of Contents	ix ✓
List of Tables	xii ✗
List of Figures	xiv ✗
List of Abbreviations	xv
List of Symbols	xvi
1 Introduction	1
1.1 Surface Electrodes.....	1
1.2 Motivation.....	2
1.3 Thesis Objectives.....	2
1.4 Thesis Contributions.....	3
1.5 Thesis Organization.....	5
2 Literature Review	6
2.1 Polarizable versus Non-Polarizable Electrodes.....	6
2.2 Electrode-Skin Impedance.....	8
2.3 Factors Influencing the Electrode-Skin Impedance.....	8
2.4 Previous Works on the Effect of an External Force on Electrode-Skin Interface Impedance.....	11
2.5 Equivalent Circuit Model for the Electrode-Skin Impedance.....	13
2.5.1 Equivalent Circuit Model Components Values for Electrode-Skin Interface.....	17
2.6 The Anticipated Results for Equivalent Circuit Model Components Values for Electrode-Skin Interface under the Influence of an External Force.....	18
2.6.1 Expected Changes on C_d Value.....	18
2.6.2 Expected Changes on R_d Value.....	19
2.6.3 Expected Changes on R_s Value.....	20
3 Materials and Methods	21
3.1 Experimental Setup.....	21

3.1.1	External Force Apparatus.....	21
3.1.2	Force Sensor.....	22
3.1.2.1	Force Sensor Drive Circuit.....	23
3.1.2.2	Calibration of the Force Sensor.....	24
3.1.3	Bioimpedance Measurement System.....	25
3.1.3.1	Computer for Data Control Unit.....	28
3.1.3.2	Frequency Response Analyzer (FRA)	28
3.1.3.3	Impedance Interface Device	29
3.2	Electrodes.....	30
3.2.1	Properties of Ag/AgCl Electrodes.....	31
3.2.2	Properties of Orbital Electrodes.....	32
3.2.3	Properties of Stainless Steel Electrodes.....	33
3.3	Data Collection.....	33
3.3.1	Electrodes Placement.....	34
3.3.2	Application of Force.....	34
3.4	Analysis of the Electrodes System Used in the Study.....	35
3.4.1	MATLAB Implementation for Estimating Electrode Circuit Components values.....	36
4	Effect of Externally Applied Force on Electrode-Skin Impedance for Ag/AgCl Electrodes with and without Electrolyte Gel	40
4.1	Introduction.....	40
4.2	Materials and Methods.....	41
4.2.1	Experimental Setup.....	42
4.2.2	Data Collection.....	42
4.3	Results.....	43
4.3.1	Responses of Electrode-Skin Impedance to Externally Different Applied Force Levels for Pregelled Ag/AgCl Electrodes.....	43
4.3.2	Results of Equivalent Circuit Model Components Values for Ag/AgCl Electrode-Skin Interface under the Influence of an External Force and an Electrolyte Gel.....	46

4.3.3	Responses of Electrode-Skin Impedance to Externally Different Applied Force Levels for Ag/AgCl Electrodes without an Electrolyte Gel.....	48
4.3.4	Results of Equivalent Circuit Model Components Values for Ag/AgCl Electrode-Skin Interface without Electrolyte Gel under the Influence of an External Force.....	50
4.4	Discussion.....	52
4.5	Conclusion.....	55
5	Effect of Externally Applied Force on Electrode-Skin Impedance for Dry Electrodes	56
5.1	Introduction.....	56
5.2	Materials and Methods.....	57
5.2.1	Experimental Setup.....	57
5.2.2	Dry Electrodes.....	57
5.2.2.1	Orbital Electrodes.....	57
5.2.2.2	Stainless Steel Electrodes.....	58
5.2.3	Data Collection.....	58
5.3	Results.....	59
5.3.1	Responses of Electrode-Skin Impedance to Externally Different Applied Force Levels for Orbital Electrodes.....	59
5.3.2	Results of Equivalent Circuit Model Components Values for Orbital Electrode-Skin Interface under the Influence of an External Force.....	62
5.3.3	Responses of Electrode-Skin Impedance to Externally Different Applied Force Levels for Stainless Steel Electrodes.....	64
5.3.4	Results of Equivalent Circuit Model Components Values for Stainless Steel Electrode-Skin Interface under the Influence of an External Force.....	66
5.4	Discussion.....	68
5.5	Conclusion.....	71
6	Effect of Externally Applied Force and Skin Preparation on Electrode-Skin Impedance for Pregelled Ag/AgCl	72
6.1	Introduction.....	72

6.2	Impact of Skin Preparation on Electrode-Skin Impedance.....	73
6.3	Materials and Methods.....	74
6.3.1	Experimental Setup.....	74
6.3.2	Data Collection.....	75
6.4	Results.....	75
6.4.1	Responses of Electrode-Skin Impedance to Force Loading/Unloading and Skin Preparation for Pregelled Ag/AgCl Electrodes.....	75
6.4.2	Results of Equivalent Circuit Model Components Values for Ag/AgCl Electrode-Skin Interface under the Influence of Force Loading/Unloading, Skin Preparation and an Electrolyte Gel.....	77
6.5	Discussion.....	81
6.6	Conclusion.....	83
6.7	Summary.....	83
7	Conclusions and Future Work	85
7.1	Conclusions.....	85
7.2	Future Work.....	87
Appendix A		89
A.1	The Applied MATLAB Code for Least Squares Curve Fitting Method.....	89
A.1.1	Loading Measured Impedance Data from Excel File to MATLAB Program.....	89
A.1.2	Electrode-Skin Impedance Circuit Model.....	89
A.1.3	Electrode-Skin Impedance Circuit Model on Logarithmic Scale.....	89
A.1.4	Estimating the Electrode Circuit Components Values.....	89
A.2	Estimating the Electrode Circuit Model Components Values.....	91
A.3	Validation for the Estimated Values of Electrode Circuit Model Components Values that was performed with MATLAB Program.....	92
A.3.1	MATLAB Code for Validation.....	94
A.4	Sample Calculation for Body Mass Index (BMI).....	95

A.5	Sample Calculation for Percentage Change of C_d	95
Appendix B		96
B.2	Impact of Electrode Settling Time and Force on Electrode-Skin Impedance....	97
B.2.1	Introduction.....	97
B.2.2	Materials and Methods.....	97
A)	Experimental Setup.....	97
B)	Data Collection.....	98
B.2.3	Results and Discussion.....	99
B.2.4	Conclusion.....	100
Appendix C		101
Appendix D		103
References		104

List of Tables

3.1.	Specifications of the force sensor (Model # A201).....	23
3.2.	Specifications of the frequency response analyzer (1255 B).....	29
3.3.	Specifications of the impedance interface device (1294 A)	30
4.1.	Information of subjects in the pregelled Ag/AgCl electrodes study.....	43
4.2.	Information of subjects in the Ag/AgCl electrodes without electrolyte gel study..	43
4.3.	Percentage increases in circuit model components values between initial stage and final stage of measurement cycle for pregelled Ag/AgCl electrodes sites, (values in brackets indicate a decrease).....	48
4.4.	Percentage increases in circuit model components values between initial state and final state of measurement cycle for Ag/AgCl electrodes sites without electrolyte gel, (values in brackets indicate a decrease).....	52
5.1.	Information of subjects in the Orbital electrodes study.....	59
5.2.	Information of subjects in the stainless steel (ST) electrodes study.....	59
5.3.	The percentage increases in circuit model components values between initial state and final state of measurement cycle for Orbital electrodes sites, (values in brackets indicate a decrease).....	64
5.4.	The percentage increases in circuit model components values between initial state and final state of measurement cycle for stainless steel electrodes sites, (values in brackets indicate a decrease)	68
6.1.	Information of subjects performed skin preparation in the pregelled Ag/AgCl electrodes study.....	75
6.2.	The percentage increases in circuit model components values between initial state (0 N – 0 min) and when the first force level (5N) was applied to pregelled Ag/AgCl electrodes on prepared skin sites, (values in brackets indicate a decrease).....	78
6.3.	The percentage increases in circuit model components values between initial state (0 N – 0 min) and final state (0 N – 36 min) for pregelled Ag/AgCl electrodes on prepared skin sites, (values in brackets indicate a decrease).....	78

B.1.	Ag/AgCl electrode's circuit component C_d values (nF) with/without electrolyte gel (G) and under the influence of different external force levels for the participated subjects.....	96
B.2.	Ag/AgCl electrode's circuit component R_d values ($k\Omega$) with/without electrolyte gel (G) and under the influence of different external force levels for the participated subjects.....	96
B.3.	Ag/AgCl electrode's circuit component R_s values (Ω) with/without electrolyte gel (G) and under the influence of different external force levels for the participated subjects.....	97
B.4.	A Comparison between the effects of force and electrode settling on electrode-skin impedance in the first 30 min at 10 Hz.....	100
C.1.	Orbital and stainless steel electrode's circuit component C_d values (nF) under the influence of different external force levels for the participated subjects.....	101
C.2.	Orbital and stainless steel electrode's circuit component R_d values ($k\Omega$) under the influence of different external force levels for the participated subjects.....	101
C.3.	Orbital and stainless steel electrode's circuit component R_s values (Ω) under the influence of different external force levels for the participated subjects.....	102
D.1.	Pregelled Ag/AgCl electrode's circuit component C_d values (nF) under the influence of 0 N and 5 N external force level for the participated subjects using skin's preparation technique.....	103
D.2.	Pregelled Ag/AgCl electrode's circuit component R_d values ($k\Omega$) under the influence of 0 N and 5 N external force level for the participated subjects using skin's preparation technique.....	103
D.3.	Pregelled Ag/AgCl electrode's circuit component R_s values (Ω) under the influence of 0 N and 5 N external force level for the participated subjects using skin's preparation technique.....	103

List of Figures

2.1.	Different equivalent electrode circuit models for electrode-skin interface. (a) Single time constant circuit model. (b) Double time constant-circuit model. (c) Double time constant- circuit model in addition to sweat duct's circuit. (d) Three time constant circuit model.....	15
2.2.	Bode plot representing impedance as a function of frequency for electrode-skin interface and electrode circuit model components.....	17
3.1.	Photo of the customized clamp device that was used to provide the externally applied force to electrodes.....	21
3.2.	Force sensor (FlexiForce Model # A201, 25 lb range, Tekscan, Boston, MA, U.S.A.).....	22
3.3.	Force-to-voltage circuit.....	24
3.4.	The calibration graph of the force sensor (FlexiForce, Model # A201, 25 lb range).....	25
3.5.	Block diagram of the experimental setup applied in this study.....	25
3.6.	Experimental setup which consists of frequency response analyzer device (Model # 1255A, Solartron Analytical, Farnborough, U.K.) and impedance interface device (Model # 1294A, Solartron Analytical, Farnborough, U.K.). Two clamps (SL300 Quick-Grip, Irwin Tools, Huntersville, NC, U.S.A.).....	27
3.7.	Pair of Ag/AgCl electrodes placed on the ventral side of the forearm, with electrode snap leads, and FlexiForce sensors (Model # A201, 25 lb range, Tekscan, Boston, MA, U.S.A.).....	27
3.8.	A simplified schematic diagram of the experimental set up.....	28
3.9.	Frequency response analyzer device (Model # 1255B, Solartron Analytical, Farnborough, U.K.).....	29
3.10.	Impedance interface device (Model # 1294A, Solartron Analytical, Farnborough, U.K.).....	30

3.11.	a) Ag/AgCl electrode (electrode's snap side). b) Ag/AgCl electrode (electrode's skin side).....	31
3.12.	a) Orbital electrode (electrode's snap side). b) Orbital electrode (electrode's kin side).....	31
3.13.	a) Stainless steel electrode (electrode's snap side). b) Stainless steel electrode (electrode's skin side).....	31
3.14.	Orbital electrode's penetration into the skin layers during biosignal recording...	33
3.15.	The simplified schematic diagram for the electrodes system used in the study...	35
4.1.	Experimental setup using pregelled Ag/AgCl electrodes.....	42
4.2.	Pregelled Ag/AgCl electrode-skin impedance frequency response to externally different applied force levels for the five subjects: (a) Ag/AgCl-G-S1, (b) Ag/AgCl-G-S2, (c) Ag/AgCl-G-S3, (d) Ag/AgCl-G-S4 and (e) Ag/AgCl-G-S5. Times in parentheses indicate the approximate start time of the impedance measurement.....	45
4.3.	Pregelled Ag/AgCl electrode's circuit model components values under the influence of force loading/unloading for the five subjects: (a) C_d , (b) R_d , and (c) R_s	47
4.4.	Ag/AgCl electrode-skin impedance frequency response to externally different applied force levels for the five subjects without electrolyte gel: (a) AgCl-No-G-S1, (b) AgCl-No-G-S2, (c) AgCl-No-G-S3, (d) AgCl-No-G-S4 and (e) AgCl-No-G-S5. Times in parentheses indicate the approximate start time of the impedance measurement.....	49
4.5.	Ag/AgCl without electrolyte gel electrode's circuit model components values under the influence of different force levels for the five subjects. (a) C_d , (b) R_d and (c) R_s	51
5.1.	Experimental setup using Orbital electrodes.....	58
5.2.	Orbital electrode-skin impedance frequency response to externally different applied force levels for the five subjects: (a) Orbital-S1, (b) Orbital-S2, (c) Orbital-S3, (d) Orbital-S4 and (e) Orbital-S5. Times in parentheses indicate the approximate start time of the impedance measurement.....	61
5.3.	Orbital electrode's circuit model components values under the influence of force loading/unloading and skin preparation for the five subjects (a) C_d , (b) R_d and (c) R_s	63

5.4.	Stainless steel electrode-skin impedance frequency response to externally different applied force levels for the five subjects: (a) ST-S1, (b) ST-S2, (c) ST-S3, (d) ST-S4 and (e) ST-S5. Times in parentheses indicate the approximate start time of the impedance measurement.....	65
5.5.	Stainless steel electrode's circuit model components values under the influence of force loading/unloading and skin preparation for the five subjects (a) C_d , (b) R_d and (c) R_s	67
6.1.	Pregelled Ag/AgCl electrode-skin impedance frequency response to externally different applied force levels and skin preparation for the five subjects. (a) AgCl-SP-S1, (b) AgCl-SP-S2, (c) AgCl-SP-S3, (d) AgCl-SP-S4 and (e) AgCl-SP-S5. Times in parentheses indicate the approximate start time of the impedance measurement.....	76
6.2.	Pregelled Ag/AgCl electrode's circuit model components values under the influence of force loading/unloading and skin preparation for the five subjects (a) C_d , (b) R_d and (c) R_s	79
6.3.	Comparison of pregelled Ag/AgCl electrode's circuit model components values under the influence of force loading/unloading and skin preparation for the five subjects. (a1) : (a2) C_d , (b1): (b2) R_d and (c1) : (c2) R_s	80
6.4.	Bars Comparison of pregelled Ag/AgCl electrode's circuit model components values under the influence of force loading/unloading and skin preparation for the five subjects. (a) C_d , (b) R_d and (c) R_s	84
A.1.	Experimental results for Orbital electrode-skin impedance frequency response (Subject, Orbital-S2) with applied force of 8.9 N at 6 min and the model plot done by least mean squares curve fitting method using MATLAB program. Estimated electrode circuit components values are located at the top of the Figure.....	91
A.2.	Equivalent circuit model for electrode-skin interface.....	92
B.1.	The effects of electrode settling and force on electrode-skin impedance at 10 Hz are with respect to time. Applied force levels are indicated on the graph (unlabeled points are at 0 N).....	99

List of Abbreviations

Abbreviation	Definition
BMI	Body Mass Index
ECG	Electrocardiogram
EEG	Electroencephalogram
EMG	Electromyogram
FRA	Frequency Response Analyzer
G	Electrolyte Gel
LTI	Liberating Technologies Inc.
Ag/AgCl	Silver/Silver Chloride
ST	Stainless Steel Electrodes

List of Symbols

Symbol	Meaning
C	Capacitance
C_d	Capacitor of electrode circuit model
cm	Centimetre
ω	Angular frequency ($2\pi f$)
ϵ_r	Dielectric constant of the material
ϵ_0	Electric constant ($8.85 \times 10^{-12} \text{ F m}^{-1}$)
A	Electrode's area (cross sectional area)
Z_e	Electrode-skin impedance
F	Farad
f	Frequency
g	Gram
GND	Ground
E_{hc}	Half cell potential of electrode circuit model
Hz	Hertz
Kg	Kilogram
$k\Omega$	Kiloohm
V_T	Input Voltage
L	Length of the material
$M\Omega$	Megaohm
m	Meter
μm	Micrometer
nF	nanoFarad
N	Newton
Ω	Ohm
$\Omega.m$	Ohm.meter
lb	Pound
R_F	Reference Resistor
R	Resistance
ρ	Resistivity of the material
R_d	Resistor of electrode circuit model
R_{se}	Sensor's Resistance
d	Separation distance between the skin and electrode
R_s	Series Resistance including underlying skin tissue
$R_{tissues}$	Tissues Resistance
V	Volt

1 Introduction

1.1 Surface Electrodes

Biological signals, such as electrocardiogram (ECG), electromyogram (EMG), and electroencephalogram (EEG), are rich in medical information. Biopotential electrodes have the ability to transduce bioelectric activity within the body (ionic current) into electrical current that can be measured and recorded [1], [2].

Biopotential electrodes can be broadly divided into two categories: 1) invasive electrodes and 2) non-invasive electrodes [1], [2].

Invasive electrodes are designed to penetrate into skin surface for detecting biopotentials near the source of interest [1], [2]. Non-invasive electrodes, which are also known as surface electrodes, are designed to be placed on the skin surface [1], [2]. Better signal quality can be obtained by using invasive electrodes than using non-invasive electrodes, since they measure near the source (other undesired bioelectric signals can be avoided) and they do not have to be contend with large amounts of tissues between the bioelectric source and the recording site, which attenuate the signal [1], [2]. However, non-invasive electrodes are the most common choice for clinical biological signals measurements and the preferred choice by patients and health care providers due to their safe usage (e.g., less chance of infection), convenience (e.g., easy to place electrodes), and better comfort for patients. This thesis will be focusing solely on non-invasive electrodes [1], [2].

Performance of non-invasive electrodes in detecting biological signals is highly dependent on electrode-skin impedance [1] - [5]. High electrode-skin impedance would result in poor biological signal quality, low signal amplitude and low signal to noise ratio (Section 2.2) [1] -

[4]. Many factors affect the electrode-skin impedance including atmospheric humidity [1], [6], heat [6], sweat secretion [1], [2], [6], skin type [7], [8] electrode size [1], [2], [9], electrode shape [2], electrode material [1], [10], electrolyte gel, and skin preparation as described in (Section 2.3) [11] - [13]. An externally applied force will also affect the electrode-skin impedance; however, its effects neither well researched nor well understood.

1.2 Motivation

Researchers in biomedical engineering field are developing new modern sensor technologies that enable continuous, remote monitoring of biological signals for patients [14]. Biopotential sensor technologies can be integrated into various devices, such as chairs [14], rollators [15], and shirts [16], to monitor biological signals, such as ECG and EMG signals of patients. Many drawbacks are facing these remote sensor technologies. One major negative aspect is the high electrode-skin interface impedance [16], [17]. In addition, wearable devices require a certain tightness to guarantee good electrode-skin contact; the tightness may change due to muscle contractions during normal physical activities and respiration [16], [17]. As a result, the force applied to the biopotential electrodes will cause fluctuations in the electrode-skin impedance [17]. Changes in electrode-skin impedance will affect biological signal quality, resulting in noise and measurement artifacts in the recorded biological signals (e.g., motion artifact) [1], [2].

Investigating the effect of external force on the electrode-skin impedance for non-invasive measurements would lead to better understanding of its impact on biological signal quality.

1.3 Thesis Objectives

The main objective of this thesis is to investigate the effects of an externally applied force on the electrode-skin impedance for non-invasive surface electrodes used in acquiring

biological signals. It will examine the effect of different force levels and force loading and unloading on a variety of non-invasive biopotential electrodes, in the presence and absence of electrolyte gel, also with and without skin preparation.

1.4 Thesis Contributions

The major contributions of this thesis are:

- 1- Analyzing the effect of an external force on electrode-skin impedance for Ag/AgCl electrodes.**

The effect of force on electrode-skin impedance for silver/silver chloride (Ag/AgCl) electrodes is analyzed based on experimental results obtained from five subjects. A circuit model of the electrode-skin impedance is employed as part of the analysis. The impact of force on the electrode-skin impedance under the presence and absence of an electrolyte gel for Ag/AgCl electrodes is assessed. The response of electrode-skin impedance to varying levels of force is analyzed (i.e., increasing the level of applied force and then decreasing the level of applied force on electrodes sites). The reasons behind the decrease in electrode-skin impedance with respect to force application and the inconsistent fluctuations in electrode-skin impedance when an electrolyte gel was applied are discussed.

- 2- Analyzing the effect of an external force on electrode-skin impedance for dry electrodes.**

The effect of force on electrode-skin impedance for different dry electrode types: 1) Stainless steel electrodes, 2) Orbital electrodes are analyzed based on experimental results obtained from five subjects. A circuit model of the electrode-skin impedance is employed as part of the analysis. The impact due to difference in shapes between stainless steel

electrodes and Orbital electrodes on electrode-skin impedance is evaluated and also the impact of Orbital electrodes spikes on electrode-skin impedance under different force levels. The response of electrode-skin impedance to varying levels of force is analyzed (i.e., increasing the level of applied force and then decreasing the level of applied force on electrodes sites). The different factors that caused a large drop in electrode-skin impedance after the application of force on dry electrodes sites are examined.

3- Analyzing the effect of repeated force loading/unloading on electrode-skin impedance for pregelled Ag/AgCl electrodes with skin preparation.

The effect of force on electrode-skin impedance for pregelled Ag/AgCl electrodes and prepared skin sites is analyzed based on experimental results obtained from five subjects. A circuit model of the electrode-skin impedance is employed as part of the analysis. The biological signal recording conditions for wearable biomedical sensor systems are mimicked in this study. Applying a repeated loading/unloading of fixed low force level (5 N) to electrodes sites resulted in a decrease in electrode-skin impedance and an increase when no force was applied. The effect of repeated loading/unloading of fixed low force level (5 N) on electrode-skin impedance is analyzed, in addition to the impact of skin preparation on the electrode-skin impedance response to applied force.

4- Comparison between the response of dry electrodes and wet electrodes to an external force level.

Dry electrodes (Stainless steel and Orbital) were found to have much larger decrease in electrode-skin impedance in response to force application as compared to wet electrodes (Ag/AgCl) with electrolyte gel.

The variations in electrode-skin impedance responses to an external force due to the differences in electrodes properties between dry and wet electrodes are evaluated.

Portions of this research have been disseminated in the following publication:

A. Albulbul and A. D. C. Chan, "Electrode-skin impedance changes due to an externally applied force," IEEE Intl. Symp. MeMeA, Budapest, Hungary, pp. 18-19, May 2012.

1.5 Thesis Organization

Chapter 2 presents background information on non-invasive electrodes, electrode-skin impedance, factors that influence the electrode-skin impedance, and an equivalent circuit model for the electrode-skin interface. This chapter includes an overview of previous research on the effect of an external force on the electrode-skin impedance.

Chapter 3 presents a detailed description of the equipment and methodology used in this thesis.

Chapter 4 examines the effect of different external force levels on the electrode-skin impedance for Ag/AgCl electrodes with electrolyte gel and Ag/AgCl electrodes without applying an electrolyte gel.

Chapter 5 examines the effect of different external force levels on the electrode-skin impedance for different dry electrode types (Orbital and stainless steel electrodes).

Chapter 6 examines the effect of repeated loading/unloading of fixed low force level and skin preparation on the electrode-skin impedance for Ag/AgCl electrodes with electrolyte gel.

Chapter 7 provides the conclusion obtained in this thesis and suggestions for future work.

2 Literature Review

This chapter highlights some fundamentals topics on biopotentials recordings. It provides a brief overview of the two types of electrodes (section 2.1): 1) polarizable and 2) non-polarizable electrodes. Electrode-skin impedance is discussed, along with its effect on biological signal quality (section 2.2). Factors that affect electrode-skin impedance are also discussed (section 2.3). An external applied force that can affect the electrode-skin impedance is an additional factor and is the focus of this study. A critical review of previously published works concerning the effect of an external applied force on electrode-skin impedance is presented (section 2.4). An equivalent circuit model, used to represent the electrode-skin impedance, is introduced (section 2.5). This model is used in this study to better understand the changes in electrode-skin impedance with respect to force application. The anticipated effect of an external force on electrode circuit model components is discussed in section 2.6.

2.1 Polarizable versus Non-Polarizable Electrodes

Biopotential electrodes perform the function of exchanging ionic current that occur in the body to electric current [1]. Non-invasive biopotential electrodes have many applications in the medical field including detecting biological signals (e.g., ECG, EMG and EEG), transferring electrical impulses to the body (e.g., cardiac pacing and defibrillation), and in bioimpedance measurements applications [1], [2]. Non-invasive electrodes can be categorized as polarizable or non-polarizable electrodes; they are also known as dry and wet electrodes, respectively. Ideal polarizable electrodes do not permit charges to pass through the electrode-skin interface [1], [2]. Instead, a change in ionic concentration at the electrode-skin interface results in

a displacement current [1], [2]; as such, polarizable electrodes are often described to function in a manner similar to a capacitor [1], [2]. Polarizable electrodes have higher electrode-skin impedance, a very large charge transfer resistance value [1], [2], [18], and higher noise in comparison to non-polarizable electrodes [1], [19]. Polarizable electrodes are applied to the skin's surface without using an electrolyte gel [20]. In general, they are not recommended for clinical measurements due to their lower signal to noise ratio [4], [20]. Polarizable electrodes have poor contact with the skin's surface resulting in electrodes movements and instability in detecting the changes in ionic concentration at the electrodes sites [1], [2]. Due to their weakness in contacting with the skin's surface, a change in the distributions of ions at the electrodes sites would cause disruptions of ions and changes to electrode's half cell potential resulting in noise and motion artifacts to biological signals [1], [18]-[20].

Ideal non-polarizable electrodes permit the charges to pass through the electrode-skin interface without hindrance [2]. In non-polarizable electrodes, reduction/oxidation reactions occur at the electrode-skin interface, exchanging charge carriers from ions to electrons and vice versa. These reactions are electrochemically reversible in non-polarizable electrodes [2]. The electrolyte gel is used with non-polarizable electrodes to facilitate the electrochemical reactions and to reduce electrode-skin interface impedance [2], [4], [12].

Stainless steel electrodes are classified as polarizable electrodes [1]. They are one of the most common polarizable electrodes used in modern wireless sensor technologies for monitoring biological signals (e.g., chairs, shirts) [21]. Ag/AgCl electrodes are classified as non-polarizable electrodes and considered as the universal electrodes in clinical measurements (e.g., ECG, EMG and EEG). They are associated with low electrode-skin impedance, low noise and motion artifact [22].

2.2 Electrode-Skin Impedance

Electrode-skin impedance plays a major role in biological signal quality. High electrode-skin impedance influences negatively biological signal quality since it is associated with low signal-to-noise ratio [1], [2], [23]. High electrode-skin impedance causes poor detection of biopotentials at the electrodes sites, because it forms a strong barrier for the potentials to cross it, causing signal attenuation [1] – [4]. High electrode-skin impedance could be linked to low mobility of ions across the highly resistant skin layer (stratum corneum) that is in contact with electrodes and low electron/ion exchange at electrodes sites [1] – [4]. Thus, that could cause weak conductivity between electrodes and skin and would reduce the biological signal amplitude (low signal to noise ratio). A mismatch in impedance between the electrodes at the skin surface during recording a biological signal would increase common mode interference (e.g., power line noise) and decrease the signal-to-noise ratio [2], [20]. With higher electrode-skin impedances, there is a higher probability of a larger mismatch in electrode-skin impedance. In addition, high electrode-skin impedance will cause a decrease in signal power and will be associated with higher susceptibility to motion artefact [8], [13], [23].

Electrode-skin impedance varies from one person to another and from one part of the body to other. For example, when Rosell *et al.* [4] measured the electrode-skin impedance at different parts of the body for ten subjects, using Ag/AgCl electrodes, they found a high electrode-skin impedance of around $1\text{ M}\Omega$ at 1 Hz at the leg site, while around $100\text{ k}\Omega$ at the forehead site.

2.3 Factors Influencing the Electrode-Skin Impedance

Skin tissue is responsible for the high electrode-skin impedance [24]-[27]; in particular, the stratum corneum, which is at the surface of the skin, with a depth of approximately 9 -19 μm [28]. The stratum corneum has a high impedance value because it is comprised of dead cells

and there is a scarceness of fluid at this tissue layer [29], [30]. Also, many factors could affect the electrode-skin interface impedance, including electrode size [18], electrode shape [2], [20], [31] electrode material [1], [20], [32] application of electrolyte gel [12], [33], [34], skin preparation [4], [13], environmental factors (e.g., humidity or heat) [1], [35] and skin type (e.g., skin thickness, skin dryness) [24], [36].

Electrode surface area is known to influence the electrode-skin impedance; larger electrode surface area results in lower electrode-skin impedance as it will be described in more details in section (2.6) [1], [2], [9]. The shape of non-invasive electrodes could influence the electrode-skin impedance. Spiked electrodes penetrate into the skin through the highly resistant stratum corneum layer and thus would result in lower electrode-skin impedance [31].

The type of electrode material determines where an electrode fits on the polarizable/non-polarizable spectrum of electrodes. Typically, electrodes could be classified as polarizable or non-polarizable, but their degree level of polarizability is different in which different kinds of electrodes have different strength of polarization. Thus, there could be very low polarizability strength or very high polarizability strength. Electrodes made of platinum are more polarizable than electrodes made of tin metal. Therefore, platinum electrodes are more polarizable than tin electrodes [22].

Non-polarizable electrodes tend to be associated with lower electrode-skin impedances in comparison to polarizable electrodes (Section 2.1) [1], [2], [32], [37].

Electrolyte gel forms conductive environment for the ionic charges to be transferred to electrode surface. The gel can penetrate into the skin, hydrating the stratum corneum layer, and providing a better conductive environment [1], [2], [33], [38]. Skin preparation is the most common procedure performed to reduce the electrode-skin impedance [11], [13], [34], [39],

[40]. Reduction of electrode-skin impedance is accomplished by the removal of stratum corneum layer [23]. Skin preparation can be performed through several techniques. Among the first techniques used was the application of adhesive tape to the skin's site for several times to remove the top skin layers of the epidermis [24]. Other techniques rely on rubbing the skin surface with sandpaper and shaving any hair at the electrode placement sites [23]. However, stripping the skin layers by adhesive tape or sandpaper can be associated with pain or discomfort. Some modern skin preparation techniques use a highly concentrated gel that contain rough elements (quartz elements), forming a rough surface on the skin's site, followed by rubbing the skin site with a fabric to remove the stratum corneum layer from the skin's surface [20]. Wiping the skin's surface with alcohol swab could also help prepare the skin's site for biological signals measurements, since it can remove the oily residues and part of the dead skin layers from the skin site [11].

Humidity can cause a change in the water's content of the stratum corneum and affect the electrolytic activity [1], [41]. Higher humidity or sweat secretion can cause higher electrolytic activity and thus lower impedance values for the skin [1], [41].

High level of hydration could lead to a better electrolytic activity of ions and such a better biological signals recording conditions [1], [35]. In addition, higher body fluid will enhance the transformation of ions by sweat to the skin surface and subsequently to the electrodes [1]. External force is also considered to affect electrode-skin impedance. This is discussed in the next section and is the main focus of this thesis.

2.4 Previous Works on the Effect of an External Force on Electrode-Skin Interface Impedance

Applying an external force to electrodes sites is found to decrease the electrode-skin impedance [42], [43]. It forces an increase in the contact strength between electrode's surface and skin such increasing the effective electrode's contact area, leading to a decrease in electrode-skin impedance [9]. Also it affects the electrode's circuit model components, capacitance (C_d), the charge transfer resistance (R_d) and the series resistance (R_s) as will be discussed in more details in section (2.6) and in the next chapters.

There are limited amount of previous works examining the effects of an external force on the electrode-skin impedance. Hill *et al.* [42], investigated the electrical impedance plethysmography and the effect of blood pressure on Ag/AgCl electrodes during measurements. A change in the electrode-skin interface impedance was found when they applied a necklace or a bracelet on the electrodes sites. The effect of a necklace or a bracelet on the electrodes sites was measured to be equivalent to approximately 100 g (0.98 N) over the electrodes sites. They found a decrease of $3.2 \text{ k}\Omega/\text{cm}^2$ when a 100 g (0.98 N) (bracelet) was placed on the electrodes sites under dry skin condition in comparison to 1 g (0.0098 N) (weight of electrode). There was a small decrease of $0.2 \text{ k}\Omega/\text{cm}^2$ when a 100 g (0.98 N) was placed on electrode-electrolyte gel sites (wet skin condition) in comparison to 1 to 2 g weight (0.0098 to 0.0196 N). This work only measured impedances at 5 kHz and did not investigate different electrode types. Moreover, there was no satisfactory explanation provided as to why there was a decrease in impedance.

The effect of an external force on the surface electrode-skin impedance measurements was examined by Swanson [43], based on the initial work by Hill *et al.* [42]. The measurements of the electrode-skin impedance were done in the frequency range of 1 Hz – 1 MHz at the

forearm, leg, back and at the chest area. Swanson applied a pressure of 70 g/cm^2 (0.69 N) on the Ag/AgCl electrodes sites in the absence of electrolyte gel and found a decrease of 10 % in impedance when it was measured at 100 Hz – 1 kHz, while there was 1-3 % decrease in impedance when it was measured at lower frequencies range (1 Hz – 10 Hz). Swanson concluded that the effect of pressure on the electrodes sites had resulted in an increase in the contact area between the electrodes and the skin leading to a decrease in electrode-skin impedance. When Swanson repeated the application of pressure on the same Ag/AgCl electrodes sites with electrolyte gel, the impedance was increased by 10 % at the low frequency range and the high frequency range. The reason behind the increase in impedance was attributed to the electrolyte gel under the electrode's cup [43]. The electrolyte gel was thought to have been squeezed out from the electrode's boundary during the application of pressure on the electrodes sites, which caused the impedance to increase. Swanson had only applied a light load 70 g/cm^2 (0.69 N) on the electrodes sites and focused on one type of electrodes (Ag/AgCl).

Dozio, Baba and Burke analyzed the electrode-skin impedance of different sizes of dry surface carbon-inlaid silicon rubber electrodes for long term ECG signal measurements, including the effect of applied force on electrodes sites [44], [45]. An electrode circuit model was used to represent the electrode-skin impedance. However, there are some concerns about the methodology they used on their measurements and its effect on the accuracy of the results. They used a two-electrode system in [44] and [45] for measurements and two time constants to estimate the values of electrode-skin interface impedance; essentially two RC circuits in series. The first time constant was used to estimate the electrode-electrolyte interface and the second time constant was used to estimate the impedance value of the electrolyte-skin interface. It turned out to be some errors in their results, as they reported of having some difficulties in

determining the time constant for each circuit. Thus, to avoid complexity, each electrode can be associated with just one time constant as described in the next section (2.5) [1], [12]. Their results showed variations in the impedance values with respect to different pressure levels. The pressure levels applied in [44] and [45] were 5 mmHg (0.067 N/cm^2) and 20 mmHg (0.27 N/cm^2). The variations in the impedance values among the tested subjects were not in agreement, as there were some decrease and increase in impedance values with increasing pressure level. Their inconsistent results may be related to the low level of pressure being applied (5 mmHg and 20 mmHg), and to the nature of the electrodes materials (dry surface carbon-inlaid silicon rubber electrodes) as the elastic property of the electrode's rubber might cause an absorption of some of the applied pressure and affect the accuracy of the results.

The tool they used to apply pressure to electrodes sites relies on customizing a belt with bladder that can be inflated to the desired level and controlled by a pressure monitor device.

The previous works on the effect of external force on electrode-skin impedance have provided some evidence of the changes that may influence the electrode-skin impedance. Furthermore, they have motivated researchers for further research on exploring the effects of different force levels on electrode-skin impedance, hence the published works on this issue were limited to light force levels $\leq 1 \text{ N}$ and did not explore the effect of force on electrode-skin impedance for different electrodes types.

2.5 Equivalent Circuit Model for the Electrode-Skin Impedance

An equivalent circuit model can be used to better understand the interactions between a surface electrode and the skin. Warburg was known to be the first to propose an equivalent electrode-electrolyte interface circuit model [46]. Feates *et al.* had identified the components of the equivalent electrode circuit model by analyzing the conductivity nature of biological tissues

[47]. Their work helped in estimating the values of capacitors and resistors in the electrode-skin model. In addition, their study provided more details on the effect of skin capacitance, impedance and electrolyte gel or sweat on the electrode-skin impedance.

(Figure 2.1a) depicts a simplified single time constant for electrode-skin interface (single interface) circuit model. The half cell potential (E_{hc}) represents the potential difference between the skin or electrolyte (gel or sweat) and the electrode as a result of the ions that reside between the electrode and skin [2]. The capacitance that accommodates the charges that are located between the electrode and skin double layer is represented by C_d [2], [25]. The resistance that would occur to the charges transfer between the skin and electrode is represented by R_d [2], [48]. The series resistance (R_s) represents the resistance of the electrolyte gel and sweat [1], [48].

There are different electrode circuit models that represent the electrode-skin interface. A double time constant model (double interface) that has two circuits as in (Figure 2.1b) is designed to represent the electrode-electrolyte (gel-sweat) interface with the first circuit and the electrolyte-skin interface with the second circuit.

The first circuit components (E_{hc} , C_d , R_d and R_s) in the double time constant model are as described previously. A half cell-potential (E_{sk}) is the first component in the second circuit of the electrolyte-skin interface and it represents the potential difference caused by the changes in ion concentration at the electrolyte (gel-sweat)-skin interface. C_e represents the capacitance of the electrolyte-skin in the upper skin layer (Epidermis) junction, R_e represents the resistance to the flow of ions across the skin surface and R_{ds} represents the resistance of the deep skin tissues (Dermis).

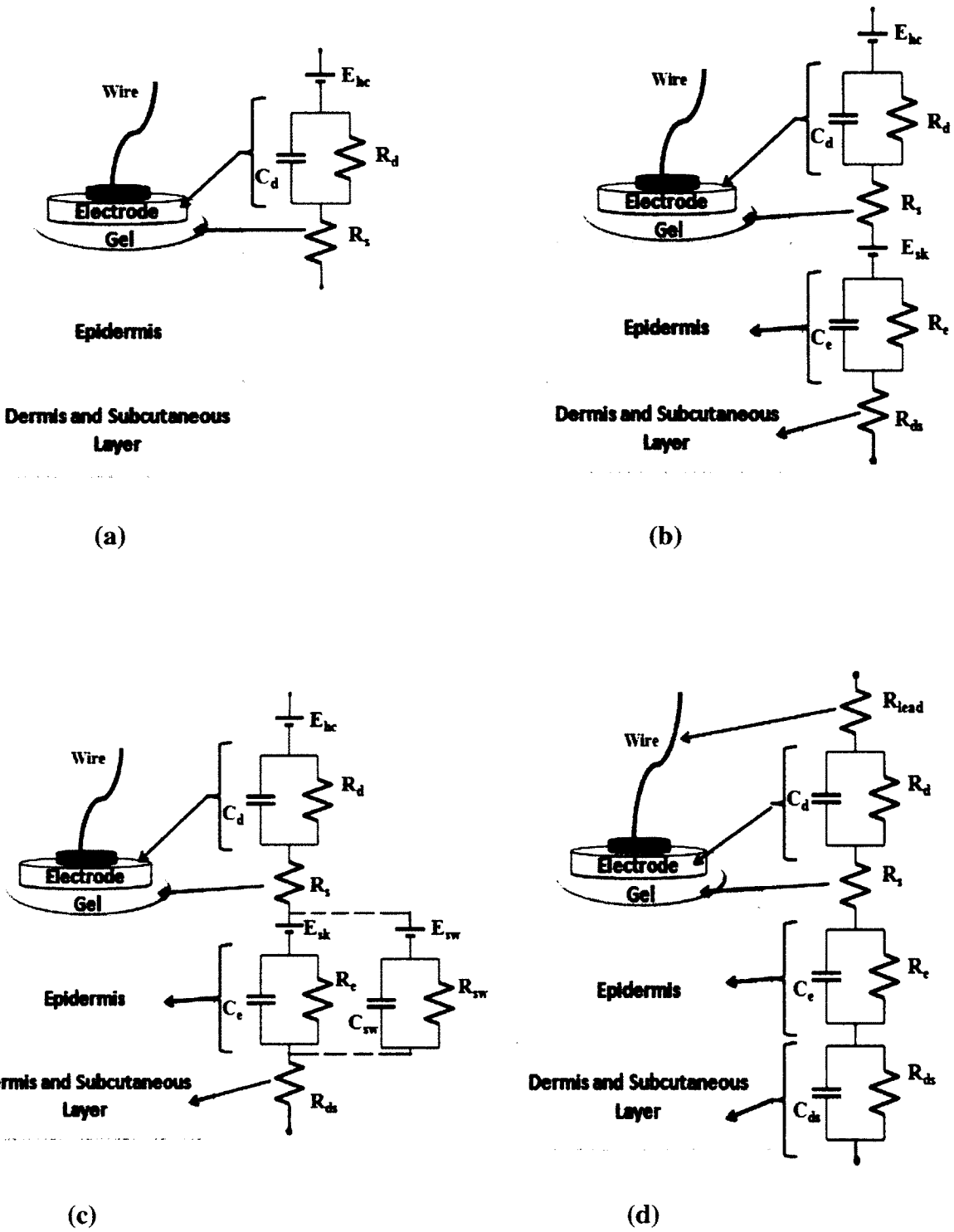


Figure 2.1. Different equivalent electrode circuit models for electrode-skin interface. (a) Single time constant circuit model. (b) Double time constant-circuit model. (c) Double time constant-circuit model in addition to sweat duct's circuit. (d) Three time constant circuit model.

The third model (electrode-skin-sweat duct's model) in Figure 2.1c is different from the previous double time constant model in Figure 2.1b by the addition of another circuit model (E_{sw} , C_{sw} and R_{sw}) that represents the involvement of sweat glands and ducts in electrode circuit modeling. (E_{sw}) is the potential changes between the sweat ducts and the surrounded skin tissue, (R_{sw}) represents the resistance of ions transfer through the sweat ducts and (C_{sw}) is the capacitance at the junction between sweat glands and sweat ducts [2]. Also, there is a three time constant model to represent the electrode-skin interface in Figure 2.1d. The three time constant model is different from the previous models by the addition of another circuit to represent the deep skin tissue (Dermis) and the ions in the tissue fluid. In the three time constant circuit model, R_{ds} represents the resistance of skin tissue in dermis (muscle and fat tissue) and C_{ds} represents the capacitance that results from the ions in the junction between the fat tissue and muscle tissue. Also, the three time constant model has R_{lead} which represents the electrode's wire resistance [5].

In this study, the simplified single time constant (single interface) circuit model (Figure 2.1a) is used in the evaluation of the effect of force on electrode-skin impedance. The simplified single time constant circuit model represents the major interface that affects the electrode-skin impedance. Analyzing the effect of force on a single time constant electrode circuit model components values would provide an understanding of the impact of an external force on electrode-skin impedance.

In addition, the other models (Figures 2.1b, c, d) have two or three circuits. So, there is a need for a time constant to be determined for each circuit and such the differentiation of each circuit components values could be problematic when having two or three circuits in the same model.

Determining different circuit model components values for different time constant circuits could be associated with errors as the difference between each time constant of two adjacent circuits is very small (could be less than 1 ms) [1], [45].

2.5.1 Equivalent Circuit Model Components Values for Electrode-Skin Interface

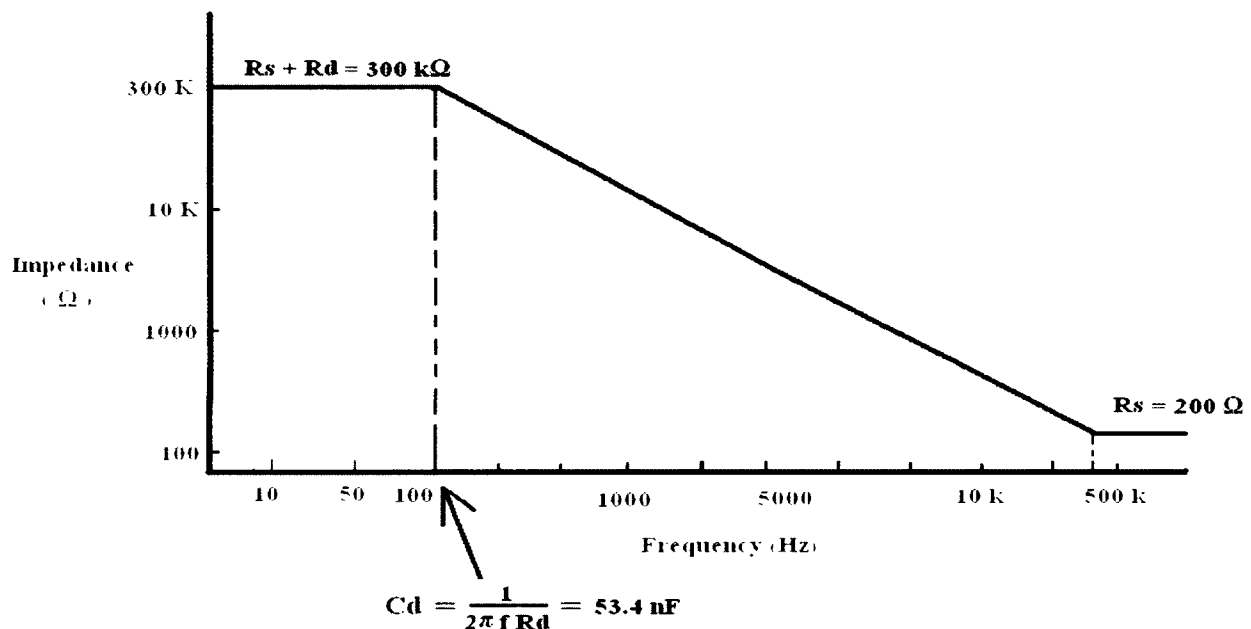


Figure 2.2. Bode plot representing impedance as a function of frequency for electrode-skin interface and electrode circuit model components.

Analyzing the behaviour of the electrode-skin impedance with respect to frequency (Figure 2.2) would lead to determination of the electrode circuit model components. In this study, the estimation of the electrode circuit model components will be based on a single electrode circuit model (Figure 2.1a).

At low frequencies and before approaching the cut-off corner frequency, the electrode-skin impedance is at its maximum value [1], [2]. At low frequencies and at the open circuit state,

capacitor C_d is at high impedance region where the electrode-skin impedance is dominated by $R_d + R_s$ [2], [48], [49]. The impedance associated with the capacitor approaches infinity at low frequencies [2]. There is a steep decline in impedance, typically around frequencies 100 Hz – 500 Hz, in which C_d value can be determined from the cut-off corner frequency [2]:

$$C_d = \frac{1}{2\pi f R_d} \quad (2.1)$$

At high frequencies 500 kHz – 1 MHz, the impedance associated with the capacitor approaches zero at the short circuit state and the electrode-skin impedance is dominated by R_s (Figure 2.1) [1], [2], [49]. The electrode-skin impedance at low frequencies is much larger than at high frequencies [1], [2], [25].

2.6 The Anticipated Results for Equivalent Circuit Model Components Values for Electrode-Skin Interface under the Influence of an External Force

Different factors would change the electrode circuit model components values as stated in section 2.3. The expected effect of external force on the electrode circuit model components C_d , R_d and R_s values will be discussed in the following subsections.

2.6.1 Expected Changes on C_d Value

It is anticipated that the effect of external force on the electrodes sites is marked by increasing the contact area between the electrode surface and the skin, which would increase the value of C_d value. The increase in the area of the parallel plates (A) (double layer charge between electrode and skin) would mean more ions to be stored between electrode and skin

resulting in an increase in capacitance value (C) in accordance with the parallel-plate capacitor's formula (2.2) [50]. Capacitance is directly proportional to the area of the parallel plates.

$$C = \epsilon_r \epsilon_0 \frac{A}{d} \quad (2.2)$$

C is the capacitance (F)

ϵ_r is the dielectric constant of the material between the parallel plates.

ϵ_0 is the electric constant (approximately $8.85 \times 10^{-12} \text{ F m}^{-1}$)

A is the area of the parallel plates (m^2)

d is the separation distance between the parallel plates (m)

Pressing the electrodes sites would decrease the separation distance between the parallel plates (d) (double layer charge) that forms between the skin and electrode, thus generating a higher capacitance value (Figure 2.4). The dielectric constant of the material between the parallel plates (ϵ_r) and the electric constant (ϵ_0) are constant.

2.6.2 Expected Changes on R_d Value

R_d value is expected to be lower after an external force is exerted on the electrodes sites because the electrode's contact area would increase if there is an external force on the electrode's site. Exerting a force on electrodes sites would force the entire electrode's surface to be in contact with the skin, and thus increasing contact area would decrease the impedance [9]. The effect of external force on R_d value can be better analyzed through the resistance of a conductor's formula (2.3) which states the relationship between resistivity, length and the cross-sectional area of the conductor material with resistance [50].

$$R = \rho \frac{L}{A} \quad (2.3)$$

R is the resistance (Ω)

ρ is the resistivity of the material that has the unit of ($\Omega \cdot m$)

L is the length of the material that has the unit of (m)

A is the cross sectional area of the conductor material that has the unit of (m^2)

According to resistance of a conductor's formula (2.3), a decrease in R_d values can be related to an increase in the electrode-skin contact area (A) and to a decrease in (ρ) resistivity value as a result of an increase in sweat quantity or the presence of an electrolyte gel, while assuming the value of L does not change in this study.

2.6.3 Expected Changes on R_s Value

The series resistance (R_s) value represents the electrolyte gel, sweat and the underlying skin tissue. R_s value is expected to be lower under the influence of force. The expected lower R_s value can be correlated with the resistance of a conductor's formula (2.3). Application of force on electrodes sites would enhance sweat activity with time causing a decrease in (ρ) resistivity and such in R_s value. Also, the presence of an electrolyte gel would decrease (ρ) resistivity and decrease R_s value [33]. In addition, the increase in the cross sectional area (A) (electrode-skin contact area) described in previous section (2.6.2) would allow more sweat-electrolyte gel to be in contact with electrode's surface, thus decreasing R_s value.

3 Materials and Methods

Section 3.1 and section 3.2 describe the experimental setup and electrodes used in this study, respectively. Section 3.3 describes the data collection procedures. Section 3.4 describes the electrode circuit used to model the electrode-skin impedance, and it also describes how electrode circuit model components were estimated.

3.1 Experimental Setup

3.1.1 External Force Apparatus

The external force being applied to electrodes in this study is provided by a customized clamp device (Figure 3.1). Since electrode-skin impedance measurements involve two electrodes, the customized device uses two clamps (Model # SL300 Quick-Grip, Irwin Tools, Huntersville, NC, U.S.A.); one for each electrode. These clamps were integrated into a fixed wooden base to provide a downward vertical force.

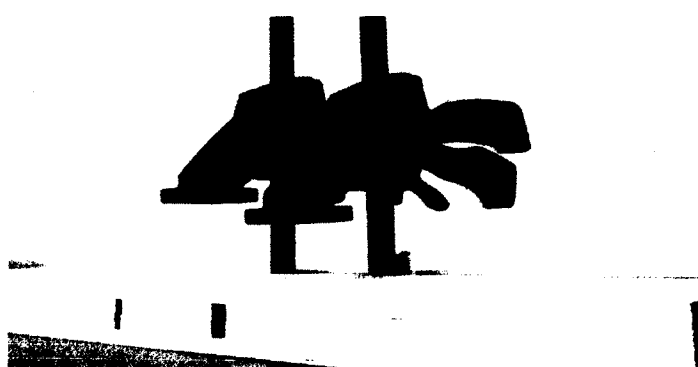


Figure 3.1. Photo of the customized clamp device that was used to provide the externally applied force to electrodes.

3.1.2 Force Sensor

A force sensor was used to measure the applied force to each electrode. FlexiForce sensors (Figure 3.2) are used in these experiments (FlexiForce, Model # A201, 25 lb range, Tekscan, Boston, MA, U.S.A.). Two force sensors are used; one associated with each clamp/electrode.

The force sensor transduces an applied force to a change in resistance. If there is no force applied to the force sensor, the force sensor will be at its maximum resistance (larger than $5 \text{ M}\Omega$) [51]. When a force is applied, the electrical resistance will decrease and the force sensor will conduct an electrical current. The conductance is set to change (i.e., reciprocal of the resistance) linearly with the applied force in the operating range.



Figure 3.2. Force sensor (FlexiForce Model # A201, 25 lb range, Tekscan, Boston, MA, U.S.A.).

This force sensor has a circular sensing area 0.375" (0.95 cm) in diameter and a sensing range of 0 lb to 25 lb (0 kg to 11.34 kg). Sensor accuracy is reported by the manufacturer to be $\pm 3.0\%$ [51]. Based on the trials performed (section 3.1.2.2), the sensor accuracy obtained is $\pm 8\%$.

The force sensor is made of two polyester thin film layers and two silver (conductive metal) layers. Each silver layer is shielded with one polyester thin film [51]. The silver metal layer covers the sensing area and ends with three pins to be connected with the force to voltage circuit. Also, there is a pressure sensitive ink which is made of an elastic polymer and contains

semi-conductive nano-particles. The pressure sensitive ink is placed between the silver layers in the sensing area. The specifications of the force sensor are available in Table 3.1 and in [51].

Temperature effect on the force sensor measurements is very minimal since the measurements are set to be done at room temperature 22°C and the recommended operating temperature range by the manufacturer is between -9°C to 60°C. Also, the sensitivity of the force sensor to 1°C change in temperature is approximately 0.4% [51]. The performance of the force sensor's operation with changes in temperature is not published or reported by the manufacturer (Tekscan).

Table 3.1. Specifications of the force sensor (Model # A201).

Force Ranges	0-25 lb (110 N)
Response Time	< 5 μ sec.
Operating Temperatures	(-9°C to 60°C)
Temperature Sensitivity	Output variance up to 0.4% per 1°C

3.1.2.1 Force Sensor Drive Circuit

The FlexiForce sensor is used with a force-to-voltage circuit. This circuit is based on Tekscan's manual recommended drive circuit [51] and is shown in Figure 3.3. An operational amplifier LM 741CN (Model # LM741CNNS-ND, National Semiconductor, TX, U.S.A.) is used to scale the output voltage. The reference resistor used to set the gain was represented by $R_F = 100 \text{ k}\Omega$, the sensing resistor (R_{Se}) has a very high resistance (larger than $5 \text{ M}\Omega$) when no force is applied.

$$V_{out} = - V_T (R_F / R_{Se}) \quad (3.1)$$

where V_T is the input voltage.

A power supply (Model # 72, TENMA laboratory, Springboro, Ohio, U.S.A.) was used for

supplying 8 V DC power to force to voltage circuit. The output voltage was measured by a digital multimeter (Model # 052-0060-2, Mastercraft, ON, Canada).

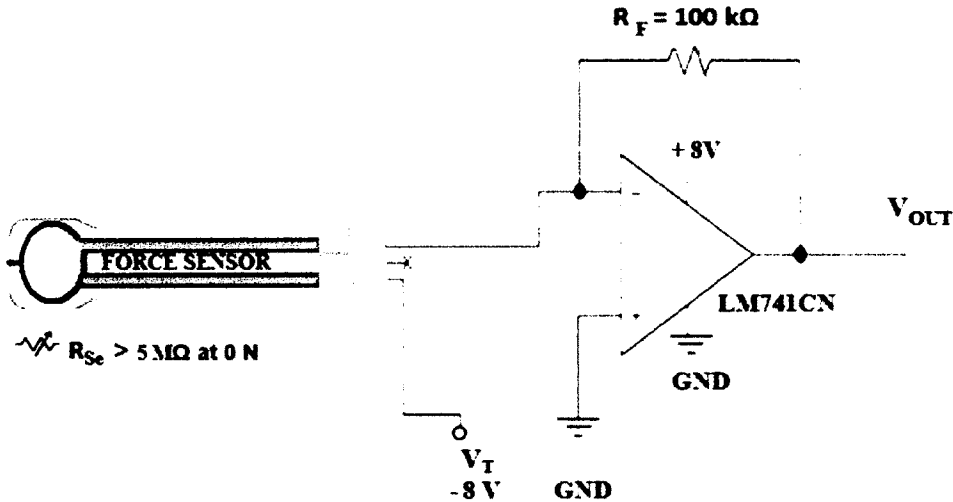


Figure 3.3. Force-to-voltage circuit.

3.1.2.2 Calibration of the Force Sensor

A calibration was performed for the 25 lb force sensor by placing different amounts of weight on the force sensor and measuring the output voltage from the force-to-voltage circuit by a digital multimeter (Model # 052-0060-2, Mastercraft, ON, Canada). The weights used are 0.250 kg (0.6 lb, 2.45 N), 0.750 kg (1.7 lb, 7.35 N), 1.76 kg (3.9 lb, 17.26 N) and 2.64 kg (5.8 lb, 25.89 N). Weights were verified using an electronic scale (Model # EJ-4100, A&D, Korea). Five calibration trials were performed. The calibration results are shown in Figure 3.4. There was a small difference between each trial. One of the reasons behind the variations in measurements between the calibration trials for the force sensor in Figure 3.4 is related to the accuracy of the force sensor. Based on the trials performed, the accuracy obtained $\pm 8\%$ is different from the reported value $\pm 3\%$ by the manufacturer (Tekscan) [51]. The reasons behind that could be attributed to the quality of the force sensor and the hysteresis effect with force

loading/unloading during the force sensor operation, since the manufacturer reported that the effect would be < 4.5 % on the measurements. The temperature effect on the calibration measurements is considered to be very minimal as described in section (3.1.2).

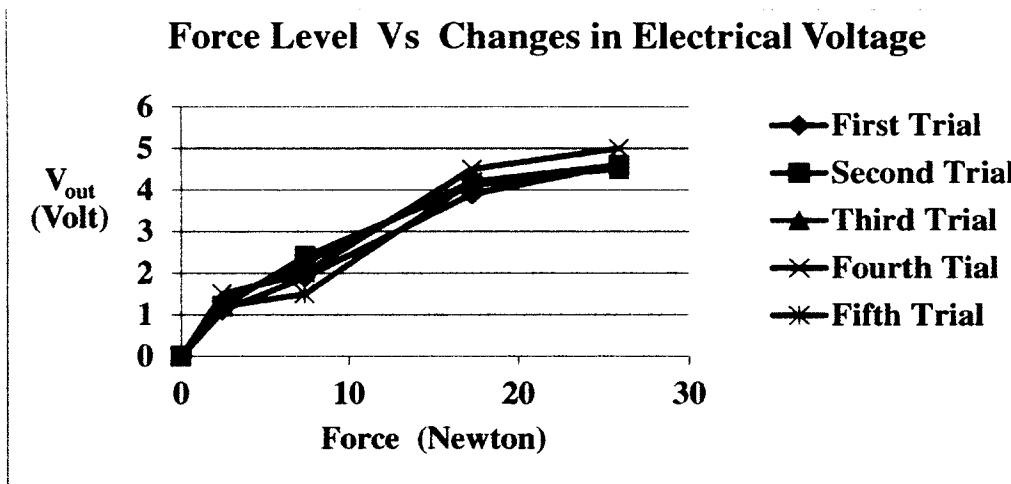


Figure 3.4. The calibration graph of the force sensor (FlexiForce, Model # A201, 25 lb range).

3.1.3 Bioimpedance Measurement System

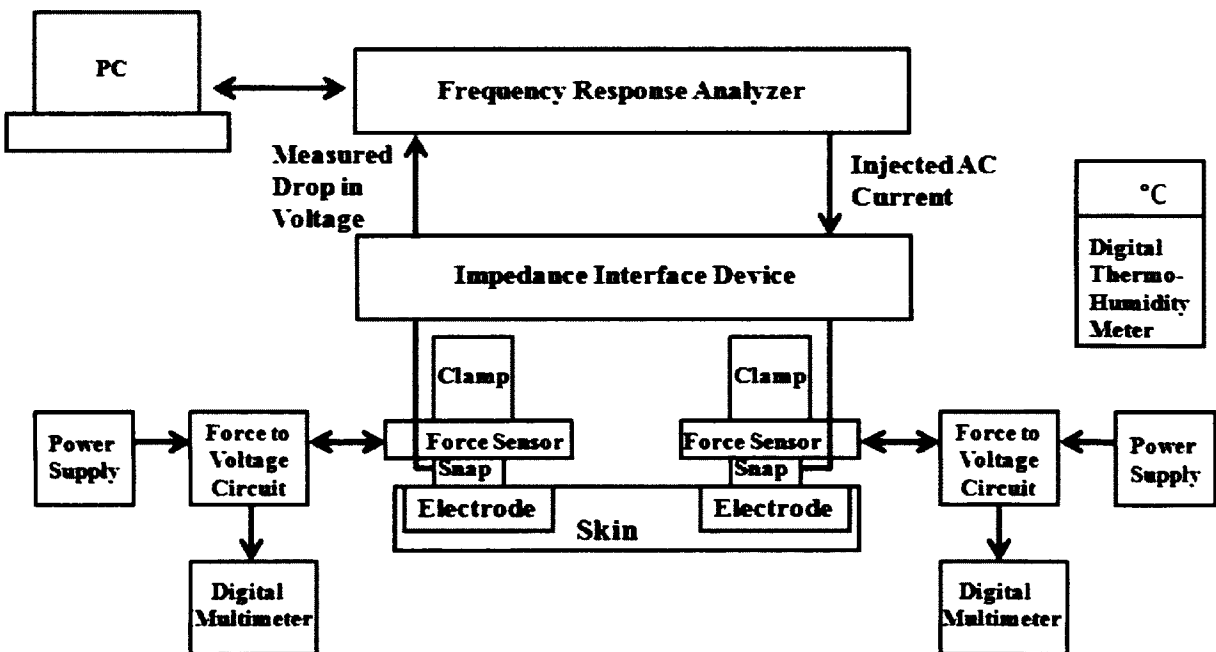


Figure 3.5. Block diagram of the experimental setup applied in this study.

A bioimpedance measurement system is used to measure the electrode-skin impedance in response to different frequencies and to an applied alternating electrical current in accordance with the safety standards (Figure 3.5).

The bioimpedance measurement system used in the study is consisted of a personal computer (PC) (Dell 390, Processor 3.0 GHz, Pentium 2, Win XP), frequency response analyzer (FRA) (Model # 1255B, Solartron Analytical, Farnborough, U.K.) and impedance interface device (Model # 1294A, Solartron Analytical, Farnborough, U.K.).

Impedance was measured from 1 Hz to 1 MHz (10 points per decade), averaging 20 cycles per frequency, applying an alternating electrical current of 100 μ A root mean square supply current. The applied alternating electrical current 100 μ A is in accordance with the safety standards [2]. 100 μ A is a low AC current value that would not harm the human body [2].

Each impedance measurement took approximately 6 min to complete. The expected change to occur for the electrode-skin impedance after the 6 min is passed is mainly a further decrease in impedance as a result of electrode settling and force effect on electrodes sites as described in the appendix (Section B2).

This bioimpedance system is set to measure the impedance of a sample (electrode-skin interface) by placing two electrodes on the arm and connecting the electrodes to the bioimpedance measurement system by shielded cables (a snap electrode lead for each electrode).

An electrical sinusoidal AC current (constant current of 100 μ A) with the frequency range between (1Hz – 1MHz) can be generated from FRA, in which the AC current can pass to impedance interface device and to the electrodes [1], [52]. The injected current will pass through the electrode-skin to measure the drop in voltage across the two electrodes.

The measured drop in voltage is returned back to FRA through impedance interface device to calculate the impedance of the sample (electrode-skin interface) by the system [1], [52]. The measured drop in voltage value over the injected AC current value will provide the impedance value.

The following sub-sections (3.1.3.1, 3.1.3.2, 3.1.3.3) describe the functions of each device used in the bioimpedance system. The following (Figures 3.6 – 3.8) show the experimental setup used in the study.



Figure 3.6. Experimental setup which consists of frequency response analyzer device (Model # 1255A, Solartron Analytical, Farnborough, U.K.) and impedance interface device (Model # 1294A, Solartron Analytical, Farnborough, U.K.). Two clamps (SL300 Quick-Grip, Irwin Tools, Huntersville, NC, U.S.A.).



Figure 3.7. Pair of Ag/AgCl electrodes placed on the ventral side of the forearm, with electrode snap leads, and FlexiForce sensors (Model # A201, 25 lb range, Tekscan, Boston, MA, U.S.A.).

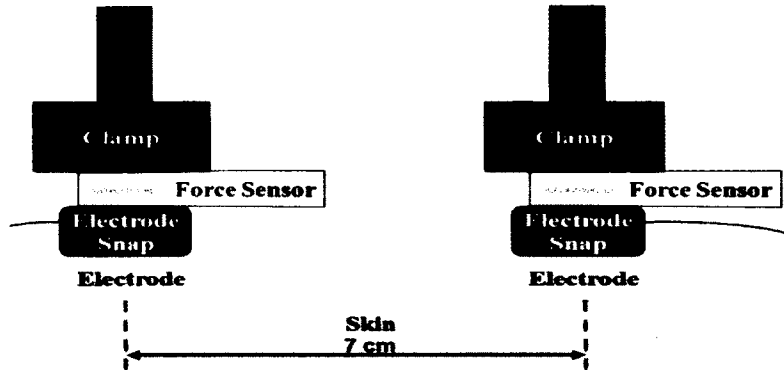


Figure 3.8. A simplified schematic diagram of the experimental set up.

3.1.3.1 Computer for Data Control Unit

A personal computer (PC) (Dell 390, Processor 3.0 GHz, Pentium 2, Win XP) is connected to the bioimpedance system. SmaRT software (Version 3.0.1, Solartron Analytical, www.solartronanalytical.com) is used to control the input data such as the supplied AC current value, frequency range, and the measurement bandwidth of the frequencies (number of cycles at each frequency). In addition, it is used for receiving the output data: impedance in ohm and phase degrees at each frequency point, Admittance magnitude, capacitance magnitude at each frequency point and the time each measurement it takes to complete.

3.1.3.2 Frequency Response Analyzer (FRA)

FRA device (Model # 1255B, Solartron Analytical, Farnborough, U.K.) (Figure 3.9) is connected to the PC to control its input data and to send its output data. It is also connected to impedance interface device. FRA important specifications are listed in Table 3.3 [53].

FRA can generate sinusoidal AC signal at wide controlled frequencies with an optional sweeping range (1 μ Hz - 1 MHz).

The sinusoidal AC signal is amplified through power amplifier and supplied to impedance interface device [1], [52].

Table 3.2. Specifications of the frequency response analyzer (1255 B)

AC Amplitude	0 to 3 V rms
Frequency range	10 μ Hz to 1 MHz
Maximum output current	± 100 mA peak
Common mode rejection	>50 dB
Output impedance	50 $\Omega \pm 1\%$

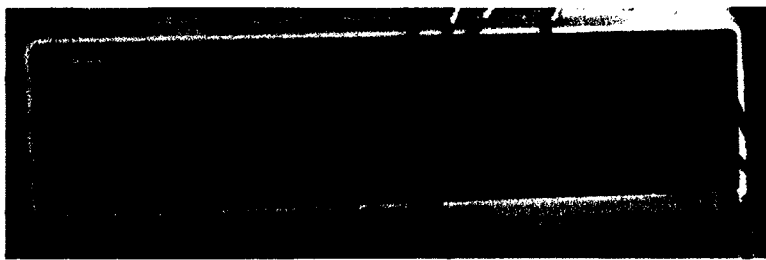


Figure 3.9. Frequency response analyzer device (Model # 1255B, Solartron Analytical, Farnborough, U.K.).

3.1.3.3 Impedance Interface Device

Impedance interface device (Model # 1294A, Solartron Analytical, Farnborough, U.K.) (Figure 3.10) is connected with frequency response analyzer device, and its important specifications are listed in Table 3.2 [54]. FRA is set to supply sinusoidal AC signal to impedance interface device as described in section (3.1.3.2). Impedance interface device is set to transfer sinusoidal AC signal to the measured sample (electrode-skin interface) and to send the measured drop in voltage signal from the electrode back to FRA [1], [52]. The signal passes the impedance interface device for many reasons. Impedance interface device is set to prevent disturbance to the supplied current and to the measured drop in voltage when it receives it back. A balanced generator system is implemented to minimize common mode voltages An adjustment in voltage is achieved with a grounded wire to allow for regaining the balance back, such improving the common mode rejection. Impedance interface device is capable of

converting a current to a voltage [1], [52]. An attenuator is included in the device to adjust the impedance associated with the output voltage by forming constant impedance and improving the received signal strength. Also, the weak signals that are sent and received are protected by shield cables to protect the current from being disturbed by noise especially with very low current (1 pA) and voltage (1 µV) that could be fed into the device.

Table 3.3. Specifications of the impedance interface device (1294 A).

Maximum input voltage	10V peak
Output resistance	50 Ω
Amplifier gain	x1
Input resistance to ground	>1 GΩ
Common mode range	±10 V

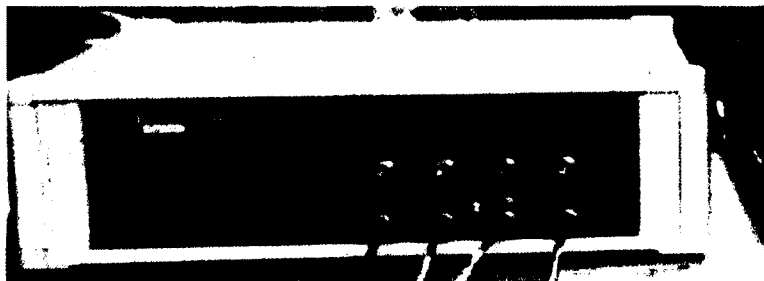
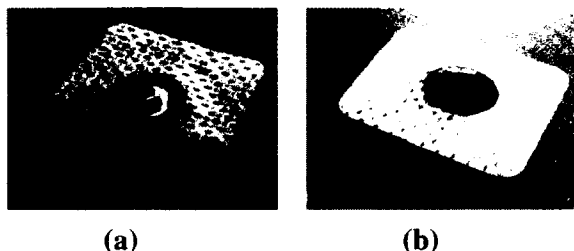


Figure 3.10. Impedance interface device (Model # 1294A, Solartron Analytical, Farnborough, U.K.).

3.2 Electrodes

Different surface electrode types were applied in this study. The applied electrodes used were pre-gelled wet surface silver/silver chloride (Ag/AgCl) electrodes (Model # FT002, MVAP II, Medical Supplies Inc., Newbury Park, CA, U.S.A.); that have a diameter of 1 cm (Figure 3.11). Dry surface Orbital electrodes (Model # ORI F6T, Orbital Research Inc, Cleveland, OH, U.S.A.), which have a diameter of 2.5 cm and penetrators (spikes) of a 150 µm length [55] (Figure 3.12) in addition to dry surface stainless steel (ST) electrodes (Model # EL12, Liberating Technologies, Inc (LTI), Holliston, MA, U.S.A.) which have a diameter of 1.42 cm and a height of 0.32 cm were also applied (Figure 3.13).



(a)

(b)

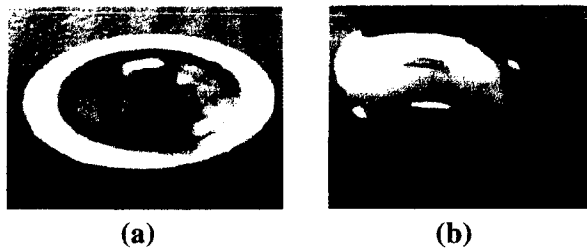
Figure 3.11. a) Ag/AgCl electrode (electrode's snap side). b) Ag/AgCl electrode (electrode's skin side).



(a)

(b)

Figure 3.12. a) Orbital electrode (electrode's snap side). b) Orbital electrode (electrode's kin side).



(a)

(b)

Figure 3.13. a) Stainless steel electrode (electrode's snap side). b) Stainless steel electrode (electrode's skin side).

3.2.1 Properties of Ag/AgCl Electrodes

Surface Ag/AgCl electrodes are the most common and favoured electrodes in clinical measurements for recording biological signals such as ECG, EMG and EEG [1], [2], [27]. The preference of Ag/AgCl electrodes over many electrode types is due to their properties. One of the main advantages of using Ag/AgCl electrodes is the low noise level it generates during biological signals recording [10], [27]. Ag/AgCl electrodes generate low electrode-skin interface impedance [1], [22], [56], [57], [58], and lower electrode-skin interface impedance

value than stainless steel electrodes [1], [18]. Ag/AgCl electrodes are considered as non-polarizable electrodes; the non-polarizable nature of Ag/AgCl electrodes allows the charges to cross the electrode-electrolyte interface [1], [2], [37].

3.2.2 Properties of Orbital Electrodes

Dry polarizable Orbital electrodes are made to last longer than the common clinical wet electrodes such as non-polarizable Ag/AgCl [55]. Orbital electrodes help to minimize the motion artifacts as the spikes at the electrode surface make tight contact with skin and, thus, prevent the movements of the electrode during the recording period [55]. Orbital electrode's coat is made of a mixture of metals: silver/silver chloride, aluminum, gold/gold chloride, nickel and titanium [55]. The Orbital Research Inc. stated that the main advantages of applying Orbital electrodes are the elimination for the need for skin preparation and an electrolyte gel application during the biological signal recording period [55].

The shape of Orbital electrode makes it more in contact with the skin than the case with regular flat stainless steel or surface Ag/AgCl electrodes. This is due to the presence of penetrators (spikes) with a height off approximately 150 µm, which allow the Orbital electrode to penetrate deeper into the stratum corneum layer that dominates the skin's surface and thus facilitates the pathways for biopotential through the skin to the Orbital electrode (Figures 3.12 and 3.14) [31], [55]. Stratum corneum has a high resistance to biopotentials and to electrical current due to the presence of dead skin cells [1], [2], [24], [27]. The application of Orbital electrode can overcome this problem by the presence of spikes [31], [55].

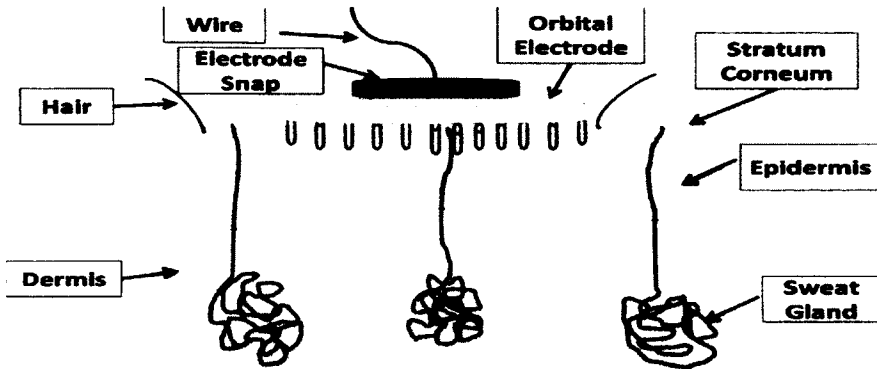


Figure 3.14. Orbital electrode's penetration into the skin layers during biosignal recording.

3.2.3 Properties of Stainless Steel Electrodes

Dry electrodes such as stainless steel electrodes are classified as polarizable electrodes [1], [18], [48]. Ragheb and Geddes [18] tested different electrode materials such as copper, rhodium, silver, palladium, aluminum and stainless steel. Their research was based on measuring the electrode-electrolyte interface impedance at frequencies range from 1 Hz – 1 MHz. The results showed that aluminum electrode had the highest impedance followed by stainless steel electrode in a range of $30 - 75 \text{ k}\Omega$ at low frequency range 100 Hz whereas copper and silver electrodes had the lowest impedance of about $10 \text{ k}\Omega$ at 100 Hz [18]. Ragheb and Geddes research [18] anticipated that the surface stainless steel electrodes would generate higher electrode-skin interface impedance than the other electrode's types. Furthermore, polarizable electrodes such as surface stainless steel electrodes are known to be reusable electrodes due to their resistance to corrosion [1].

3.3 Data Collection

This study was reviewed and approved by Carleton University Research Ethics Committee, approval # 12-0350.

Subject information, including height, weight and body mass index (BMI) are reported in each part of the study. Nine different subjects were participated in the study in which each experiment was conducted on five subjects and the same subject could participate in different experiments. The room temperature and humidity were recorded by digital thermo-humidity meter (Model # 91588CTC, Springfield, China) before conducting any measurements.

3.3.1 Electrodes Placement

Two electrodes from the same type were placed on the ventral side of the right forearm, spaced 7 cm apart, with the distal electrode approximately 11 cm from the wrist. This common configuration is used because the measured impedance would include the entire desired electrode-skin impedance value (Section 3.4) [1], [5]. It evaluates the effect of force on the whole electrode-skin impedance value. The electrodes were placed on a convenient place (ventral side of the right forearm) for better comfort when applied to subjects. Other configurations such as the four electrodes system is not applied in this study because it is used to measure the underling skin tissue impedance and not the entire electrode-skin impedance [1], [5].

3.3.2 Application of Force

Exerting an external force on electrodes sites was made through two clamps as stated in section 3.1.1. Different force levels were exerted on the electrodes sites to determine their impact on electrode-skin interface impedance measurements. The three force levels that were applied are as follow: 0 N (0 lb) (no externally applied force), 8.9 N (2 lb) and 22.2 N (5 lb). The application of an external force on electrodes sites was started at 0 N followed by

an increase to 8.9 N and 22.2 N then, returning back to 8.9 N and 0 N in order to examine any hysteresis effect.

3.4 Electrode-Skin Impedance Circuit Model

The bioimpedance measurements were performed by applying two electrodes on the ventral side of the right forearm spaced 7 cm apart (section 3.3.1). Figure 3.15 is a schematic of the measured impedance, consisting of two electrode-skin interfaces and the impedance associated with the underlying tissue.

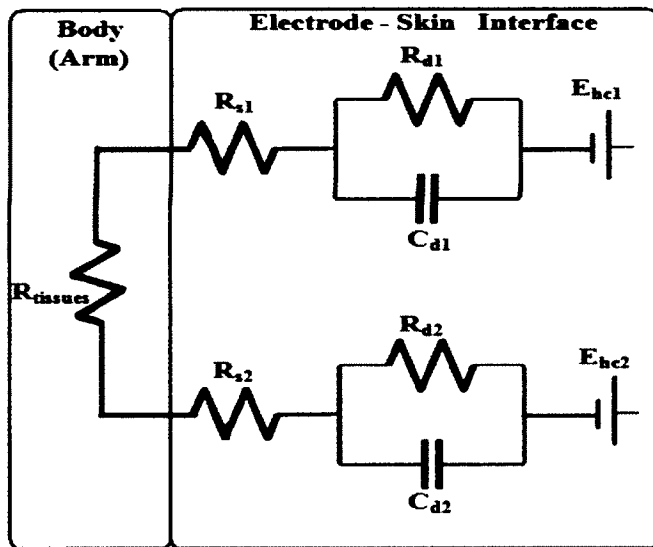


Figure 3.15. The simplified schematic diagram for the electrodes system used in the study.

In order to determine the impedance associated with the electrode-skin interface, two assumptions are made: 1) the electrode-skin interfaces are identical for the two electrodes (i.e., $C_d=C_{d1}=C_{d2}$, $R_d=R_{d1}=R_{d2}$, and $R_s=R_{s1}=R_{s2}$), and 2) $R_{tissues}$ is assumed to be negligible (i.e., $R_{tissues} = 0$). The first assumption is reasonable, if the two electrodes are the same (e.g., identical

size, identical material, produced from the same manufacture). For the second assumption, the value of $R_{tissues}$ is generally small relative to the impedance value of the electrode-skin interface in the frequencies of interest (biosignals measurements is mainly contained in the low frequency region, generally below 500 Hz). The impedance value for healthy human arm's tissue is found to be less than 500Ω [12], while the impedance value for electrode-skin interface can be larger than $1 M\Omega$ [4]. If the electrode-skin impedance is high, the effect of $R_{tissues}$ will be negligible. The effect of assuming $R_{tissues} = 0$ is that its contributions to the total measured impedance will be included in the R_s estimate (i.e., the estimate of R_s would be equal to $R_s + R_{tissues} / 2$, where R_{tissue} is divided by two electrodes).

The following formula (3.2) is the impedance for the electrode-skin interface for a single electrode.

$$Z_e = R_s + \frac{R_d}{1 + j2\pi f C_d R_d} \quad (3.2)$$

where f is the frequency (Hz).

3.4.1 MATLAB Implementation for Estimating Electrode Circuit Components values.

In this study, a least squares nonlinear curve fitting method is applied using MATLAB (MATLAB version 7.7, R2008b, MathWorks Inc., Massachusetts, U.S.A., 2008) to estimate the electrode circuit model components (R_s , R_d , and C_d) values. The complete MATLAB code is provided in Appendix A.1.

Least squares nonlinear curve fitting determines the optimized best fit impedance model, in terms of total square difference from the measured impedance values. Impedance has both real

and complex values (3.2). Only the absolute value of the impedance is considered in this least squares nonlinear curve fitting method.

In order to determine the impedance values for a single electrode-skin's site, the measured impedance values are divided by two, as there are two electrodes used in the measurements [48], [59]. The measured electrode-skin impedance values (Z) and the frequencies values (f) are provided by the bioimpedance measurement system. Curve fitting is performed in a logarithmic scale. The following code is used to convert the impedance and frequency into the log domain.

MATLAB Code:

```
LogF = log10(f);  
LogZ = log10(Z);
```

The impedance function (3.2) is needed in least squares nonlinear curve fitting method to estimate the electrode circuit components values. The MATLAB code for the impedance formula (3.2) is provided in the Appendix (Section A.1.2).

An initial estimate for circuit model components values (R_s , R_d , and C_d) are needed to start the least squares curve fitting process.

The impedance value at high frequencies approaches the value of R_s [1], [5] (Section 2.5.1). The highest frequency measured in this study is at 1 MHz. R_s is initialized to the impedance measured at 1 MHz, which is the last recorded impedance value.

MATLAB Code:

```
Rs0 = Z(length(Z));
```

At low frequencies, the impedance value approaches $R_d + R_s$ (Section 2.5.1). The lowest frequency used in this study is 1 Hz. Using the initial R_s value, we can subtract it from the estimated value of $R_s + R_d$ to obtain an initial estimate of R_d .

MATLAB Code:

```
Rd0 = (Z(1) - Rs0);
```

C_d value can be determined from the corner frequency (Section 2.5.1). However, the corner frequency may be hard to determine. An initial arbitrarily value for C_d (1 nF) was chosen.

MATLAB Code:

```
Cd0 = 1e-9;
```

Using the initial circuit components values (R_{s0} , R_{d0} , and C_{d0}) which are stored in the variable `circuitParameter0` and the impedance function (3.2), an optimal estimate for R_s , R_d , and C_d values can be determined by applying the `(lsqcurvefit)` function.

MATLAB Code:

```
[curCircuitParameter, curResnorm] =
    lsqcurvefit(@logElectrodeSkinImpedance,circuitParameter0,logF,logZ,[0
    0 0],[inf inf inf]);
```

The `lsqcurvefit` function outputs the residual error (`resnorm`) associated with the estimated circuit components (R_s , R_d and C_d) values.

Least squares curve fitting can be sensitive to the initial value of C_{d0} and may result in finding local minima. To help avoid this, a brute force search is performed using alternative initial

values of C_{d0} between 1 fF and 10 μ F (100 initial values are chosen within this range, logarithmically spaced). For each iteration, the model with the lowest residual error is retained.

MATLAB Code:

```
N = 100;  
Cd0 = logspace(-15, -5, N);  
  
for i = 1:N  
    Rs = Rs0;  
    Rd = Rd0;  
    circuitParameter0 = [Rs Rd Cd0(i)];  
    [curCircuitParameter, curResnorm] =  
        lsqcurvefit(@logElectrodeSkinImpedance, circuitParameter0, logF, logZ,  
        [0 0 0], [inf inf inf]);  
    if curResnorm < resnorm  
        circuitParameter = curCircuitParameter;  
    end
```

The least squares curve fitting method for estimating the electrode circuit model component values was validated (Appendix A.3).

4 Effect of Externally Applied Force on Electrode-Skin Impedance for Ag/AgCl Electrodes with and without Electrolyte Gel

4.1 Introduction

Surface silver/silver chloride (Ag/AgCl) electrodes are known as the “universal electrodes” for biological signals measurements [1], [37]. The use of surface Ag/AgCl electrodes is high due to their high quality performance in clinical measurements for recording biological signals, such as ECG, EMG and EEG. Ag/AgCl electrodes are considered non-polarizable electrodes [1], [2], [60] (see section 2.1 and section 3.2.1 for more information regarding non-polarizable electrodes and Ag/AgCl electrodes, respectively). Ag/AgCl electrodes measurements are generally performed with an electrolyte gel. The presence of an electrolyte gel reduces the electrode-skin interface impedance and motion artifacts [4], [12], [25], [33]. Electrolyte gel can penetrate into the skin through the pores that are located at the stratum corneum layer, hydrating the stratum corneum layer and providing a better conductive environment for the charges to be transferred to electrodes [2], [60]. It can also fill up the wrinkles that exist on the skin resulting in better electrodes contact with the skin and lower electrode-skin impedance [2], [12], [33]. The application of an electrolyte gel can help in reducing noise in biological signal recordings [1], [34], [61].

The purpose behind this study is to analyze the effect of an externally different applied force levels and electrolyte gel on electrode-skin impedance. An equivalent circuit model representing the electrode-skin interface is used in this analysis. Pregelled surface Ag/AgCl electrodes and Ag/AgCl electrodes without electrolyte gel are used in this study.

It is anticipated that the effect of an external force level on the electrode-skin impedance for pregelled Ag/AgCl electrodes to be marked by a decrease in electrode-skin impedance. The

presence of electrolyte gel and the increase in contact strength between electrodes and skin (increase in contact area) would cause the decrease in impedance values [9], [33]. For electrode circuit components values, it is expected an increase in C_d values, a decrease in R_d values and a decrease in R_s values (Section 2.6). The increase in force level is anticipated to be associated with further decrease in electrode-skin impedance, further increase in C_d values and further decrease in R_d and R_s values and vice versa with the decrease in force level except R_s values will continue to decrease as sweat secretion will stay active.

The second part of this chapter is done to determine the reason behind the unexpected fluctuations in electrode-skin impedance obtained with pre-gelled Ag/AgCl electrodes. The second experiment is designed to follow the same exact procedures as in the first part, except without applying an electrolyte gel.

The anticipated results for the effect of an external force on the electrode-skin impedance for Ag/AgCl electrodes without electrolyte gel would be a decrease in electrode-skin impedance values and elimination for any fluctuations in impedance values. For electrode circuit components values, it is expected an increase in C_d values, a decrease in R_d values and a small decrease in R_s values since the sweat will be the only electrolyte to be present in these measurements.

4.2 Materials and Methods

The equipment and experimental setup used in this section are generally the same as described in chapter three. Additional materials and procedures used in this study are described in the following sections.

4.2.1 Experimental Setup

Disposable, pregelled Ag/AgCl surface electrodes (Model # FT002, MVAP II, Medical Supplies Inc., Newbury Park, CA, U.S.A.), which have a diameter of 1 cm were used in the first part of the study (Figure 3.11). New pregelled Ag/AgCl surface electrodes were applied on every subject. In the second part of the study, the pregelled Ag/AgCl surface electrodes were modified to be used without electrolyte gel. The electrolyte gel was removed from the Ag/AgCl electrodes by rubbing the electrode's surface with a fabric. New Ag/AgCl electrodes without electrolyte gel were applied on each subject. The schematic diagram of pregelled Ag/AgCl electrode-skin contact area is different from electrodes without electrolyte gel (Figure 3.10) used in this study due to the presence of an electrolyte gel (Figure 4.1).

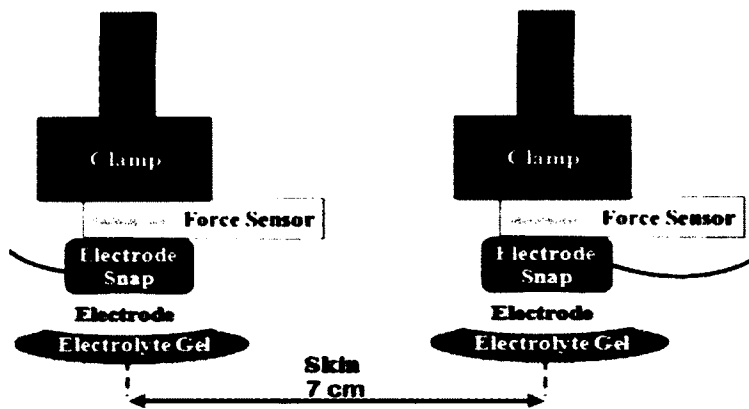


Figure 4.1. Experimental setup using pregelled Ag/AgCl electrodes.

4.2.2 Data Collection

Information regarding the subjects in the pregelled Ag/AgCl and Ag/AgCl without electrolyte gel studies is contained in Table 4.1 and Table 4.2, respectively. Measurements were conducted on different days on the same subjects, except the fifth subject who is different in both studies. The formula applied for calculating the body mass index (BMI) can be found in

appendix A. Skin preparation was not performed in this study. The room temperature and humidity were measured as 22°C and 32%, respectively.

Table 4.1. Information of subjects in the pregelled Ag/AgCl electrodes study.

Subject	Height (cm)	Weight (kg)	Body Mass Index	Age	Gender
Ag/AgCl-G-S1	163	68	25.6	25	Male
Ag/AgCl-G-S2	174	78	26.1	28	Male
Ag/AgCl-G-S3	172	80	27.0	29	Male
Ag/AgCl-G-S4	168	65	22.9	29	Male
Ag/AgCl-G-S5	170	65	22.5	27	Male

Table 4.2. Information of subjects in the Ag/AgCl electrodes without electrolyte gel study.

Subject	Height (cm)	Weight (kg)	Body Mass Index	Age	Gender
AgCl-No-G-S1	163	68	25.6	25	Male
AgCl-No-G-S2	174	78	26.1	28	Male
AgCl-No-G-S3	172	80	27.0	29	Male
AgCl-No-G-S4	168	65	22.9	29	Male
AgCl-No-G-S5	175	67	21.9	24	Male

4.3 Results

4.3.1 Responses of Electrode-Skin Impedance to Externally Different Applied Force Levels for Pregelled Ag/AgCl Electrodes

Changes in electrode-skin impedance for all subjects were observed in response to applied forces (Figure 4.2). The general trend observed was a decrease in electrode-skin impedance with increasing force applied to electrodes sites, as observed for subjects Ag/AgCl-G-S3 to

Ag/AgCl-G-S5. For subjects Ag/AgCl-G-S4 and Ag/AgCl-G-S5, the majority of the decrease occurred with the initial application of force (8.9 N – 6 min). A smaller decrease occurred when the force was increased (22.2 N) and the impedance remained relatively unchanged as the force was removed. Subject Ag/AgCl-G-S3, exhibited a similar trend, except for a small decrease in impedance that was observed when the force was initially decreased to (8.9 N – 18 min).

The results for subjects Ag/AgCl-G-S1 and Ag/AgCl-G-S2 were inconsistent. At low frequencies, the effect of a high force level (22.2 N) caused higher impedance for subject Ag/AgCl-G-S1, while it caused lower impedance for subject Ag/AgCl-G-S2. At high frequencies, the effect of a high force level (22.2 N) caused lower impedance for subject Ag/AgCl-G-S1, while it caused higher impedance for subject Ag/AgCl-G-S2.

For all subjects, the lowest impedance was observed when the force was removed from the electrodes sites (0 N – 24 min), except at high frequencies for Ag/AgCl-G-S1. A hysteresis effect was present with all the subjects; the electrode-skin impedance at the beginning of the measurements (0 N – 0 min) was not the same as at the end of the measurements (0 N – 24 min), despite both having no externally applied force.

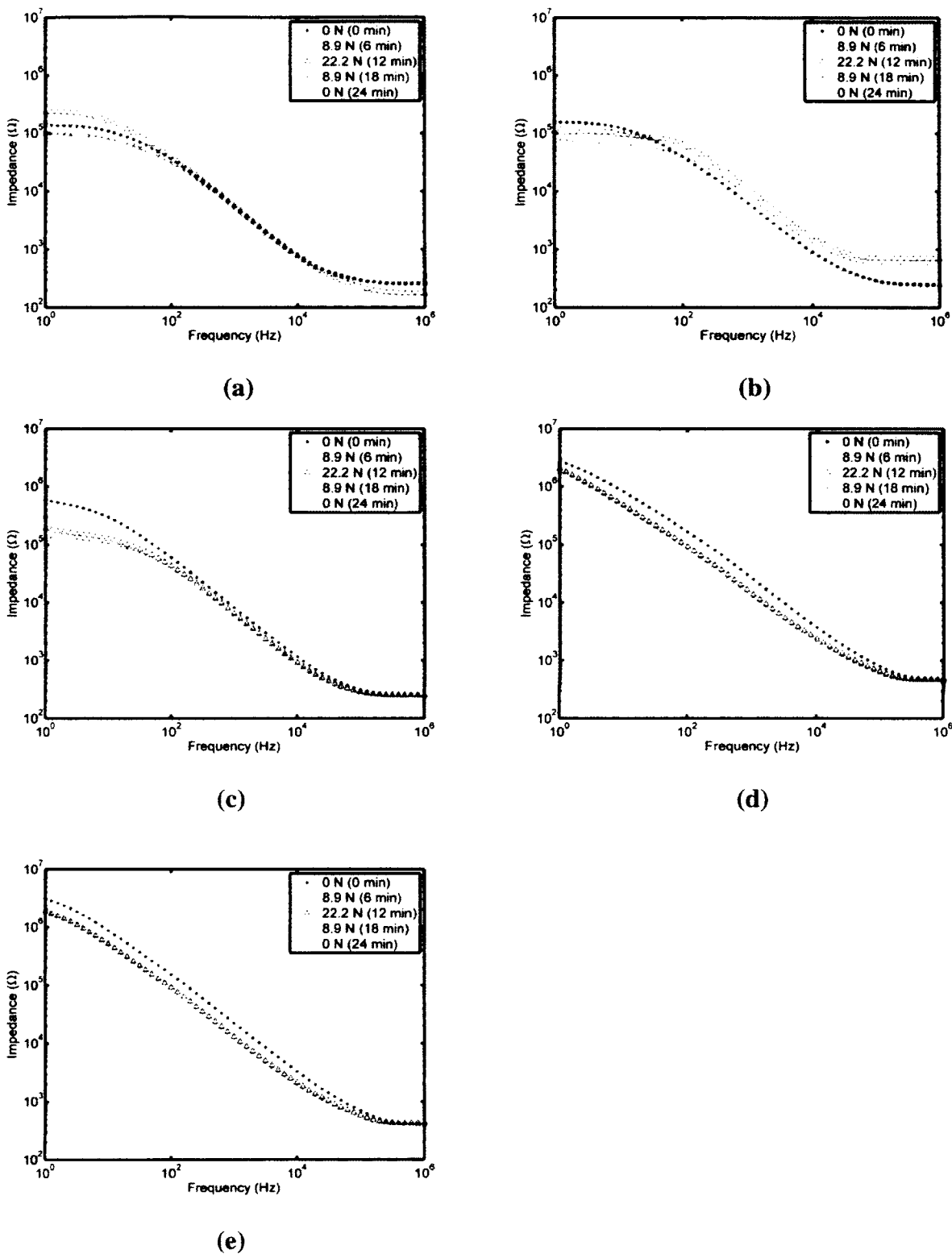


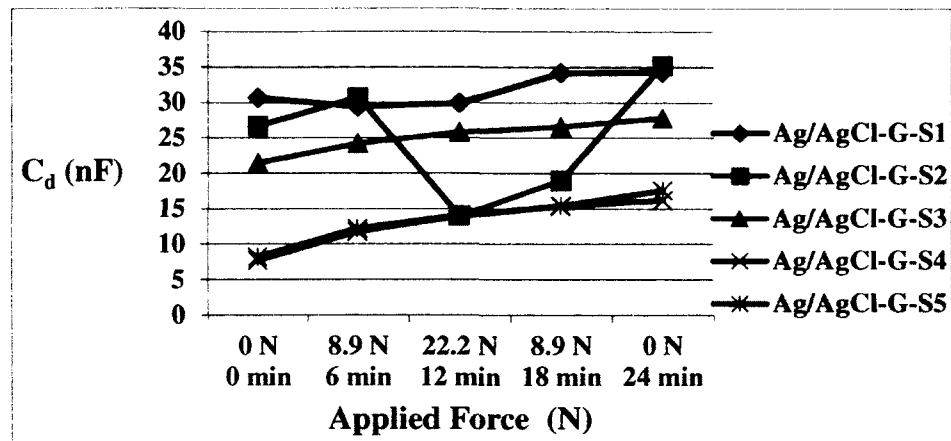
Figure 4.2. Pregelled Ag/AgCl electrode-skin impedance frequency response to externally different applied force levels for the five subjects: (a) Ag/AgCl-G-S1, (b) Ag/AgCl-G-S2, (c) Ag/AgCl-G-S3, (d) Ag/AgCl-G-S4 and (e) Ag/AgCl-G-S5. Times in parentheses indicate the approximate start time of the impedance measurement.

4.3.2 Results of Equivalent Circuit Model Components Values for Ag/AgCl Electrode-Skin Interface under the Influence of an External Force and an Electrolyte Gel.

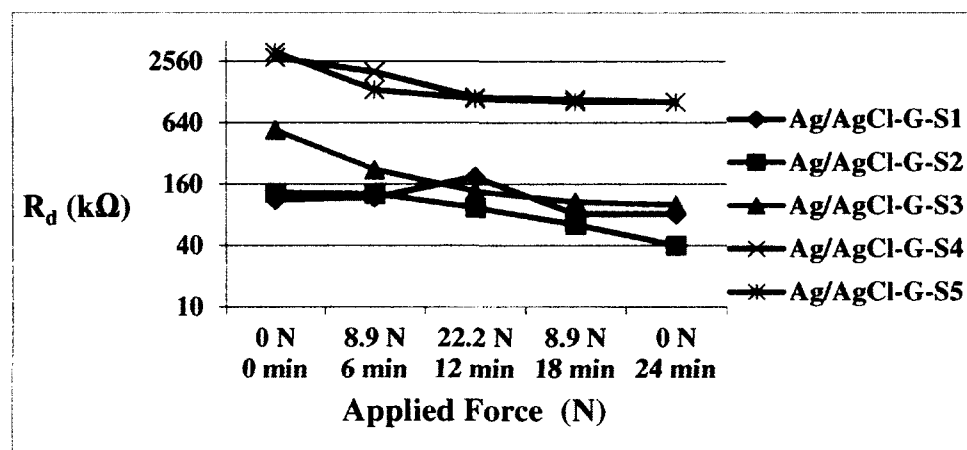
The estimated values for the electrode circuit model components (C_d , R_d and R_s) are available in appendix B, Tables B.1, B.2 and B.3 for all subjects.

For C_d values, the general trend was an increase with force application and a further increase when the force was removed (Figure 4.4a). This behaviour was observed in all the subjects except for subject Ag/AgCl-G-S1, who did not exhibit a change in C_d values when the force was applied, and subject Ag/AgCl-G-S2, where there was a sudden decrease in C_d value at 22.2 N, which remained low when the force was decreased to 8.9 N. For all subjects, C_d values were at highest at the end of the force loading/unloading cycle (0 N – 24 min). The average percentage increase in C_d values across all subjects between initial state and final state was 57.4% (Table 4.3), sample calculation for percentage changes of C_d is available in (Section A.5).

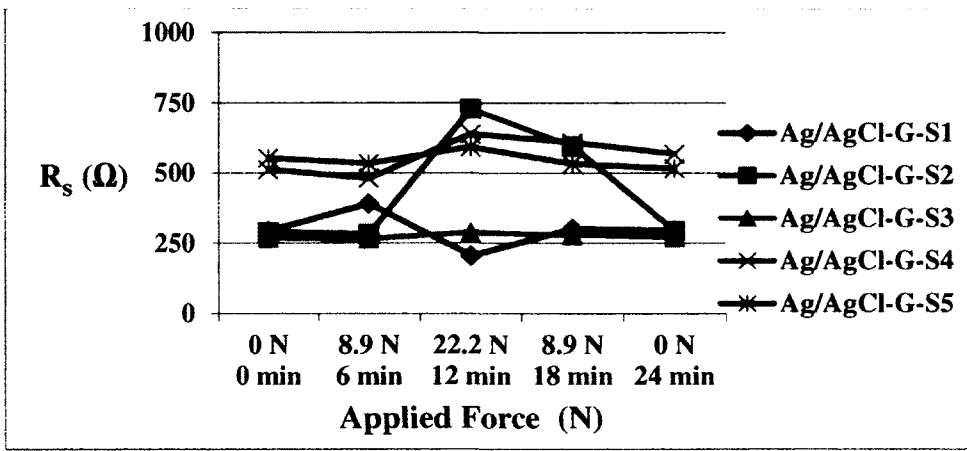
R_d values decreased with increasing force level in all subjects except an increase from 8.9 N to 22.2 N for subject Ag/AgCl-G-S1 (Figure 4.3b). A further decrease in R_d values was observed as the force was removed, although the change in impedance was generally smaller as compared to the change observed when the force was applied. The lowest R_d values were observed at the end of the force loading/unloading cycle (0 N – 24 min). The average percentage decrease in R_d values across all subjects between initial state and final state was 55.5% (Table 4.3). There was not a consistent trend observed for R_s values during the force loading/unloading (Figure 4.3c).



(a)



(b)



(c)

Figure 4.3. Pregelled Ag/AgCl electrode's circuit model components values under the influence of force loading/unloading for the five subjects: (a) C_d , (b) R_d , and (c) R_s .

Table 4.3. Percentage increases in circuit model components values between initial state and final state of measurement cycle for pregelled Ag/AgCl electrodes sites (values in brackets indicate a decrease).

Circuit Model Components	Subjects					Average
	Ag/AgCl-G-S1	Ag/AgCl-G-S2	Ag/AgCl-G-S3	Ag/AgCl-G-S4	Ag/AgCl-G-S5	
C _d	11.7%	31.7%	32.0%	109.6%	102.1%	57.4%
R _d	(28.0%)	(69.5%)	(76.4%)	(54.8%)	(48.6%)	(55.5%)
R _s	0.2%	1.4%	(9.4%)	1.6%	(6.7%)	(2.6%)

R_s values varied inconsistently among the subjects. A large change in R_s value was observed in subject Ag/AgCl-G-S2 at 22.2 N and 8.9 N (18 min). The average percentage decrease in R_s values across all subjects between initial state and final state was 2.6% (Table 4.3). Note that the estimate of R_s, includes any contribution from R_{tissues} (Section 3.4). As such, the percentage changes reported for estimated R_s will be smaller than the actual changes in R_s.

4.3.3 Responses of Electrode-Skin Impedance to Externally Different Applied Force Levels for Ag/AgCl Electrodes without an Electrolyte Gel

Noticeable changes in electrode-skin impedance for all subjects were observed in response to applied forces to Ag/AgCl electrodes without electrolyte gel (Figure 4.4). The general trend observed was a decrease in electrode-skin impedance with increasing force applied to electrodes sites. A large drop in electrode-skin impedance was observed after the addition of 8.9 N for all subjects (Figure 4.4). A smaller decrease occurred when the force level was increased to 22.2 N. The impedance remained relatively unchanged as the force level was decreased. For all subjects, the lowest impedance was observed when the force was removed from the electrodes sites (0 N – 24 min). A hysteresis effect was present with all the subjects; the electrode-skin impedance at the beginning of the measurements (0 N – 0 min) was different than at the end of the measurements (0 N – 24 min), despite both having no externally applied force.

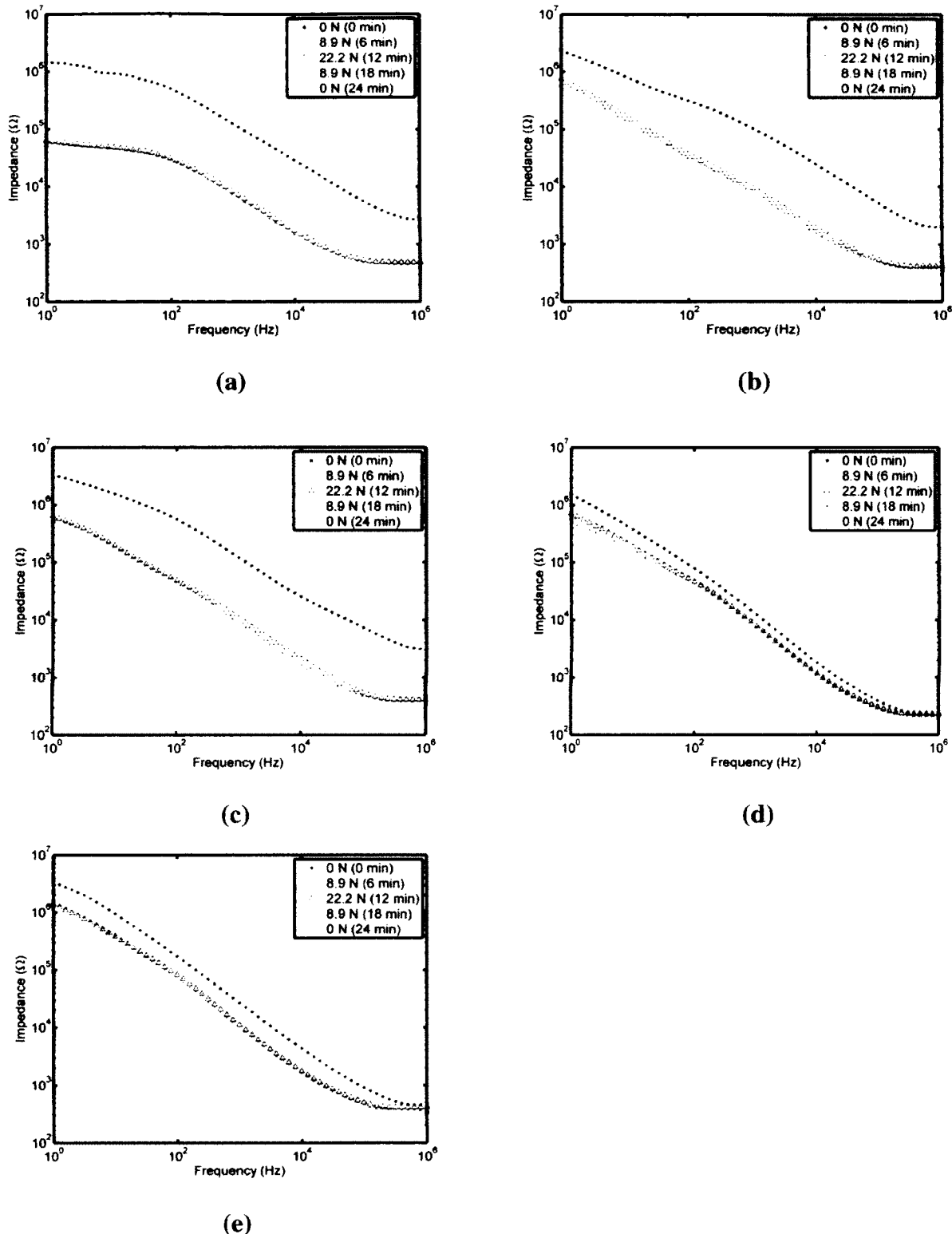


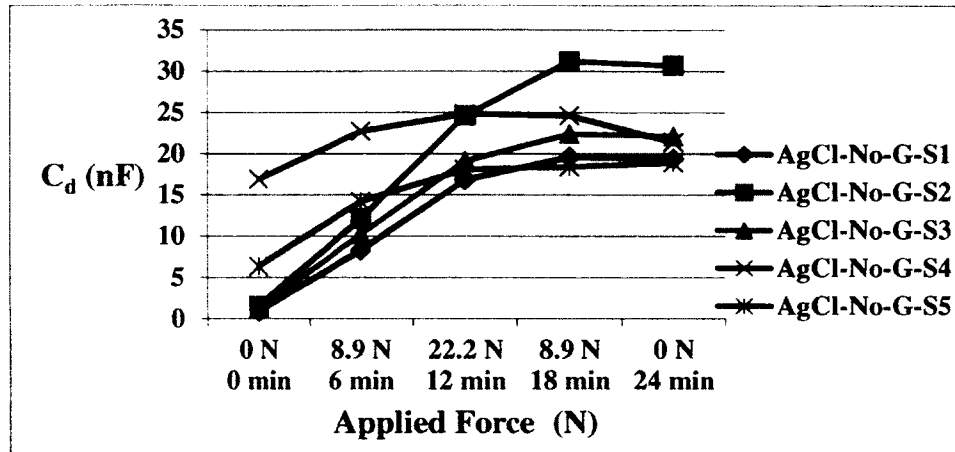
Figure 4.4. Ag/AgCl electrode-skin impedance frequency response to externally different applied force levels for the five subjects without electrolyte gel: (a) AgCl-No-G-S1, (b) AgCl-No-G-S2, (c) AgCl-No-G-S3, (d) AgCl-No-G-S4 and (e) AgCl-No-G-S5. Times in parentheses indicate the approximate start time of the impedance measurement.

4.3.4 Results of Equivalent Circuit Model Components Values for Ag/AgCl Electrode-Skin Interface without Electrolyte Gel under the Influence of an External Force.

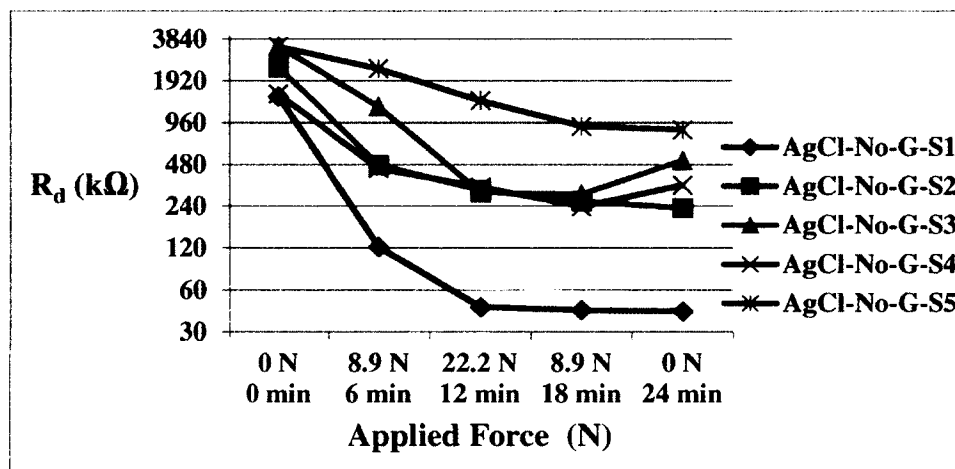
The results showed an increase in C_d values with increasing force levels (Figure 4.5a). A further increase was observed when the force was reduced from 22.2 N to 8.9 N, but no change when the force was further reduced to 0 N, except for subject AgCl-No-G-S4, where no change was observed when the force was reduced from 22.2 N to 8.9 N and a decrease in C_d value occurred when the force was further reduced to 0 N. The average percentage increase in C_d values across all subjects between initial state and final state was 1207.6% (Table 4.4).

The sharp decrease in R_d values occurred after the addition of the first force level 8.9 N on electrodes sites and it continued to decrease at higher force level 22.2 N (Figure 4.5b). The low R_d values were relatively maintained during force unloading, except for an increase when the force was reduced from 8.9 N to 0 N in subjects AgCl-No-G-S3 and AgCl-No-G-S4. The average percentage decrease in R_d values across all subjects between initial state and final state was 85% (Table 4.4).

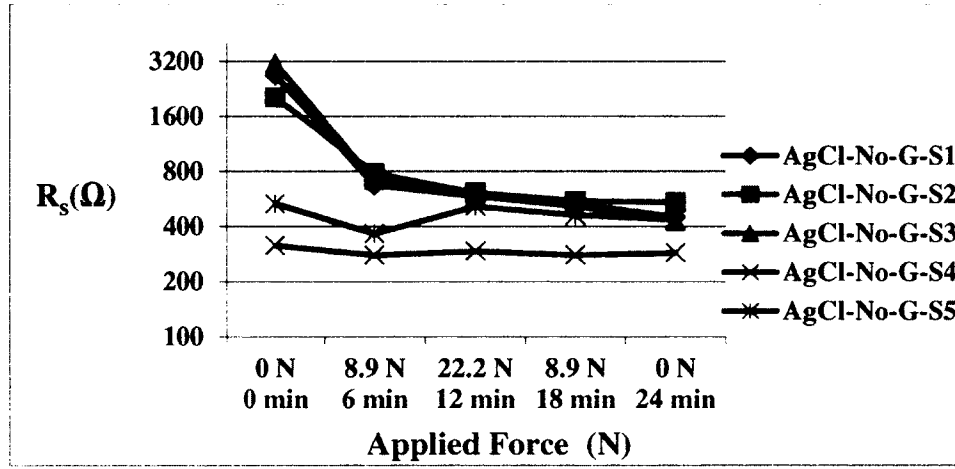
A steep decrease in R_s values occurred after the addition of the first force level 8.9 N on electrodes sites for subjects AgCl-No-G-S1 to AgCl-No-G-S3 (Figure 4.5c); R_s values decreased slightly as force was further increased and then removed. R_s values remained relatively unchanged for subject AgCl-No-G-S4 and AgCl-No-G-S5 during the force loading/unloading cycle. The average percentage decrease in R_s values across all subjects between initial state and final state was 54% (Table 4.4).



(a)



(b)



(c)

Figure 4.5. Ag/AgCl without electrolyte gel electrode's circuit model components values under the influence of different force levels for the five subjects. (a) C_d , (b) R_d and (c) R_s .

Table 4.4. Percentage increases in circuit model components values between initial state and final state of measurement cycle for Ag/AgCl electrodes sites without electrolyte gel, (values in brackets indicate a decrease).

Circuit Model Components	Subjects					Average
	AgCl-No-G-S1	AgCl-No-G-S2	AgCl-No-G-S3	AgCl-No-G-S4	AgCl-No-G-S5	
C_d	2132.5 %	1933.1 %	1742.7 %	26.6 %	199.1 %	1206.8 %
R_d	(97.1 %)	(90.3 %)	(84.9 %)	(77.8 %)	(74.8 %)	(85.0 %)
R_s	(83.2 %)	(73.2 %)	(86.3 %)	(9.0 %)	(18.2 %)	(54.0 %)

4.4 Discussion

As explained in section 2.6, a decrease in electrode-skin impedance was anticipated with increasing force [43]. Electrolyte gel has the ability to adapt to the skin's surface by filling up the skin wrinkles, enhancing the electrode-skin contact area and thus lowering electrode-skin impedance [2], [4], [25], [38], [39]; an applied force could result in such redistribution of electrolyte gel. This redistribution of electrolyte gel could remain, even when the applied force is removed; this is consistent with the sustained decrease in electrode-skin impedance that was observed. Moreover, exerting a force on the electrodes sites could result in more secretion of sweat, which could also be attributed to a decrease in electrode-skin impedance [62]. The hypothesis of an increase in contact strength between electrodes and skin, such increasing in effective electrode contact area is consistent with the increase in C_d values (section 2.6.1) and decrease in R_d values (section 2.6.2) that observed for Ag/AgCl with and without electrolyte gel. A decrease in the distances that separate the skin layers caused by the applied force could attribute to the observed increase in C_d values (section 2.6.1).

Results for subjects Ag/AgCl-G-S1 and Ag/AgCl-G-S2 were unexpected. Exerting a large force on the electrodes sites could result in the electrolyte gel being redistributed away from the electrodes sites, which would result in a higher impedance level. In [43], such redistribution

was used to explain an increase in electrode-skin impedance, observed in recessed electrodes that employed electrolyte gel. It was hypothesized in these results that the electrolyte gel was redistributed from underneath the electrode, due to the applied force, which led to the increased electrode-skin impedance. The fluctuations in R_s values in Figure 4.3c would support this hypothesis, as R_s is associated with the impedance of the electrolyte gel. The decrease in C_d value that was occurred for subject Ag/AgCl-G-S2 at 22.2 N can be associated with the electrolyte gel being redistributed away from electrode-skin contact area (Figure 4.3a).

As already indicated, increased sweat activity could account for decreases in impedance [62]. Sweat activity varies among subjects, which could help explain the observed inconsistencies, as that was apparent to be a result of other differences among subjects (e.g., skin type). For Ag/AgCl electrodes without electrolyte gel, a redistribution of electrolyte gel away from the electrodes sites is not possible, which could explain why these results were more consistent across subjects.

The initial electrode-skin impedance values for pregelled Ag/AgCl electrodes were lower than Ag/AgCl electrodes without electrolyte gel. As expected, exerting a force of 8.9 N on Ag/AgCl electrodes without electrolyte gel had decreased the electrode-skin impedance by a larger amount compared to pregelled Ag/AgCl electrodes. The force likely causes the Ag/AgCl electrodes without electrolyte gel to be in better contact with skin. Increasing the force level to 22.2 N improved the electrode-skin contact area, thus resulting in a further decrease in electrode-skin impedance [9], [42], [43].

The impedance did not return to initial value when force was removed from electrodes sites (0 N- 24 min). The reasons behind this hysteresis effect could be attributed to the long term effect of force on skin deformation, sweat accumulation with time and electrode settling

(section B2). Skin deformation causes the separation distance between the double layer charge that formed between electrodes and skin (section 2.6) to stay small until the skin retains back to its original state. The results in Figure 4.5 and (Appendix B) show relatively stable values for C_d , R_d and R_s at 0 N-24 min. For Ag/AgCl electrodes without electrolyte gel, the elapsed time and force could have resulted in sweat under the electrodes, which would behave similar to electrolyte gel; this would explain why the long terms effects were similar to Ag/AgCl electrodes with electrolyte gel. This is also consistent with the larger decreases in R_s observed for subjects AgCl-No-G-S1 to AgCl-No-G-S3 when the initial force of 8.9 N was applied (Figure 4.5c); these subjects also exhibited the largest decreases in electrode-skin impedance when the initial force of 8.9 N was applied (Figure 4.4). The sharp decrease in R_s values could indicate the introduction of sweat under the electrodes.

R_s values did not decrease below 200 Ω when a high force level (22.2 N) was applied to the Ag/AgCl electrodes sites with or without electrolyte gel, for all the subjects (Figures 4.5c and 4.3c). The estimated value of R_s might not have decreased below 200 Ω with higher force levels because of the contributions of the impedance of underlying skin tissue, which are included in the estimated values of R_s (Section 3.4); that is, $R_{tissues}$ is responsible for a fixed impedance value within the R_s estimate. Large decreases in the R_s estimate are associated with actual decreases in R_s rather than changes in $R_{tissues}$. If there was a large effect from the applied force on $R_{tissues}$, these would have been observed as the force level was increased and later decreased.

Electrode settling would decrease electrode-skin impedance with time [45]; however, its effect is slow and cannot be accounted for the observed decreases alone. The results showed in

(Section B.2) that the long term effect of force on decreasing the electrode-skin impedance was stronger than the electrode settling effect.

4.5 Conclusion

The application of an external force causes a decrease in electrode-skin impedance. Decreases in electrode-skin impedance were relatively small for Ag/AgCl electrodes with electrolyte gel compared to Ag/AgCl electrodes without electrolyte gel; this is primarily due to the initial impedance of Ag/AgCl electrodes being much lower when electrolyte gel was present. Decreases in electrode-skin impedance remained even as the force was removed from electrodes sites. Exerting high force level on electrodes using electrolyte gel could result in fluctuations in electrode-skin impedance due to the electrolyte gel being redistributed away from the electrode site, which was not expected in this study. The fluctuations in R_s values in Figure 4.3c that reflect the resistance of electrolyte gel and the similar reported fluctuations in impedance values during force application to pregelled Ag/AgCl electrodes [43] would support the findings of this study. The observed increase in C_d values and decrease in R_d and R_s values are an indication of the influence of force on their values, and it is consistent with the stated hypothesis of this study.

5 Effect of Externally Applied Force on Electrode-Skin Impedance for Dry Electrodes

5.1 Introduction

Dry electrodes benefit from the formation of sweat on the skin's surface to lower the electrode-skin interface impedance and to improve biological signals measurements [32], [63]. Dry electrodes are sometimes the comfort choice for patients who have sensitive skin and may develop skin irritation after applying electrolyte gel to their skins. Dry electrodes, however, are weakly attached to skin; hence they can be easily affected by motion artifacts [32], [63].

The objective behind this study is to analyze the effect of an externally different applied force levels on electrode-skin impedance. An equivalent circuit model representing the electrode-skin interface is applied in this analysis. Two types of dry electrodes (Orbital and stainless steel electrodes) are used in this study.

It is anticipated that the effect of external force on the electrode-skin impedance for dry electrodes to be marked by a decrease in electrode-skin impedance. The increase in contact strength between electrodes and skin (increase in contact area) would cause the decrease in impedance values [9]. Orbital electrodes are expected to have larger decrease in impedance than stainless steel electrodes due to the spikes of Orbital electrodes that could penetrate the highly resistant skin layer (startum corneum). For electrode circuit components values, it is expected an increase in C_d values (Section 2.6), a decrease in R_d values and a decrease in R_s values as a reflection of formation of sweat with time. The increase in force level is anticipated to be associated with further decrease in electrode-skin impedance, further increase in C_d

values and further decrease in R_d and R_s values and vice versa with the decrease in force level except R_s values will continue to decrease as sweat secretion will stay active.

5.2 Materials and Methods

5.2.1 Experimental Setup

The equipment and experimental setup used in this section are generally the same as described in chapter three. Additional materials and procedures used in this study are described in the following sections.

5.2.2 Dry Electrodes

5.2.2.1 Orbital Electrodes

Orbital electrodes (Model # ORI F6T, Orbital Research Inc., Cleveland, OH, U.S.A.), which have a diameter of 2.5 cm and penetrators (spikes) of a 150 μm length are used in this study (Figure 3.12). The Orbital electrodes properties are described in section 3.2.2. An adhesive tape was used to affix the Orbital electrode to the skin. The same Orbital electrodes were used on all subjects. Orbital electrodes were washed with water and dried off before conducting any new set of measurements. The schematic diagram of Orbital electrode-skin contact area is different from other electrodes (Figure 3.10) used in this study (Figure 5.1); the difference is due to the presence of spikes, which may penetrate into the upper layers of the skin.

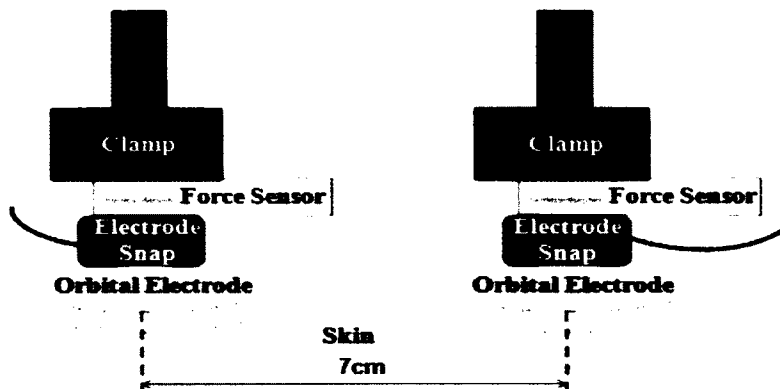


Figure 5.1. Experimental setup using Orbital electrodes.

5.2.2.2 Stainless Steel Electrodes

Stainless steel (ST) electrodes (Model # EL12, Liberating Technologies Inc, (LTI), Holliston, MA, U.S.A.) which have a diameter of 1.5 cm (Figure 3.13) were used. The Stainless steel electrodes properties are described in section 3.2.3. An adhesive tape was used to affix the stainless steel electrode to the skin. The same stainless steel electrodes were used on all subjects. Stainless steel electrodes were washed with water and dried off before conducting any new set of measurements. The schematic diagram of the experimental set up for stainless steel electrode is identical to Figure 3.10.

5.2.3 Data Collection

In this study, measurements were conducted on five subjects. Information regarding the subjects is contained in Table 5.1 and Table 5.2, respectively. Measurements were conducted on the same subjects, for both electrode types, on different days. The first and second subjects are different than in the application of Ag/AgCl electrodes with and without electrolyte gel (chapter 4). Skin preparation was not performed in this study. The room temperature and humidity were 23°C and 31%, respectively.

Table 5.1. Information of subjects in the Orbital electrodes study.

Subject	Height (cm)	Weight (kg)	Body Mass Index	Age	Gender
Orbital-S1	158	67	26.8	25	Male
Orbital-S2	180	90	27.8	64	Male
Orbital-S3	172	80	27.0	29	Male
Orbital-S4	168	65	22.9	29	Male
Orbital-S5	170	65	22.5	27	Male

Table 5.2. Information of subjects in the stainless steel (ST) electrodes study.

Subject	Height (cm)	Weight (kg)	Body Mass Index	Age	Gender
ST-S1	158	67	26.8	25	Male
ST-S2	180	90	27.8	64	Male
ST-S3	172	80	27.0	29	Male
ST-S4	168	65	22.9	29	Male
ST-S5	170	65	22.5	27	Male

5.3 Results

5.3.1 Responses of Electrode-Skin Impedance to Externally Different Applied Force Levels for Orbital Electrodes

The results obtained from the subjects showed a decrease in electrode-skin impedance with response to the external force applied to Orbital electrodes sites (Figure 5.2). The general

trend observed was a decrease in electrode-skin impedance with increasing force applied to electrodes sites.

The initial application of force (8.9 N) on Orbital electrodes sites caused a large decrease in impedance to all subjects. A further decrease in impedance values was observed as the force level was increased to 22.2 N for all the subjects except subject Orbital-S2, where the impedance was mainly unchanged.

As the force level was decreased from 22.2 N to 8.9 N, the impedance remained unchanged for subjects Orbital-S1, Orbital-S2 and Orbital-S5: subject Orbital-S3 exhibited a slight decrease in impedance and subject Orbital-S4 exhibited a slight increase in the lower frequencies.

For all subjects, the electrode-skin impedance increased when force was removed from the electrodes sites (0 N - 24 min); however, the electrode-skin impedance remained lower than initial level (0 N - 0 min).

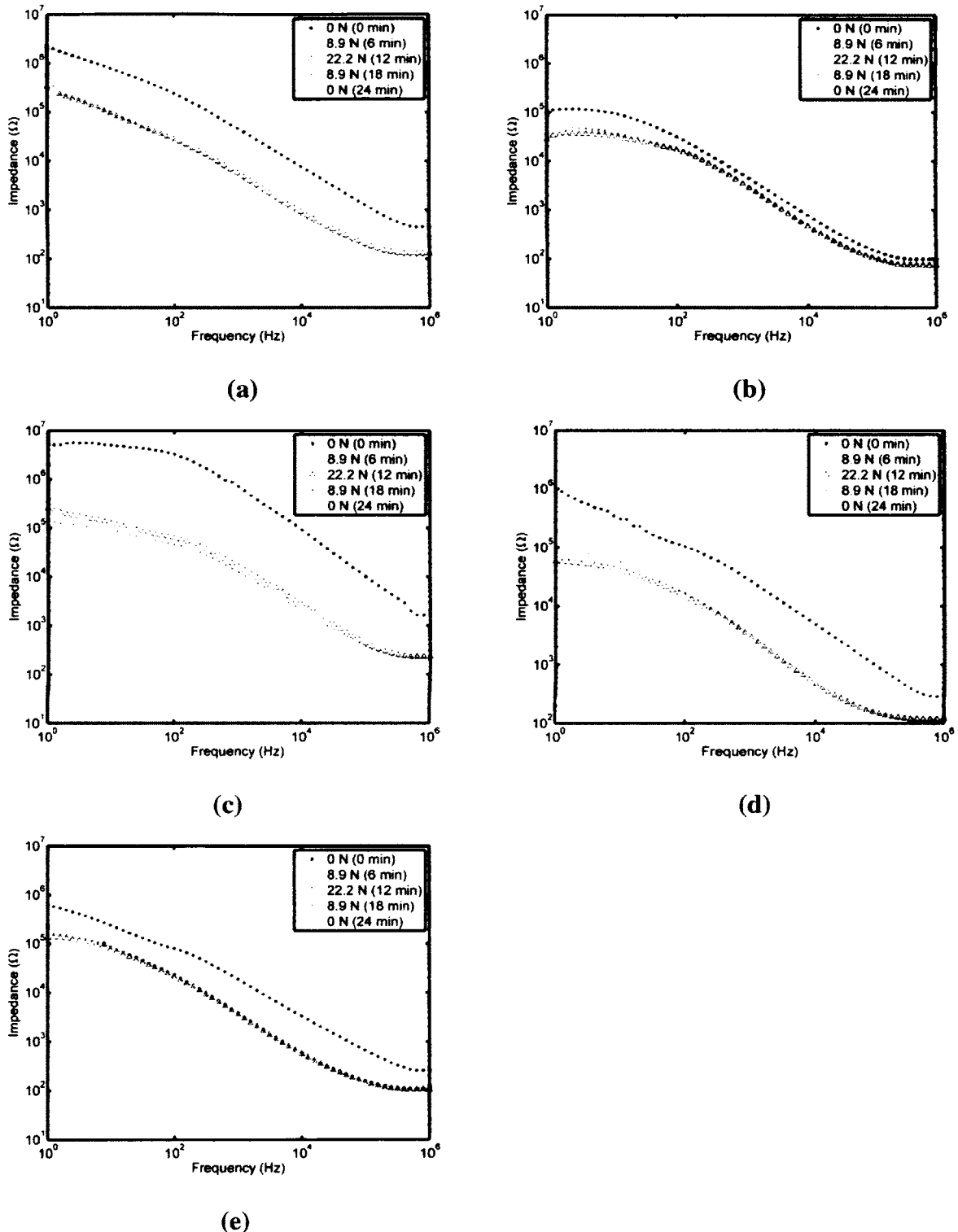


Figure 5.2. Orbital electrode-skin impedance frequency response to externally different applied force levels for the five subjects: (a) Orbital-S1, (b) Orbital-S2, (c) Orbital-S3, (d) Orbital-S4 and (e) Orbital-S5. Times in parentheses indicate the approximate start time of the impedance measurement.

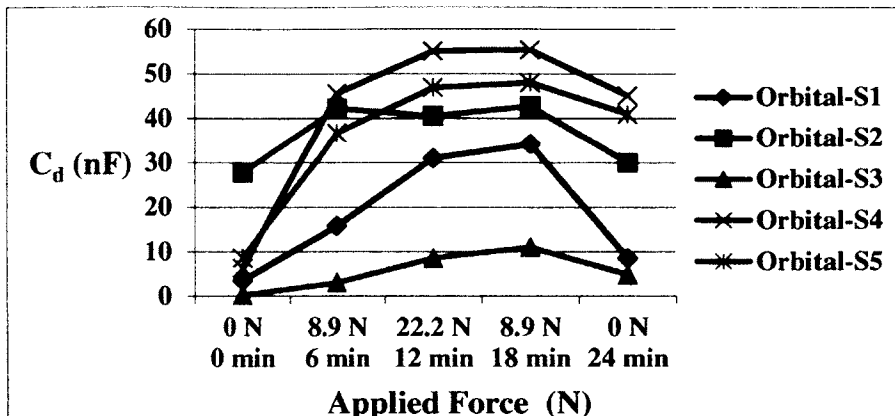
5.3.2 Results of Equivalent Circuit Model Components Values for Orbital Electrode-Skin Interface under the Influence of an External Force

The estimated values for the electrode circuit model components (C_d , R_d and R_s) are available in appendix C, Tables C.1, C.2 and C.3 for all subjects.

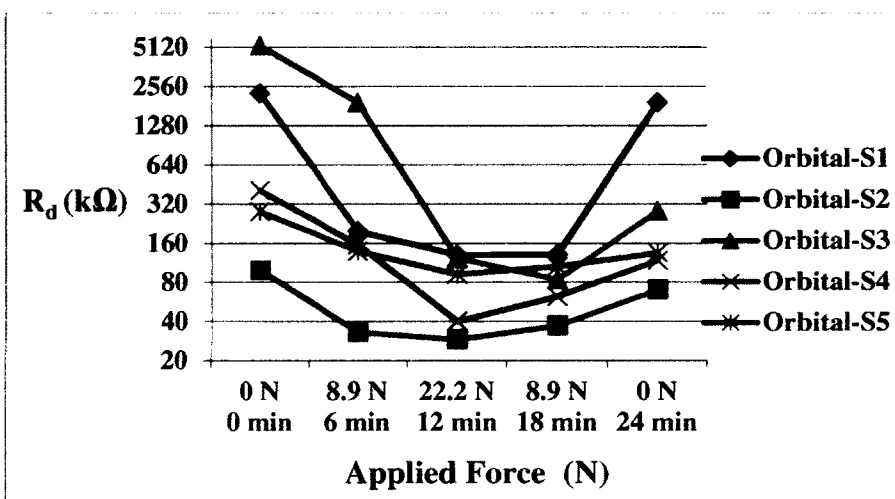
C_d values were sharply increased with the initial application of force (8.9 N) for all the subjects (Figure 5.3a). C_d values continued to increase at higher force level (22.2 N) for all the subjects except subject Orbital-S2 who exhibited relatively static C_d value. C_d values remained relatively unchanged, when the force was reduced from 22.2 N to 8.9 N. C_d values decreased when the force was removed from the electrodes sites (0 N – 24 min). The average percentage increase in C_d values across all subjects between initial state and final state (0 N- 24 min) was 669% (Table 5.3).

R_d values in all subjects decreased when force was applied to Orbital electrodes sites (Figure 5.3b). R_d values dropped at first force level (8.9 N) and continued to drop at high force level (22.2 N). R_d values remained relatively unchanged when the force was reduced from 22.2 N to 8.9 N. R_d values increased after the force was removed from the electrodes sites. The average percentage decrease in R_d values across all subjects between initial state and final state was 59.4% (Table 5.3).

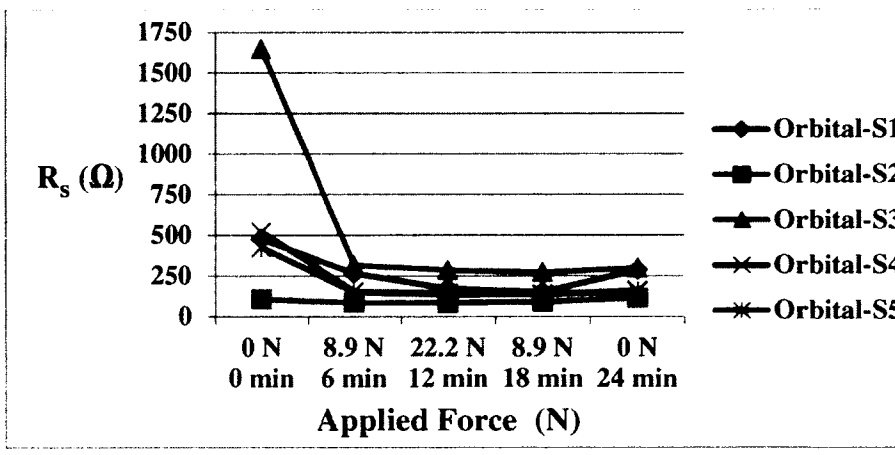
R_s values were sharply decreased when the first force level (8.9 N) was applied on electrodes sites for subjects Orbital-S1 and Orbital-S3 to Orbital-S5 (Figure 5.3c). R_s value remained generally steady for subject Orbital-S2. The third subject, Orbital-S3 had the largest decrease in R_s value at the first force level (8.9 N).



(a)



(b)



(c)

Figure 5.3. Orbital electrode's circuit model components values under the influence of force loading/unloading and skin preparation for the five subjects (a) C_d , (b) R_d and (c) R_s .

R_s values did not change when the force level was increased to 22.2 N and remained relatively stable when the force was removed from the electrodes sites, except for subject Orbital-S1 who exhibited an increase in R_s value when the force was decreased from 8.9 N to 0 N. The average percentage decrease in R_s values across all subjects between initial state and final state was 44.9% (Table 5.3).

Table 5.3. The percentage increases in circuit model components values between initial state and final state of measurement cycle for Orbital electrodes sites, (values in brackets indicate a decrease).

Circuit Model Components	Subjects					Average
	Orbital-S1	Orbital-S2	Orbital-S3	Orbital-S4	Orbital-S5	
C_d	138.5%	6.7%	2180.0%	641.9%	377.8%	669.0%
R_d	(55.1 %)	(29.2 %)	(95.4 %)	(66.2 %)	(51.0 %)	(59.4 %)
R_s	(12.7 %)	1.2%	(80.4 %)	(69.1 %)	(63.5 %)	(44.9 %)

5.3.3 Responses of Electrode-Skin Impedance to Externally Different Applied Force Levels for Stainless Steel Electrodes

A decrease in electrode-skin impedance for all subjects was observed in response to applied forces on stainless steel electrodes (Figure 5.4). A marked decrease in impedance was observed as the applied force was increased from (0 N) to (8.9 N) in all subjects. A smaller decrease in impedance was observed as the force was increased to 22.2 N. As the force was decreased (8.9 N), the impedance remained relatively unchanged for all subjects. When the force was removed (0 N - 24 min), the impedance remained relatively unchanged or increased in the lower frequencies, but did not return to the original impedance value as measured in the initial state (0 N - 0 min). A hysteresis effect was present with subjects ST-S2, ST-S4 and ST-S5; the electrode-skin impedance at the beginning of the measurements (0 N – 0 min) was not the same as at the end of the measurements (0 N – 24 min).

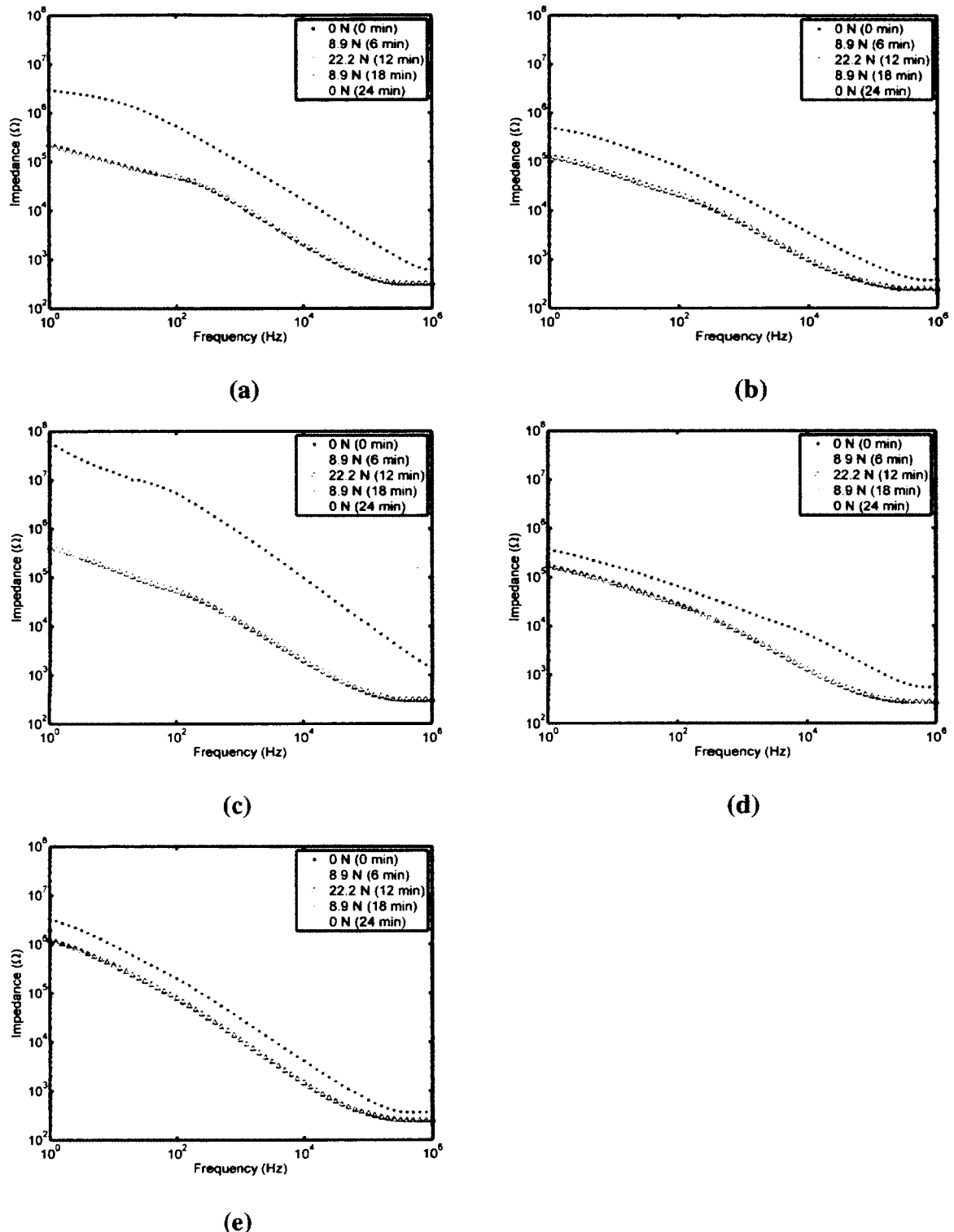


Figure 5.4. Stainless steel electrode-skin impedance frequency response to externally different applied force levels for the five subjects: (a) ST-S1, (b) ST-S2, (c) ST-S3, (d) ST-S4 and (e) ST-S5. Times in parentheses indicate the approximate start time of the impedance measurement.

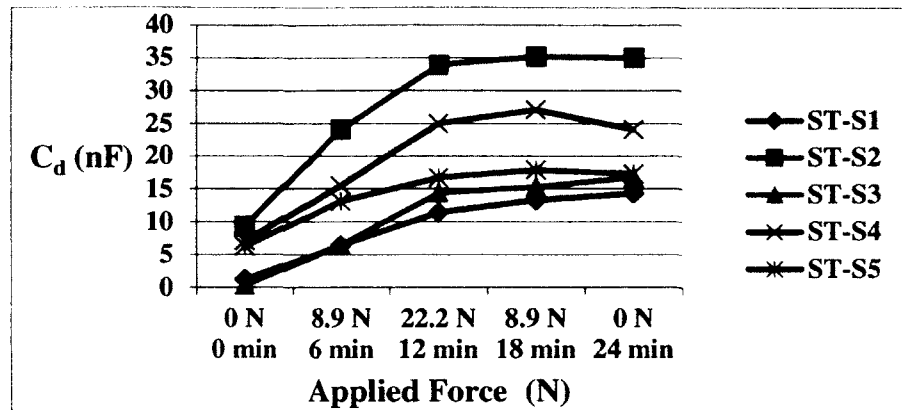
5.3.4 Results of Equivalent Circuit Model components values for Stainless Steel Electrode-Skin Interface under the influence of an External Force.

The increase in C_d values occurred under the influence of force on stainless steel electrodes sites for all the subjects (Figure 5.5a). C_d value was highly increased after applying the first force level (8.9 N) to the electrodes sites and continued to increase at higher force level (22.2 N) for all subjects.

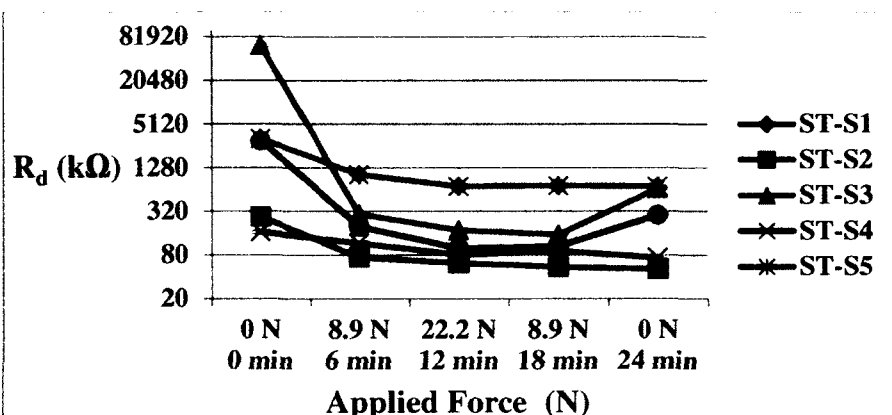
C_d values tended to be stable at 0 N – 24 min, as the force was subsequently removed from the electrodes sites for all subjects, except for subject ST-S4 who exhibited a decrease in C_d value. The average percentage increase in C_d values across all subjects between initial stage and final state (0 N- 24 min) was 1535.8% (Table 5.4).

The decrease in R_d values in response to force occurred for all the subjects (Figure 5.5b). A large decrease in R_d values was observed when the first force level (8.9 N) was exerted on the electrodes sites. A smaller decrease in R_d values occurred with exerting higher force level (22.2 N) on electrodes sites. R_d values were stable in most of the subjects when the force level was returned back to 0 N, except for subjects ST-S1 and ST-S3 who exhibited an increase in R_d values when the force was decreased from 8.9 N to 0 N. The average percentage decrease in R_d values across all subjects between initial stage and final state was 78.8% (Table 5.4).

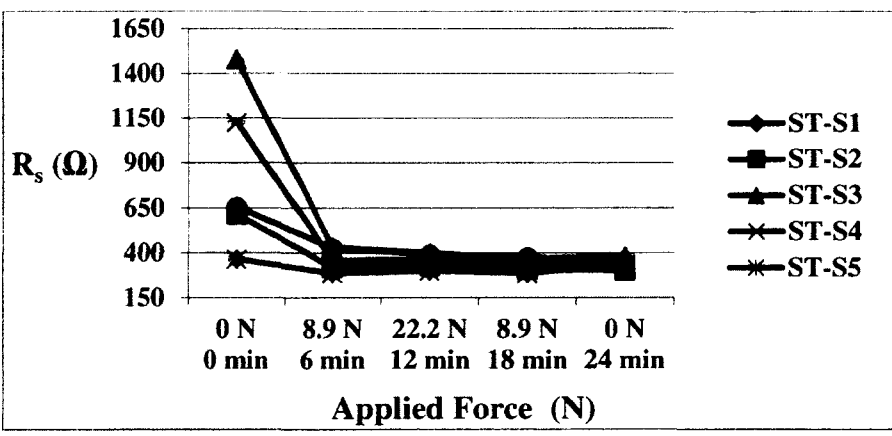
R_s values decreased sharply at first force level (8.9 N) for all subjects (Figure 5.5c). R_s values tended to be stable after the first force level was exerted on electrodes sites and as the applied force was further increased and then removed. The average percentage decrease in R_s values across all subjects between initial stage and final state was 53.5% (Table 5.4).



(a)



(b)



(c)

Figure 5.5. Stainless steel electrode's circuit model components values under the influence of force loading/unloading and skin preparation for the five subjects (a) C_d , (b) R_d and (c) R_s .

Table 5.4. The percentage increases in circuit model components values between initial state and final state of measurement cycle for stainless steel electrodes sites, (values in brackets indicate a decrease).

Circuit Model Components	Subjects					Average
	ST-S1	ST-S2	ST-S3	ST-S4	ST-S5	
C_d	964.9%	274.0%	6023.1%	239.4%	177.5%	1535.8%
R_d	(90.7%)	(81.1%)	(99.0%)	(55.4%)	(67.7%)	(78.8%)
R_s	(45.4%)	(51.0%)	(76.0%)	(72.0%)	(22.8%)	(53.5%)

5.4 Discussion

The results for stainless steel electrodes appeared to have some differences in electrode-skin impedance in comparison to Orbital electrodes. Stainless steel electrodes are different in their shape and metal properties than Orbital electrodes. Orbital electrodes are designed to overcome the effect of highly resistant skin layer (stratum corneum) by the presence of spikes [31], [55]. Stainless steel electrodes are flat dome electrodes that do not penetrate into the skin surface and they are made of highly polarizable metal [1], [18], [57].

Exerting a force of 8.9 N on Orbital and stainless steel electrodes sites caused the impedance value to be much lower compared to 0 N – 0 min. It resulted in enlarging the electrode-skin contact area and thus lowering impedance value [9], [43]. Moreover, secretion of sweat could result from exerting a force on the electrodes sites, which could cause a decrease in electrode-skin impedance value [62]. In the absence of electrolyte gel in dry electrodes applications, the addition of sweat would act similar to electrolyte gel and would be associated with a large decrease in electrode-skin impedance. The effect of high force level 22.2 N was more noticeable on Orbital electrodes sites (Figure 5.2) than stainless steel electrodes (Figure 5.4) potentially due to the presence of spikes. Adding more force on Orbital electrodes would allow the spikes to penetrate further into the skin's surface.

The hysteresis effect was observed when the force was removed from Orbital and stainless steel electrodes sites at 0 N- 24 min (Figure 5.4) as the impedance did not return back to the initial state.

This hysteresis effect could be a result of the long term effect of force on skin deformation, sweat accumulation with time and electrode settling (section B2) [45]. Skin deformation causes the separation distance between the double layer charge that formed between electrodes and skin (section 2.6) to stay small until the skin retains back to its original state.

The components of electrode circuit model C_d , R_d and R_s were heavily influenced by the strong contact between the dry electrode and the skin. An increase in electrode-skin contact area, caused by an applied force, would result in an increase in C_d values and a decrease in R_d values. Larger contact area is associated with higher capacitance value according to the parallel-plate capacitor's formula (section 2.6.1). The decrease in R_d values can be attributed to an increase in electrode-skin contact area; larger cross-sectional area is associated with lower resistance according to resistance of a conductor's formula (section 2.6.2) [9], [43]. In addition, as the distance that separates the skin layers becomes smaller by an applied force, the capacitance value increases.

As the applied force was removed from Orbital electrodes sites, a decrease in C_d values and an increase in R_d values were observed; a reduction in electrode-skin contact area could be formed as the contact between the spikes of Orbital electrodes and skin became weaker, so the area between the spikes would lose contact with the skin. Stainless steel electrodes, which do not have spikes, did not exhibit this decrease in C_d nor increase in R_d in comparison to the Orbital electrodes.

A large decrease in R_s values in Orbital and stainless steel electrodes was observed with the initial application of force. This is attributed to improved contact between the electrode and skin, established by the applied force. This hypothesis is substantiated as the estimated R_s values remained relatively unchanged as the force level was further increased and later decreased. The absolute change in the estimate of R_s is attributed to actual changes in R_s and not to $R_{tissues}$. If there were changes in $R_{tissues}$ values, then these changes would have been observed as the force level was further increased and decreased, which was not observed here (or in Section 4.3.4).

Despite the presence of spikes in Orbital electrodes, which could penetrate the highly resistant skin layer (stratum corneum) into the underlying skin tissue [31], [55], R_s values did not decrease below a 100Ω when a high force level (22.2 N) was applied to Orbital electrodes sites for all the subjects (Figure 5.3c). The R_s values also did not decrease below 300Ω when a high force level (22.2 N) was applied to stainless steel electrodes sites for all the subjects (Figure 5.5c). The estimated value of R_s might not have decreased below a 100Ω for Orbital electrodes or below 300Ω for stainless steel electrodes with high force levels because of the contributions of the impedance of underlying skin tissue, which are included in the estimated values of R_s . The explanation is the same as given in Section 4.4.

The effect of applied force on electrode-skin impedance for Ag/AgCl electrodes without electrolyte gel (Section 4.3.3) were similar to the dry electrodes examined in this study. Electrode-skin impedance changes for Ag/AgCl electrodes without electrolyte gel were more like stainless steel electrodes; this is potentially because both of these electrodes do not have spikes like the Orbital electrodes, so less change in electrode-skin impedance when force is removed. The response of electrode-skin impedance to external force with dry electrodes was

quite consistent between subjects unlike Ag/AgCl electrodes with electrolyte gel (chapter 4). This further substantiates that the inconsistent behavior observed for Ag/AgCl electrodes with electrolyte gel could be attributed to the electrolyte gel and the hypothesis that it was redistributed away from the electrodes sites under high force levels.

5.5 Conclusion

The effect of an external force on dry electrodes sites is found to decrease the electrode-skin impedance as hypothesised. Electrode-skin impedance is sensitive to the application of force when dry electrodes are applied. A large drop in electrode-skin impedance occurred after the application of first force level. The decrease in electrode-skin impedance was maintained even after the force was removed. This implies that when using dry electrodes, ensuring an initial force is applied will help achieve lower impedance in long term. Orbital electrodes have lower electrode-skin impedance than stainless steel electrodes when an external force is maintained on electrodes. These spikes can penetrate into the upper layers of the skin, such providing a good electrode-skin contact; however, without force, the strength of electrode-skin contact can become weak as the areas between the spikes and skin may lose contact. This behaviour is observed in Figure 5.3b as there is an increase in R_d values at 0 N- 24 min with all the participated subjects (five subjects).

6 Effect of Repeated Force Loading/Unloading on Electrode-Skin Impedance for Pregelled Ag/AgCl Electrodes with Skin Preparation

6.1 Introduction

One of the main sources that cause impairment to biological signal is the high electrode-skin impedance and noise [1], [2], [64], [65]. Reducing electrode-skin impedance and noise associated with biological signals measurements is a crucial measure in health care sector in which reliable medical information can be extracted. The appropriate skin impedance for recording biological signals, such as ECG, EEG, and EMG is around $5\text{ k}\Omega$ [64], [65]. Techniques that can be employed to achieve low electrode-skin impedance include: skin preparation, the use of non-polarizable electrodes and the use of electrolyte gel [1], [2]. The efficiency of these techniques needs to be examined under the effect of repeated force loading/unloading that may face modern wearable sensor technologies for monitoring biological signals. For example, electrodes integrated in a stretchable material (e.g., spandex) would have experience varying applied force levels due to changing in anatomical size (e.g., due to a muscle contraction, due to respiration). In this study, measurements conditions for biological signals in wearable sensor technologies are mimicked, by employing a skin preparation protocol, using pregelled Ag/AgCl surface electrodes, ensuring that the initial electrode-skin impedance value is around $5 - 10\text{ k}\Omega$. Repeated loading/unloading of a low force level (5 N) is applied to the electrodes sites. This study differs from the previous studies (chapters 4 and 5), as skin preparation is employed and applying repeated loading/unloading of a fixed low force level (5 N) is applied to the electrodes sites. In the previous study, there was a gradual increase and decrease in force levels (0 – 22.2 N). No skin preparation was performed in the previous study, which would better represent the initial application of a wearable system.

With sufficient time, electrode settling would like result in a large decrease in electrode-skin impedance; the electrode settling effect is reduced (or removed) by skin preparation.

The objective behind this study is to analyze the effect of repeated loading/unloading of low fixed force level (5 N) on electrode-skin impedance. An equivalent circuit model representing the electrode-skin interface is used in this analysis. Pregelled surface Ag/AgCl electrodes and skin preparation are applied in this study.

It is anticipated that the initial electrode-skin impedance values to be low with skin preparation. The effect of repeated application of force loading/unloading of a fixed light force level (5 N) on the electrode-skin impedance for pregelled Ag/AgCl electrodes sites to be a small decrease with force loading and a small increase with unloading state. For electrode circuit components values, it is expected a small increase in C_d values with force loading and a small decrease with the unloading state (Section 2.6). A small decrease in R_d values with force loading and small increase with unloading state. Initial R_s values are expected to be low with the presence of electrolyte gel and to decrease with force loading with the formation of sweat. It is expected to be a small increase in R_s values with unloading state with some fluctuations as occurred with pregelled Ag/AgCl in chapter 4.

6.2 Impact of Skin Preparation on Electrode-Skin Impedance

The main target of skin abrasion is the removal of top skin layers. The skin is mainly composed of three major layers; epidermis, dermis and hypodermis or subcutaneous layer [30]. The first layer of the skin is epidermis and it has the following layers: 1) stratum corneum 2) stratum lucidum, 3) stratum granulosum, 4) stratum spinosum and 5) stratum basale [28], [30]. Stratum corneum is the outermost layer of the skin and has a depth of about 9 -19 μm [28]. The stratum corneum is primarily made up of dead dry skin cells. The dryness of the stratum

corneum represents an electrical obstacle for biological signals to be fully detected through surface electrodes [12], [33], [34], [66], [67].

A sharp decrease in electrode-skin impedance can be achieved when the stratum corneum is removed [11], by allowing the surface electrodes to be placed on a better part of the epidermis that has more living skin cells and body fluid [12], [33], [34], [66], [67]. Skin preparation often includes some form of skin abrasion that removes the stratum corneum or parts of it. Furthermore, skin abrasion could also remove the residues on the skin's surface and the traces of oil that impose noise to biological signals and high impedance values [1], [40], [68]. Thus, skin preparation is a practical way to reduce electrode-skin impedance and noise associated with biological signals [11], [13], [23], [40], [68], [69].

6.3 Materials & Methods

The equipment and experimental setup used in this section are generally the same as described in chapter three. However, some additional materials and procedures used for performing skin preparation are described in the following sections.

6.3.1 Experimental Setup

Skin preparation was performed by applying Nuprep Skin Prep Gel (Model # 10-30, Weaver and Company, Aurora, Colorado, U.S.A.) to the skin to remove the stratum corneum layer followed by rubbing the skin's site with a piece of fabric. The skin's surface was then cleaned with an alcohol swab (Model # 326895, BD, Becton Dickinson, ON, Canada) in order to remove oily residues from the skin's surface and to clean up the electrodes sites. Skin preparation was performed before conducting measurements to reduce the electrode-skin impedance level to near $5 \text{ k}\Omega$ - $10 \text{ k}\Omega$ matching the acceptable impedance level for ECG and EMG measurements. Disposable pregelled Ag/AgCl surface electrodes (Model # FT002,

MVAP II, Medical Supplies Inc., Newbury Park, CA, U.S.A.) which have a diameter of 1 cm were used in this study (Figure 3.11). New pregelled Ag/AgCl surface electrodes were used on every subject. Impedance measurements were performed by conducting subsequent force loading/unloading with 0 N (no externally applied force) and 5 N (equivalent to applying a weight of 1.12 lb).

6.3.2 Data Collection

Information regarding the subjects in this study is contained in Table 6.1. All the subjects are the same as in previous study (Chapter 4) except the first subject is different. The room temperature and humidity were 24°C and 39%, respectively. The schematic diagram of the experimental set up is the same as in Figure 4.1.

Table 6.1. Information of subjects performed skin preparation in the pregelled Ag/AgCl electrodes study.

Subject	Height (cm)	Weight (kg)	Body Mass Index	Age	Gender
AgCl-SP-S1	181	75	22.9	28	Male
AgCl-SP-S2	174	78	26.1	28	Male
AgCl-SP-S3	172	80	27.0	29	Male
AgCl-SP-S4	168	65	22.9	29	Male
AgCl-SP-S5	170	65	22.5	27	Male

6.4 Results

6.4.1 Responses of Electrode-Skin Impedance to Repeated Force Loading/Unloading and Skin Preparation for Pregelled Ag/AgCl Electrodes

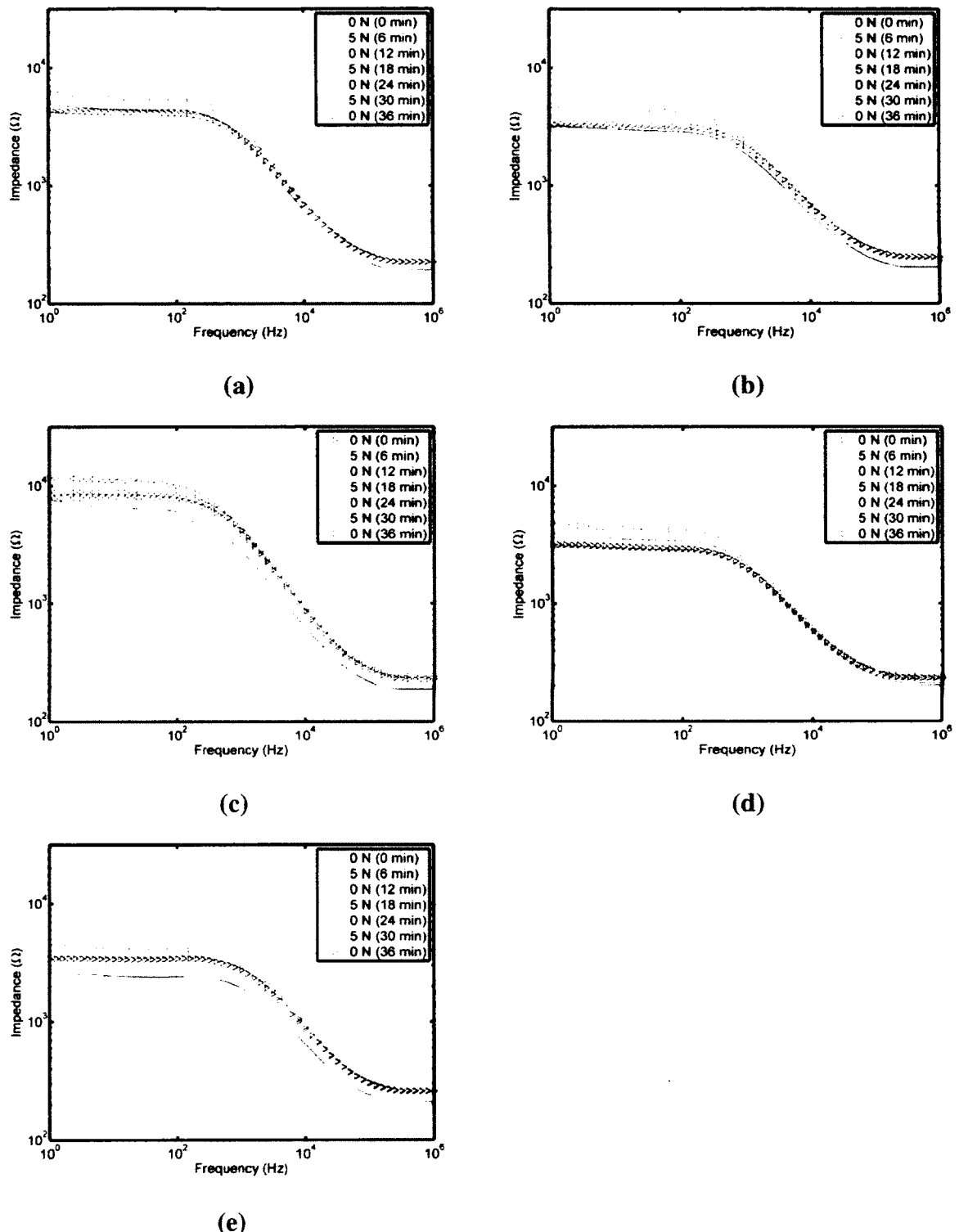


Figure 6.1. Pregelled Ag/AgCl electrode-skin impedance frequency response to externally different applied force levels and skin preparation for the five subjects. (a) AgCl-SP-S1, (b)AgCl-SP-S2, (c) AgCl-SP-S3, (d) AgCl-SP-S4 and (e) AgCl-SP-S5. Times in parentheses indicate the approximate start time of the impedance measurement.

The changes in electrode-skin impedance for all subjects were observed in response to force loading/unloading (Figure 6.1). The results were consistent across subjects. A decrease in electrode-skin impedance was observed with force application. Electrode-skin impedance level increased at low frequencies when the force was removed from electrodes sites, but remained lower than the initial state (0 N – 0 min) and tended to return to their initial state at high frequencies. Electrode-skin impedance at the first force loading/unloading cycle (0 min – 6 min) was higher than the second (12 min – 18 min) and third (24 min – 30 min) cycles.

6.4.2 Results of Equivalent Circuit Model Components Values for Ag/AgCl Electrode-Skin Interface under the Influence of Repeated Force Loading/Unloading, Skin Preparation and Electrolyte Gel.

The estimated values for the electrode circuit model components (C_d , R_d and R_s) are available in appendix D, Tables D.1, D.2 and D.3 for all subjects.

The general trend for C_d values is higher values associated when there is a force applied, compared to when there is no force applied; this behaviour is observed with all the subjects except for subject AgCl-SP-S4, who exhibited a slight change in C_d values after the second cycle of force loading/unloading was applied (Figure 6.2a). The average percentage increase in C_d values across all subjects between initial state (0 N – 0 min) and first force level (5 N- 6 min) was 22.7% (Table 6.2). The average percentage decrease in C_d values across all subjects between initial state (0 N – 0 min) and final state (0 N – 36 min) was 2.5% (Table 6.3) (Figure 6.3a1).

R_d values decreased with exerting a force (5 N) on the electrodes sites and increased when force was removed (0 N), as appeared in all subjects except for subject AgCl-SP-S4, who exhibited a slight change in R_d values after the second cycle of force loading/unloading was

applied (Figure 6.2b). The average percentage decrease in R_d values across all subjects between initial state (0 N – 0 min) and first force level (5 N - 6 min) was 29.8% (Table 6.2). The average percentage decrease in R_d values across all subjects between initial state (0 N – 0 min) and final state (0 N – 36 min) was 24.5% (Table 6.3) (Figure 6.3b1).

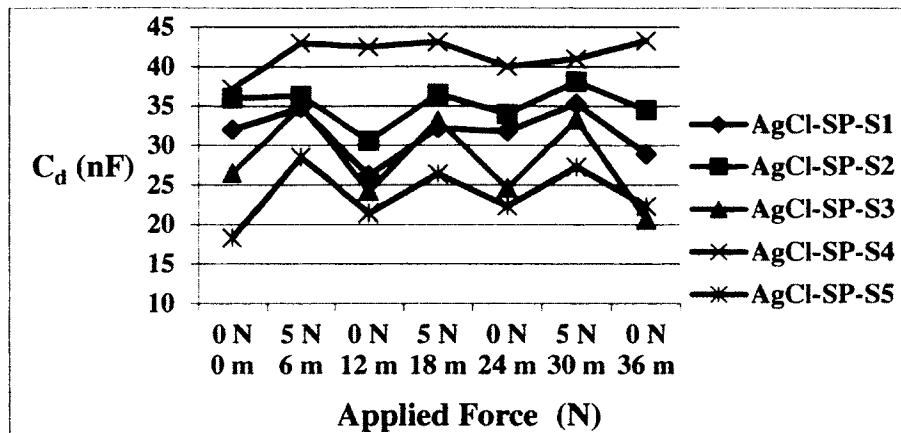
Table 6.2. The percentage increases in circuit model components values between initial state (0 N – 0 min) and when the first force level (5N) was applied to pregelled Ag/AgCl electrodes on prepared skin sites, (values in brackets indicate a decrease).

Circuit Model Components	Subjects					Average
	AgCl-SP-S1	AgCl-SP-S2	AgCl-SP-S3	AgCl-SP-S4	AgCl-SP-S5	
C_d	8.8%	0.8%	32.5%	15.6%	55.7%	22.7%
R_d	(22.6%)	(30.6%)	(40.3%)	(18.0%)	(37.7%)	(29.8%)
R_s	(15.6%)	(21.9%)	(19.0%)	(10.9%)	(21.4%)	(17.8%)

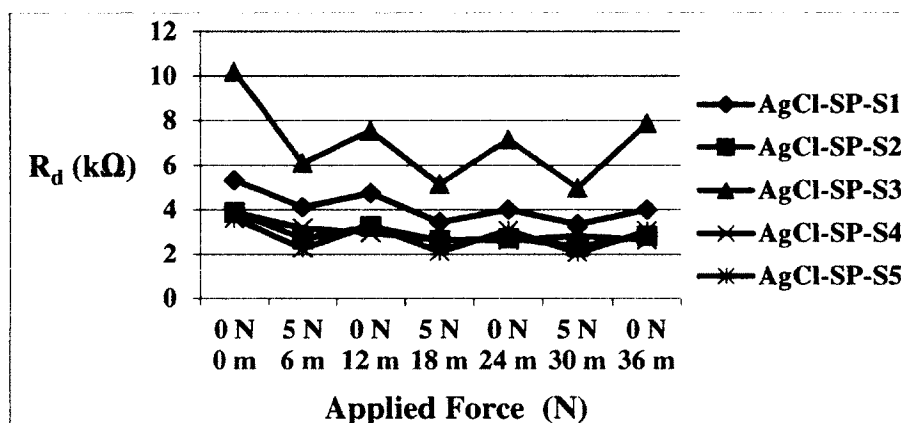
Table 6.3. The percentage increases in circuit model components values between initial state (0 N – 0 min) and final state (0 N – 36 min) for pregelled Ag/AgCl electrodes on prepared skin sites, (values in brackets indicate a decrease).

Circuit Model Components	Subjects					Average
	AgCl-SP-S1	AgCl-SP-S2	AgCl-SP-S3	AgCl-SP-S4	AgCl-SP-S5	
C_d	(9.7%)	(4.2%)	(22.3%)	1.6%	21.9%	(2.5%)
R_d	(24.8%)	(27.2%)	(22.6%)	(32.0%)	(16.0%)	(24.5%)
R_s	(11.1%)	(1.1%)	(0.04%)	(3.3%)	(1.0%)	(3.3%)

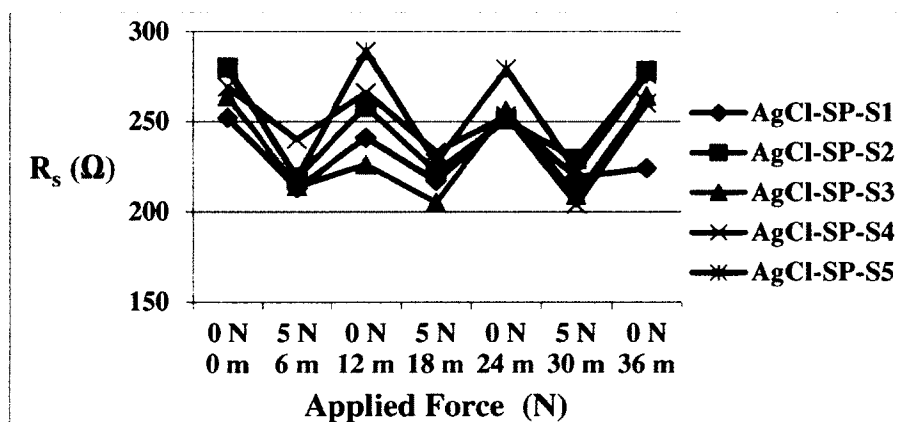
R_s values sharply decreased with exerting a force (5 N) on the electrodes sites and sharply increased when force was removed (0 N), as appeared in all subjects (Figure 6.2c). The average percentage decrease in R_s values across all subjects between initial state (0 N – 0 min) and first force level (5 N- 6 min) was 17.8% (Table 6.2). The average percentage decrease in R_s values across all subjects between initial state (0 N – 0 min) and final state (0 N – 36 min) was 3.3% (Table 6.3) (Figure 6.3c1). R_d values were more consistent to repeated application of force loading/unloading with time than C_d or R_s values as there was a general trend for decreasing R_d values with time (Figure 6.3).



(a)

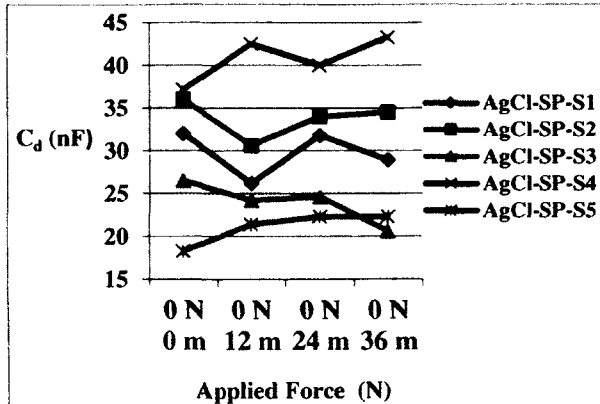


(b)

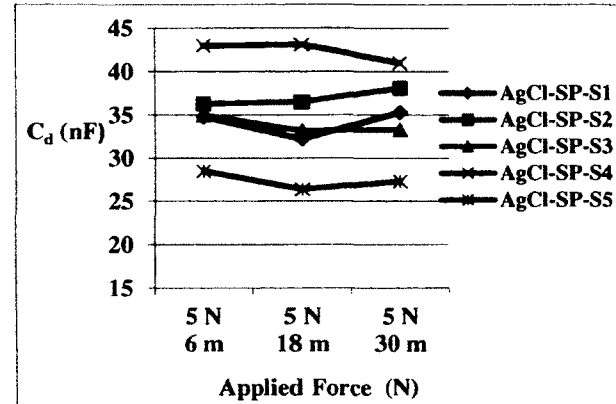


(c)

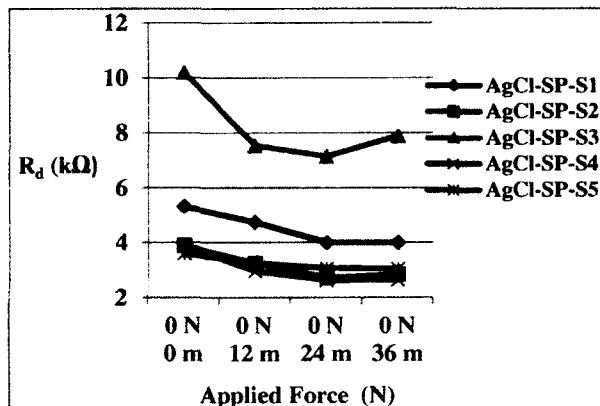
Figure 6.2. Pregelled Ag/AgCl electrode's circuit model components values under the influence of force loading/unloading and skin preparation for the five subjects (a) C_d , (b) R_d and (c) R_s .



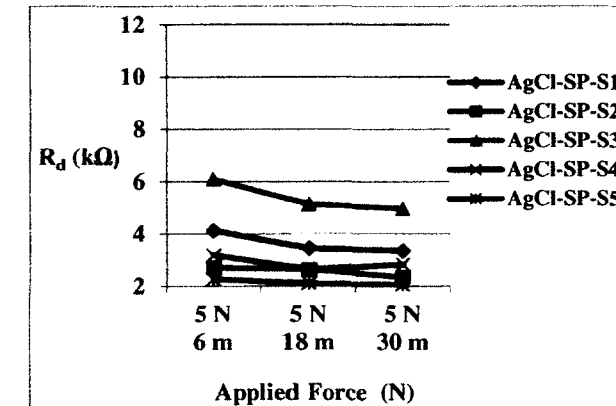
(a1)



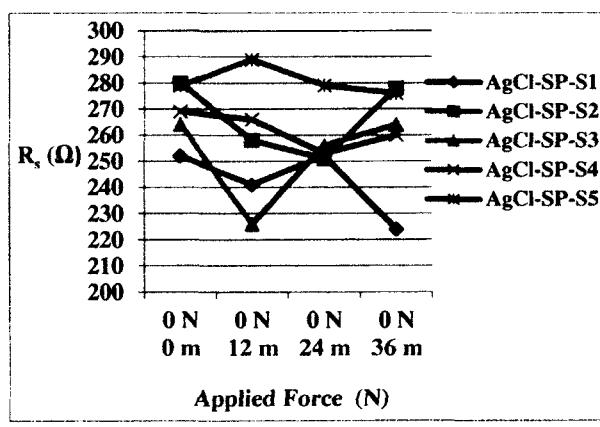
(a2)



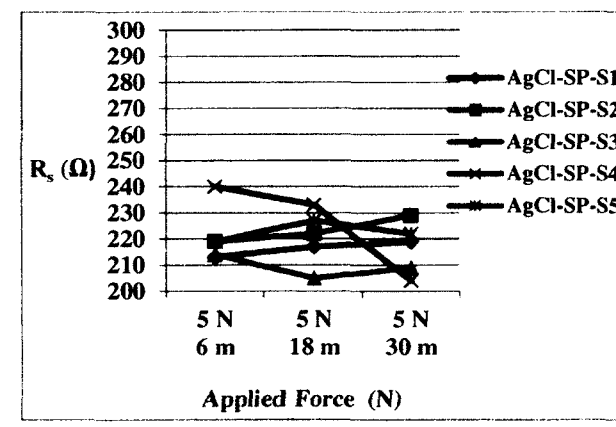
(b1)



(b2)



(c1)



(c2)

Figure 6.3. Comparison of pregelled Ag/AgCl electrode's circuit model components values under the influence of force loading/unloading and skin preparation for the five subjects. (a1) : (a2) C_d , (b1): (b2) R_d and (c1) : (c2) R_s .

6.5 Discussion

The initial low impedance value measured for all subjects is attributed to removing the stratum corneum layer by skin preparation [11], [13], [23], [40], [68], [69] and to the application of electrolyte gel [4], [70], [71], [72].

The decrease and increase in electrode-skin impedance for all subjects indicate its sensitivity to force application. A decrease in electrode-skin impedance was anticipated with applying force and thus enlarging electrode-skin contact area [9], [43]. While an increase in electrode-skin impedance was anticipated with removing force from electrodes sites and thus decreasing electrode-skin contact area.

Applying repeated force loading/unloading to the electrodes sites at the same force level (5 N) resulted in lower impedance at second and third force loading/unloading cycles in comparison to the initial values of measurements at first force loading/unloading cycle. The reasons behind that can be associated with sweat secretion with time [62], electrode settling, and the long time effect of force on electrode-skin contact area. The long term effect of force on electrode-skin impedance and the effect of electrodes settling were tested and compared in (Section B) and these results were published [73]. These results indicated that the decrease in impedance as a result of force can last for a long period of time and the decrease as a result of electrodes settling effect was smaller than the force effect. Compared to results with pregelled Ag/AgCl electrodes, where no skin-preparation was performed (chapter 4), changes in impedance were much smaller. This is attributed to the skin-preparation, which provided a better electrode-skin contact and thus lower initial electrode-skin impedance. The increase in C_d values occurred by the applied force is attributed to enlarging the contact area between electrode and skin. Initial R_d values obtained in the range of 3-10 k Ω are low reflecting the

impact of skin preparation and electrolyte gel on the electrode-skin impedance. R_d values became lower when a 5 N force was exerted on the electrodes sites because of the increase in contact strength between electrodes and skin (increase in contact area). The presence of an electrolyte gel and an increased sweat activity between the electrode and skin contact area with time could also attribute to the decrease in R_d values with time, as the electrolyte gel and sweat would provide lower resistivity (ρ) in accordance to resistance of a conductor's formula (section 2.6.2). A decrease in (ρ) resistivity is caused by the additional sweat formed during force loading stage [62]. R_s values did not seem to change much from its initial value (0 N – 0 min) to its final value (0 N – 36 min); however, R_s values did decrease when a force was applied. This suggests that the force caused a redistribution of the electrolyte, perhaps improving the electrode-skin contact, but that redistribution was a reversible process, returning the R_s value to its original state. As indicated in Section 3.4, the estimate value of R_s does include the contributions of $R_{tissues}$. The changes observed in the estimated values of R_s , were smalls (10s of ohms) and it is not possible to rule out an effect of force on $R_{tissues}$; however, the consequences of changes in the estimated R_s values is inconsequential because the changes were small and the value of the estimated R_s is also small and would not influence biosignal quality as much as C_d and R_d . R_s values did not decrease below 200 Ω when a light force level (5 N) was applied to pregelled Ag/AgCl electrodes sites for all the subjects (Figure 6.2c). The estimated value of R_s might not have decreased below 200 Ω with higher force levels because of the contributions of the impedance of underlying skin tissue, which are included in the estimated values of R_s . The explanation is the same as given in Section 4.4. The response of electrode-skin impedance to repeated loading/unloading of fixed low force level (5 N) with pregelled Ag/AgCl electrodes

was quite consistent between subjects unlike the inconsistent behaviour observed in the previous study (section 4.3.1). Those inconsistencies were associated with pregelled Ag/AgCl electrodes at high level of applied force (22.2 N) and attributed to a redistribution of the electrolyte gel from underneath the electrode. However, in this part of study, the level of applied force was much lower (5 N).

6.6 Conclusion

Skin preparation caused the electrode-skin impedance to be sensitive to force application. Applying a force (5 N) to electrodes sites resulted in a decrease in electrode-skin impedance and an increase when no force was applied. Performing skin preparation enabled low initial electrode-skin impedance; however, lower electrode-skin impedance was observed with the application of force on the electrodes sites. The magnitude of change between force loading/unloading in electrode-skin impedance decreased with subsection force loading/unloading. A light initial force (5 N) application showed to cause noticeable changes in C_d , R_d , and R_s values, 22.7% increase, 29.8% decrease, and 17.8% decrease, respectively between the initial unloaded state (0 N – 0 min) and loaded state (5 N – 6 min).

6.7 Summary

The results of this study indicate the sensitiveness of electrode-skin impedance to force application. The responses of electrode circuit components to repeated application of force loading/unloading demonstrate that applying an external force would increase C_d values and decrease R_d and R_s values. In the force unloading state, it shows the opposite; a decrease in C_d values and an increase in R_d and R_s values (Figure 6.2). In addition, based on a comparison made to the responses of C_d , R_d and R_s values to repeated force loading/unloading in Figures 6.4a, b and c, a better perspective for the effect of force loading/unloading can be observed.

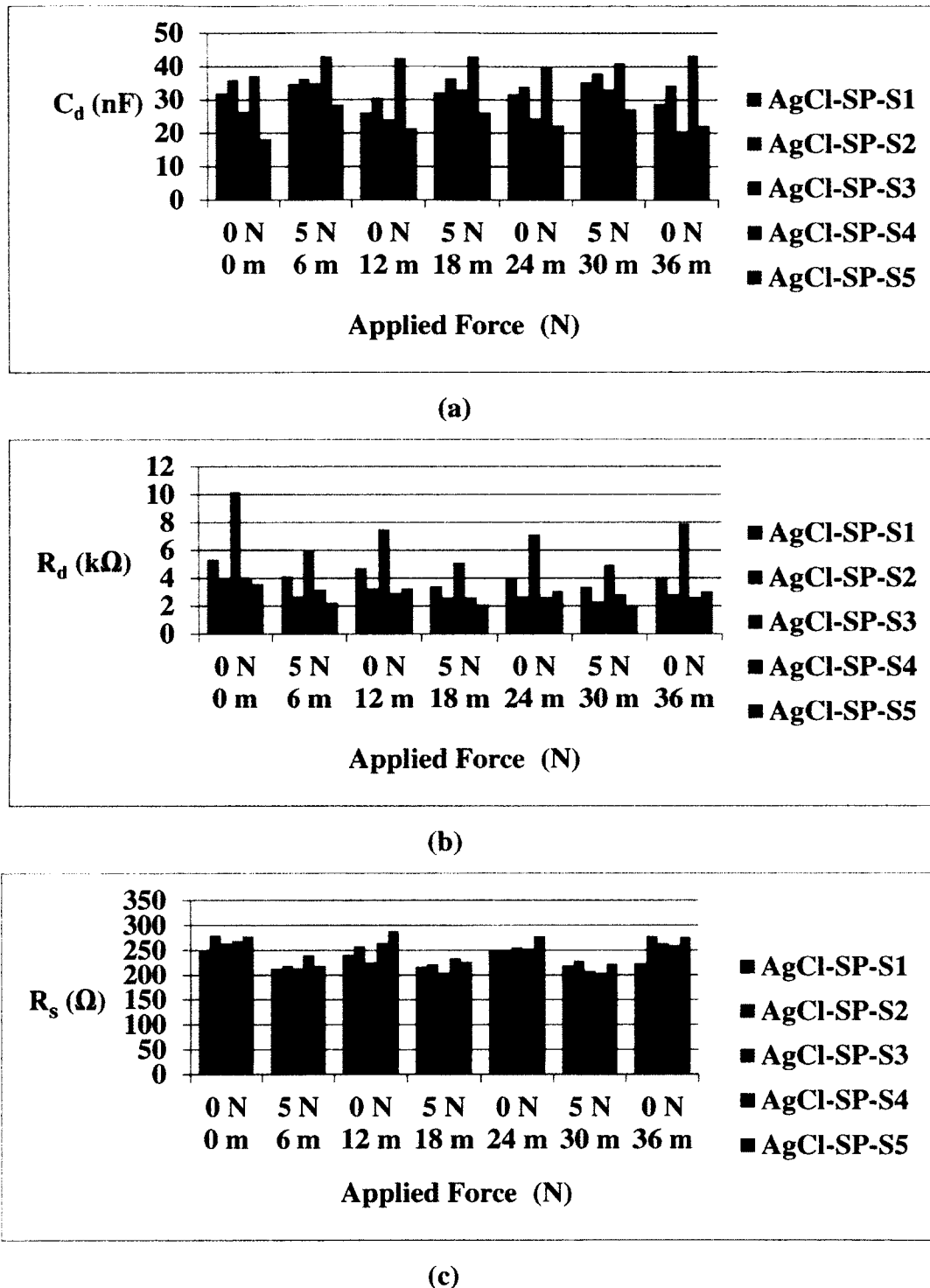


Figure 6.4. Bars Comparison of pregelled Ag/AgCl electrode's circuit model components values under the influence of force loading/unloading and skin preparation for the five subjects. (a) C_d , (b) R_d and (c) R_s .

7 Conclusions and Future Work

7.1 Conclusions

It was anticipated that exerting a force on the electrodes sites can decrease the electrode-skin impedance, which was generally observed with the majority of results obtained. Results are consistent with the hypothesis that an applied force on electrodes sites would increase the contact strength between the electrodes and skin surface, increasing the effective contact area and such decreasing the electrode-skin impedance [9].

A sharp decrease in impedance was experienced during the application of dry electrodes and in the absence of electrolyte gel with Ag/AgCl electrodes. However, pregelled Ag/AgCl electrodes exhibited inconsistent results among the tested subjects. The presence of electrolyte gel could affect electrode-skin impedance measurements under high level of force (22.2 N). The reason behind that is attributed to the strong force (22.2 N) being applied to the electrodes sites, forcing the electrolyte gel to be redistributed away from the electrodes centers. The fluctuations in R_s values in Figure 4.3c that reflect the resistance of electrolyte gel and the similar reported fluctuations in impedance values during force application to pregelled Ag/AgCl electrodes [43] support the findings of this study. Performing skin preparation would result in a low range of initial electrode-skin impedance, which could reduce part of the impact of applying an external force on electrodes sites and such not observing a sharp decrease in electrode-skin impedance. The effect of force on electrode's circuit model components is in agreement with the anticipated results; an increase in capacitance value (C_d) and a decrease in resistance values (R_d and R_s). Electrode-skin impedance and electrode's circuit model components were found highly responsive at initial force level (8.9 N). Electrode-skin

impedance for most of the measurements sustained their lower values even after the applied force was removed.

Furthermore, applying an external force on the electrodes sites would decrease the electrode-skin impedance for dry electrodes and in the absence of electrolyte gel.

Based on the results of this study a moderate force level (8.9 N) would be sufficient to sharply reduce the electrode-skin impedance when dry electrodes are applied. Increasing the force level to more than 8.9 N would further decrease the electrode-skin impedance. Caution should be taken when exerting a force level higher than 8.9 N on electrodes sites because it may cause some pain to the subjects.

In this thesis, five subjects were participated in each experiment, from the total number of nine subjects who participated in the thesis. However, the results of this study can be generalized when considering the following. Firstly, this study has more than a hundred measurements that have a common main result, which is applying an external force on the electrodes, would result in a decrease in the electrode-skin impedance regardless of the type of electrodes being applied in each experiment. Secondly, the existence of a general trend in the responses of different variables of electrode circuit model to force application could support the findings of this study, as an increase in capacitance (C_d) and decrease in resistance values of (R_d) and (R_s).

R_s or $R_{tissues}$ don't form a large part of the electrode-skin impedance in low frequencies, unlike at high frequencies. Biosignals measurements are mainly contained in the low frequency region; generally (below 500 Hz), so their impacts on biosignal quality are inconsequential.

The similarities in age and gender between the subjects are assumed not to be critical factors in influencing the overall results. However, it would be better in future work to include larger sample of old and young male and female subjects.

7.2 Future Work

A further analysis on the effect of an external force on the biological signals needs to be done in order to provide a better assessment on the usefulness of this technique in recording biological signals. Exploring more on the application of an external force on the electrodes sites can be achieved through several ways.

1- Increasing the number of subjects in the future study

In the future study, including large number of young and old, male and female subjects is important for a valid statistical analysis testing.

2- Analyzing the effect of an external force on electrodes sites during ECG, EMG and EEG signals measurements.

Performing an analysis on the effect of different external force levels on the electrodes sites for recording ECG, EMG and EEG signals would be beneficial for a future work. Recording EEG signal requires specific electrodes placements sites on head which could be highly sensitive to force effect. EMG signal could have a different response when external force is placed on muscle as well as ECG signal. In the future work, these factors need to be analyzed for better understanding of the force effect on recording biological signals.

3-The effect of external force technique on physiological monitoring system's measurements would be worth trying in the future.

Applying an external force on wearable physiological monitoring system needs to be under controllable standards by considering the comfort of the person who is wearing the physiological monitoring system. Moreover, the muscle's movements during breathing (inflation and deflation) and normal physical activity may influence the physiological monitoring system measurements. Analyzing more in depth the effect of external force on the wearable physiological monitoring system measurements would be crucial for improving the physiological monitoring system measurements.

Appendix A

Section A.1 MATLAB Code for Least Squares Curve Fitting Method

A.1.1 Loading Measured Impedance Data from Excel File to MATLAB Program

```
function [f,Z,startDateTime] = loadImpedanceData(filename)
[data,textdata] = xlsread(filename);
f = data(:,5);
Z = abs(data(:,9)/2);
% 5 (column number) belongs to the frequencies values obtained from Excel file.
% 9 (column number) belongs to the impedance values obtained from Excel file.
experimentStartTime = textdata{2};
% 2 (column number) belongs to the experiment start time obtained from Excel file.
startDate = experimentStartTime(25:length(experimentStartTime));
startDateTime = datevec(startDate);
```

A.1.2 Electrode-Skin Impedance Circuit Model

```
% Compute the magnitude of the electrode-skin impedance for a single electrode.
function Zelectrode = electrodeSkinImpedance(circuitParameter, f)
circuitParameter = [Rs Rd Cd];

Rs = circuitParameter(1);
Rd = circuitParameter(2);
Cd = circuitParameter(3);
s = j*2*pi*f;
Zelectrode = abs(Rs + (Rd./(1 + s*Rd*Cd)));
```

A.1.3 Electrode-Skin Impedance Circuit Model on Logarithmic Scale

```
function logZelectrode = logElectrodeSkinImpedance(circuitParameter, logF)
f = 10.^logF;
Zelectrode = electrodeSkinImpedance(circuitParameter, f);
logZelectrode = log10(Zelectrode);
```

A.1.4 Estimating the Electrode Circuit Components Values

```
function [Rs,Rd,Cd] = findElectrodeModel(f,Z)
% Convert the impedance and frequencies into log domain.
logF = log10(f);
```

```

logZ = log10(Z);

% Initialize a guess of parameters.

Rs0 = Z(length(Z)); % For high frequencies Z approaches Rs

Rd0 = (Z(1) - Rs0); % For low frequencies Z approaches Rs + Rd

Cd0 = 1e-9; % Arbitrarily use 1nF

% Compute the curve fitting model

circuitParameter0 = [Rs0 Rd0 Cd0];

[circuitParameter, resnorm] =

    lsqcurvefit(@logElectrodeSkinImpedance,circuitParameter0,logF,logZ,[0 0 0],[inf inf inf]);

% Curve fitting seems to be sensitive to initial value of Cd (hitting local minima). Search for
better fit (smaller residual area) over a range of Cd.

N = 100;

Cd0 = logspace(-15,-5,N);

for i = 1:N

    Rs = Rs0;

    Rd = Rd0;

    circuitParameter0 = [Rs Rd Cd0(i)];

    [curCircuitParameter, curResnorm] =

        lsqcurvefit(@logElectrodeSkinImpedance,circuitParameter0,logF,logZ,[0 0 0],[inf inf inf]);

    if curResnorm < resnorm

        circuitParameter = curCircuitParameter;

    end

    %compute the curve fitting figure.

    loglog(f,Z,'s',f,electrodeSkinImpedance(circuitParameter,f),'o');

    title([datestr(startTime) 'Rs =' num2str(Rs) 'Rd =' num2str(Rd) 'Cd =' num2str(Cd) ]);

    ylabel('|Z| (ohms)');
    xlabel('Frequency (Hz)');
    legend('Measured','Model');

```

A.2 Estimating the Electrode Circuit Model Components Values

Electrode circuit model components values were estimated by applying the least mean squares curve fitting method using MATLAB Program (MathWorks Inc.). An example of the least mean squares curve fitting output is presented in Figure A.1. The estimated R_s , R_d and C_d values are located at the top of Figure A.1.

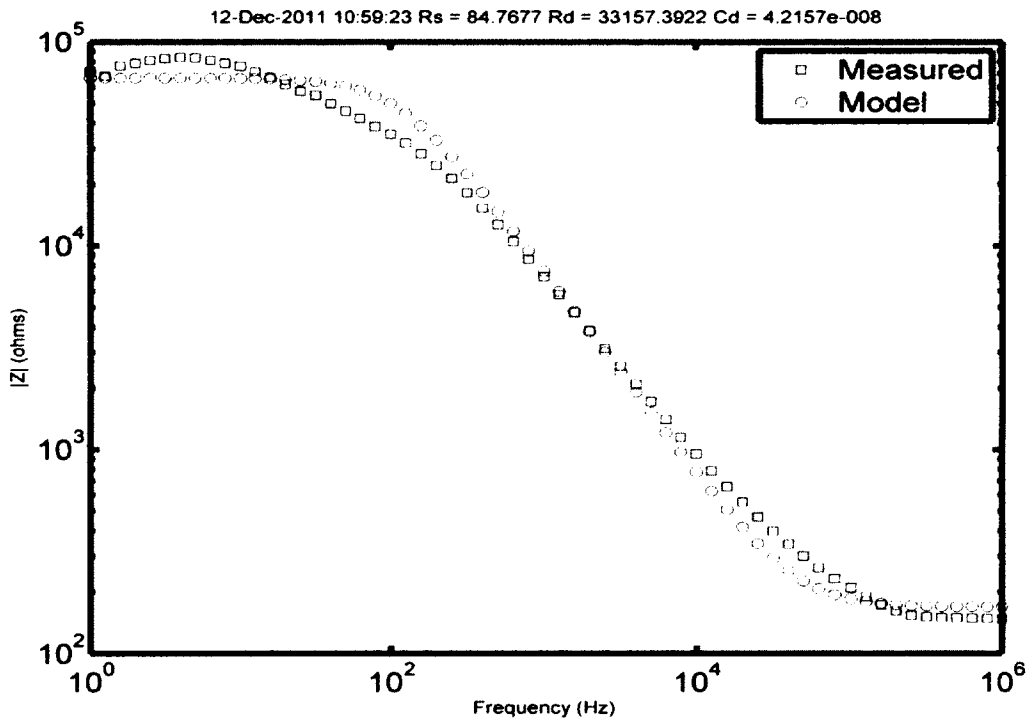


Figure A.1. Experimental results for Orbital electrode-skin impedance frequency response (Subject, Orbital-S2) with applied force of 8.9 N at 6 min and the model plot done by least mean squares curve fitting method using MATLAB program. Estimated electrode circuit components values are located at the top of the Figure.

The percent residual difference between the measured and model values is in the range of 5 – 10 % for most of the measurements.

A.3 Validation for the Estimated Values of Electrode Circuit Model Components Values that was performed with MATLAB Program

To validate the equivalent circuit model components values for electrode-skin interface (Figure A.2), the following formulas were applied

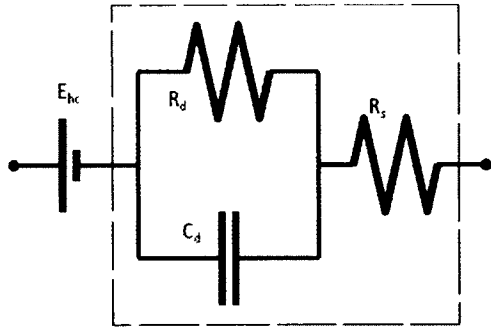


Figure A.2. Equivalent circuit model for electrode-skin interface.

$$Z_e = R_s + \frac{1}{\frac{1}{R_d} + j\omega C_d} \quad (A.3.1)$$

where $\omega = 2\pi f$ and f stands for frequency

$$Z_e = R_s + \frac{R_d}{1 + j\omega C_d R_d} \quad (A.3.1.1)$$

$$Z_e = \frac{R_s + R_d + i\omega C_d R_s R_d}{1 + j\omega C_d R_d} \quad (A.3.2)$$

The formula that was used in MATLAB program to generate the impedance versus frequency model plot is

$$Z_e = \left| R_s + \frac{1}{\frac{1}{R_d} + j\omega C_d} \right| \quad (A.3.1)$$

Two methods were applied to verify the validity of the estimated electrode circuit model components values (C_d , R_d and R_s) generated by MATLAB program. The first method relies on comparing the values of C_d , R_d and R_s that were determined from distinguished points in impedance versus frequency plot as described in section 2.5.1 with the values obtained from MATLAB program. The second method relies on running a verification formula using MATLAB program and comparing the values obtained from impedance versus frequency model plot with the values obtained from verification formula. The verification formula is the derived impedance formula of equivalent circuit model for electrode-skin interface (A.3.2).

$$Z_e = \left| \frac{R_s + R_d + i\omega C_d R_s R_d}{1 + j\omega C_d R_d} \right| \quad (\text{A.3.2})$$

Assigning arbitrary values for C_d , R_d and R_s [$(C_d = 50 \times 10^{-6} \text{ nF})$, $(R_d = 10000\Omega)$, $(R_s = 100\Omega)$] and substituting these values in the derived impedance formula (A.3.2) will provide the absolute impedance (Z_e) value, and then inserting the impedance value into the original formula (A.3.1.1) using MATLAB program will generate values for C_d , R_d and R_s . If the percentage difference between the arbitrary values for C_d , R_d and R_s and the values generated by MATLAB is zero as obtained in this study, then the estimation for electrode circuit model components values (C_d , R_d and R_s) generated by MATLAB program is correct.

A.3.1 MATLAB Code for Validation

```
[f,Z,startDateTime] = loadImpedanceData([dataDirectory filename]);  
[data,textdata] = xlsread(filename);  
  
Rs =100 + 10*rand(1,1);  
Rd =10000 + 1000*rand(1,1);  
Cd =50e-6 + 5e-6*rand(1,1);  
  
s =j*2*pi*f;  
  
%Computing the impedance value of two electrodes as in the original data file.  
Ze = (Rs+Rd+s*Rs*Rd*Cd)./(1+s*Rd*Cd) + (Rs+Rd+s*Rs*Rd*Cd)./(1+s*Rd*Cd);  
Z = abs(Ze);  
  
%Computing the impedance value for a single electrode.  
Z = Z/2;  
  
n = 100;  
x = rand(1,n);  
  
% Estimating the circuit model components values from the impedance value.  
[RsEst,RdEst,CdEst] = findElectrodeModel(f,Z);  
  
%Computing the percent error in the model components values  
[((RsEst-Rs)/Rs*100) ((RdEst-Rd)/Rd*100) ((CdEst-Cd)/Cd*100)]  
loglog(f,Zmag)
```

A.4 Sample Calculation for Body Mass Index (BMI)

The calculation for Body Mass Index (BMI) is based on the height and the weight of the subject [74]. The following sample calculation is for subject Orbital-S2 (Table 5.1).

$$\text{BMI} = \frac{\text{Weight in Kilograms}}{\text{Height in Meters} \times \text{Height in Meters}} \quad (\text{A.4})$$

$$27.8 = \frac{90 \text{ Kg}}{1.8 \text{ m} \times 1.8 \text{ m}}$$

A.5 Sample Calculation for Percentage Change of C_d Values

The percentage C_d values change between initial value (16.55 nF) at 0 N – 0 min and final value (8.19 nF) when force was removed from pre-gelled Ag/AgCl electrodes sites at 0 N- 24 min is 102.1% increase.

These values belong to Subject Ag/AgCl-G-S5 (Table B.1)

Final C_d value (0 N - 24 min) = 16.55 nF

Initial C_d value (0 N - 0 min) = 8.19 nF

$$\text{Percentage Change} = \frac{\text{Final } C_d \text{ value} - \text{Initial } C_d \text{ value}}{\text{Initial } C_d \text{ Value}} \times 100 \quad (\text{A.5})$$

$$\frac{16.55 - 8.19}{8.19} \times 100 = 102.1 \%$$

A negative percentage change would indicate a decrease in value.

Appendix B

The results of equivalent circuit model components values for Ag/AgCl electrode-skin interface with and without an electrolyte gel and under the influence of an external force are available in following tables.

Table B.1: Ag/AgCl electrode's circuit component C_d values (nF) with/without electrolyte gel (G) and under the influence of different external force levels for the participated subjects.

Subject	Electrode Type	Force (N)	0	8.9	22.2	8.9	0
		Time (min)	0	6	12	18	24
Ag/AgCl-G-S1	Ag/AgCl		30.73	29.37	29.91	34.23	34.33
Ag/AgCl-G-S2	Ag/AgCl		26.75	30.69	14.06	19.00	35.24
Ag/AgCl-G-S3	Ag/AgCl		21.06	24.32	25.80	26.60	27.81
Ag/AgCl-G-S4	Ag/AgCl		7.73	11.77	13.96	15.38	16.20
Ag/AgCl-G-S5	Ag/AgCl		8.19	12.21	14.10	15.45	16.55
AgCl-No-G-S1	Ag/AgCl		0.869	8.27	16.9	19.7	19.4
AgCl-No-G-S2	Ag/AgCl		1.51	12.1	24.6	31.2	30.7
AgCl-No-G-S3	Ag/AgCl		1.20	10.2	19.1	22.4	22.1
AgCl-No-G-S4	Ag/AgCl		16.9	22.7	24.8	24.6	21.4
AgCl-No-G-S5	Ag/AgCl		6.32	14.2	18.4	18.4	18.9

Table B.2: Pregelled Ag/AgCl electrode's circuit component R_d values (k Ω) with/without electrolyte gel (G) and under the influence of different external force levels for the participated subjects.

Subject	Electrode Type	Force (N)	0	8.9	22.2	8.9	0
		Time (min)	0	6	12	18	24
Ag/AgCl-G-S1	Ag/AgCl		112.3	118.0	186.8	80.8	80.9
Ag/AgCl-G-S2	Ag/AgCl		131.2	128.0	95.8	63.5	40.0
Ag/AgCl-G-S3	Ag/AgCl		422.8	225.4	134.8	106.7	99.6
Ag/AgCl-G-S4	Ag/AgCl		2261.2	1255.4	1129.1	1075.6	1021.7
Ag/AgCl-G-S5	Ag/AgCl		2046.5	1360.5	1093.1	1056.6	1052.7
AgCl-No-G-S1	Ag/AgCl		1475.6	122.3	45.5	43.4	42.7
AgCl-No-G-S2	Ag/AgCl		2401.3	472.69	312.67	261.1	232.5
AgCl-No-G-S3	Ag/AgCl		3402.8	1252.7	302.3	293.4	512.6
AgCl-No-G-S4	Ag/AgCl		1539.6	448.3	330.3	237.7	341.3
AgCl-No-G-S5	Ag/AgCl		3385.9	2353.1	1384.2	903.6	852.5

Table B.3: Pregelled Ag/AgCl electrode's circuit component R_s values (Ω) with/without electrolyte gel (G) and under the influence of different external force levels for the participated subjects.

Subject	Electrode Type	Force (N)	0	8.9	22.2	8.9	0
		Time (min)	0	6	12	18	24
Ag/AgCl-G-S1	Ag/AgCl		294.1	390.8	205.5	302.0	294.8
Ag/AgCl-G-S2	Ag/AgCl		290.0	283.8	719.6	596.6	294.1
Ag/AgCl-G-S3	Ag/AgCl		300.6	267.1	287.5	278.9	272.2
Ag/AgCl-G-S4	Ag/AgCl		560.2	598.1	640.0	608.9	569.4
Ag/AgCl-G-S5	Ag/AgCl		553.4	533.7	593.0	532.9	516.3
AgCl-No-G-S1	Ag/AgCl		2682.0	673.1	586.3	531.8	450.6
AgCl-No-G-S2	Ag/AgCl		2030.5	781.6	612.2	552.3	543.2
AgCl-No-G-S3	Ag/AgCl		3130.6	715.1	585.8	513.7	429.1
AgCl-No-G-S4	Ag/AgCl		315.0	278.7	292.9	278.9	286.8
AgCl-No-G-S5	Ag/AgCl		532.5	365.6	515.0	461.2	435.7

B.2 Impact of Electrode Settling Time and Force on Electrode-Skin Impedance

B.2.1 Introduction

Electrode settling allows the electrode to start interacting with the ions on the skin and would result in lowering electrode-skin impedance with time [1], [45]. In this study, the effect of force on electrodes sites caused a decrease in electrode-skin impedance. The effect of electrode settling time needs to be examined in order to compare its impact with the effect of force on electrode-skin impedance.

This study is designed to compare the effect of force with the effect of electrode settling on electrode-skin impedance.

The results of this study were published in [73].

B.2.2 Materials and Methods

A) Experimental Setup

Pregelled wet surface silver/silver chloride (Ag/AgCl) electrodes (Model # FT002, MVAP II, Medical Supplies Inc., Newbury Park, CA, U.S.A.) that have a diameter of 1 cm were used

(Figure 3.11). Bioimpedance measurement system stated in section 3.1.3 was used to measure electrode-skin interface impedance. Impedance was measured from 1 Hz to 1 MHz (10 points per decade), averaging 20 cycles per frequency, and using a 100 μ A root mean square supply current. The applied alternating electrical current 100 μ A is in accordance with the safety standards. 100 μ A is a low AC current that would not harm the human body [2]. A custom device was constructed to provide an externally applied force (Figure 3.12). It is consisted of two clamps (SL300 Quick-Grip, Irwin Tools, Huntersville, NC, U.S.A.), integrated into a fixed wooden base, and used to provide a downward vertical force. Force sensors (FlexiForce A201, 25 lb range, Tekscan, Boston, MA, U.S.A.) were used to measure the applied force.

B) Data Collection

The first Ag/AgCl electrode pair was placed on the ventral side of the right forearm, spaced 7 cm apart, with the distal electrode approximately 11 cm from the wrist. The second Ag/AgCl electrode pair was placed on the ventral side of the left forearm, spaced 7 cm apart, with the distal electrode approximately 11 cm from the wrist. In this study, skin preparation was not performed in any electrode-skin impedance measurements.

The first sets of measurements for electrode-skin impedance of the right forearm were measured under different force levels in the following sequence: 0 N, 8.8 N, 22.5 N, 8.8 N, and 0 N for the first 30 min. The electrode-skin impedance at the last load 0 N continued to be recorded for additional 50 min to analyze the long term effect of force on electrode-skin impedance. The second sets of measurements for electrode-skin impedance of the left forearm were measured without applying any force to the electrodes to analyze the effect of electrodes

settling time on electrode-skin impedance for 30 min. The room temperature and humidity were 22°C and 31%, respectively.

B.2.3 Results and Discussion

The measured electrode-skin impedance at 10 Hz as a function of time decreased in a faster base with force application than without force application (Figure B.1).

The percentage decrease in electrode-skin impedance under force effect was 73% for subject 1 and 36% for subject 2 (Table B.4) while it was 30% for subject 1 and 17% for subject 2 under electrode settling effect (Table B.4). The effect of force on electrode-skin impedance remained even when there was not any force being applied on the electrodes sites; subject 1 has almost constant electrode-skin impedance value of 32 k Ω at 31 min and 30 k Ω at 83 min under force effect.

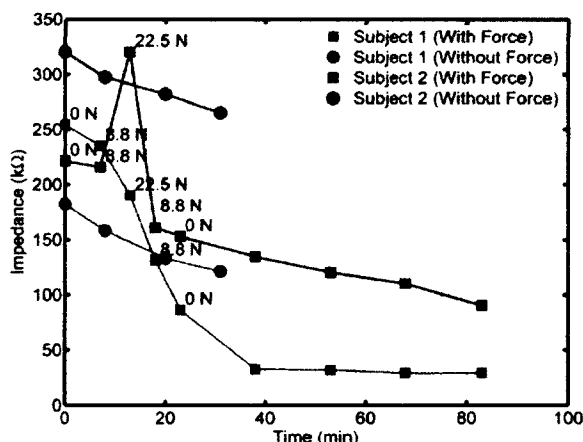


Figure B.1. The effects of electrode settling and force on electrode-skin impedance at 10 Hz are with respect to time. Applied force levels are indicated on the graph (unlabeled points are at 0 N).

The electrode-skin impedance for subject 2 continued to decrease even when the force was removed from the electrodes sites as it was $135\text{ k}\Omega$ at 31 min and $100\text{ k}\Omega$ at 83 min. The

electrode settling can cause a decrease in electrode-skin impedance [45], but at a slower base in comparison to the effect of force on electrodes sites.

Table B.4: A Comparison between the effects of force and electrode settling on electrode-skin impedance in the first 30 min at 10 Hz.

Subject	With Force	Without Force
1	73 %	30 %
2	36 %	17 %

The results indicated that the effect of force on electrode-skin impedance can decrease the electrode-skin impedance for a longer period of time. The sudden increase in electrode-skin impedance at high force level 22.5 N can be attributed to the gel being redistributed away from the electrodes sites under heavy load [43]. However, the increase in impedance was then changed to a decrease at lower force levels (8.8 N and 0 N).

B.2.4 Conclusion

The results obtained in this study indicate that the impact of force on electrode-skin impedance is much larger than electrode settling time. Moreover, the effect of force on electrode-skin impedance results in hysteresis effect and could continue for longer period of time.

Appendix C

The results of equivalent circuit model components values for Orbital and stainless steel electrode-skin interface under the influence of an external force are available in following tables.

Table C.1: Orbital and stainless steel electrode's circuit component C_d values (nF) under the influence of different external force levels for the participated subjects.

Subject	Electrode Type	Force (N)	0	8.9	22.2	8.9	0
		Time (min)	0	6	12	18	24
Orbital-S 1	Orbital		3.66	15.77	30.66	34.22	8.73
Orbital-S 2	Orbital		28.16	42.12	42.20	42.68	30.04
Orbital-S 3	Orbital		0.20	2.50	8.55	10.97	4.56
Orbital-S 4	Orbital		6.11	45.58	55.37	57.38	45.33
Orbital-S 5	Orbital		8.56	36.69	46.89	48.01	40.90
ST-S 1	Stainless Steel		1.34	6.29	11.41	13.20	14.27
ST-S 2	Stainless Steel		9.37	24.06	33.88	35.15	35.04
ST-S 3	Stainless Steel		0.26	6.56	14.36	15.31	15.92
ST-S 4	Stainless Steel		7.09	15.54	24.97	27.11	24.06
ST-S 5	Stainless Steel		6.22	13.13	16.65	17.92	17.26

Table C.2: Orbital and stainless steel electrode's circuit component R_d values ($k\Omega$) under the influence of different external force levels for the participated subjects.

Subject	Electrode Type	Force (N)	0	8.9	22.2	8.9	0
		Time (min)	0	6	12	18	24
Orbital-S 1	Orbital		2268.4	197.8	129.6	130.5	1018.5
Orbital-S 2	Orbital		99.2	33.2	29.2	37.4	70.2
Orbital-S 3	Orbital		5277.3	1291.3	122.7	83.7	244.1
Orbital-S 4	Orbital		370.2	156.4	40.1	62.4	125.0
Orbital-S 5	Orbital		273.7	138.8	91.6	106.0	134.0
ST-S 1	Stainless Steel		3026.0	192.3	98.5	104.0	281.4
ST-S 2	Stainless Steel		272.5	74.1	61.6	55.3	51.4
ST-S 3	Stainless Steel		62522.0	305.1	176.5	153.8	655.9
ST-S 4	Stainless Steel		166.3	117.4	81.2	90.6	74.1
ST-S 5	Stainless Steel		2187.3	1029.7	705.6	724.1	705.8

Table C.3: Orbital and stainless steel electrode's circuit component R_s values (Ω) under the influence of different external force levels for the participated subjects

Subject	Electrode Type	Force (N)	0	8.9	22.2	8.9	0
		Time (min)	0	6	12	18	24
Orbital-S 1	Orbital		449.2	266.4	172.3	151.1	392.2
Orbital-S 2	Orbital		112.9	85.0	87.1	90.4	114.2
Orbital-S 3	Orbital		1645.7	454.9	283.9	271.5	321.8
Orbital-S 4	Orbital		501.7	153.1	142.2	139.7	154.8
Orbital-S 5	Orbital		424.4	149.7	133.5	135.8	155.0
ST-S 1	Stainless Steel		626.2	458.6	391.1	370.0	341.7
ST-S 2	Stainless Steel		614.0	316.7	325.4	307.4	300.6
ST-S 3	Stainless Steel		1478.8	478.9	399.0	367.3	354.5
ST-S 4	Stainless Steel		1131.4	356.6	361.9	336.8	316.7
ST-S 5	Stainless Steel		431.7	285.9	298.8	284.6	333.1

Appendix D

The results of equivalent circuit model components values for Ag/AgCl electrode-skin interface with electrolyte gel under the influence of an external force and skin preparation are available in following tables.

Table D.1: Pregelled Ag/AgCl electrode's circuit component C_d values (nF) under the influence of 0 N and 5 N external force level for the participated subjects using skin's preparation technique.

Subject	Electrode Type	Force (N)	0	5	0	5	0	5	0
		Time (min)	0	6	11	17	23	28	33
AgCl-SP-S1	Ag/AgCl		32.0	34.8	26.2	32.2	31.8	35.3	28.9
AgCl-SP-S2	Ag/AgCl		36.0	36.3	30.6	36.5	34.0	38.1	34.5
AgCl-SP-S3	Ag/AgCl		26.5	35.1	24.2	33.2	24.6	33.3	20.6
AgCl-SP-S4	Ag/AgCl		37.2	43.0	42.5	43.1	39.7	41.0	43.3
AgCl-SP-S5	Ag/AgCl		18.3	28.5	21.4	26.4	22.3	27.3	22.3

Table D.2: Pregelled Ag/AgCl electrode's circuit component R_d values (kΩ) under the influence of 0 N and 5 N external force level for the participated subjects using skin's preparation technique.

Subject	Electrode Type	Force (N)	0	5	0	5	0	5	0
		Time (min)	0	6	11	17	23	28	33
AgCl-SP-S1	Ag/AgCl		5.32	4.12	4.74	3.44	3.99	3.35	4.00
AgCl-SP-S2	Ag/AgCl		3.89	2.70	3.25	2.63	2.72	2.34	2.83
AgCl-SP-S3	Ag/AgCl		10.2	6.09	7.54	5.14	7.15	4.97	7.89
AgCl-SP-S4	Ag/AgCl		3.88	3.18	2.96	2.63	2.64	2.83	2.64
AgCl-SP-S5	Ag/AgCl		3.63	2.26	3.26	2.11	3.07	2.06	3.05

Table D.3: Pregelled Ag/AgCl electrode's circuit component R_s values (Ω) under the influence of 0 N and 5 N external force level for the participated subjects using skin's preparation technique.

Subject	Electrode Type	Force (N)	0	5	0	5	0	5	0
		Time (min)	0	6	11	17	23	28	33
AgCl-SP-S1	Ag/AgCl		252.4	212.9	240.7	217.0	251.8	218.7	224.4
AgCl-SP-S2	Ag/AgCl		280.8	219.3	258.2	222.0	251.6	229.0	277.7
AgCl-SP-S3	Ag/AgCl		263.8	213.8	226.2	205.3	256.4	209.2	263.7
AgCl-SP-S4	Ag/AgCl		269.1	239.8	265.7	232.7	253.0	203.8	260.3
AgCl-SP-S5	Ag/AgCl		278.6	218.9	289.25	227.4	278.5	222.5	275.9

References

- [1] S. Grimnes and Ø. G. Martinsen, "Bioimpedance and bioelectricity basics", 2nd ed., Academic Press, Amsterndam, Elsevier, pp. 206-281, 2008.
- [2] J. G. Webster, "Medical instrumentation application and design", 4th ed., John Wiley & Sons, New York, pp. 181-262, 2010.
- [3] Y. Yamamoto and T. Yamamoto, "Dispersion and correlation of the parameters for skin impedance", *Med. Biol. Eng. Comput.*, vol. 16, no. 5, pp. 592-594, 1978.
- [4] J. Rosell, J. Colominas, P. Riu, R. Pallas-Areny, and J. G. Webster, "Skin impedance from 1 Hz to 1 MHz", *IEEE Trans. Biomed. Eng.*, vol. 35, no. 8, pp. 649-651, 1988.
- [5] E.T. McAdams, J. Jossinet, A. Lackermeier, and R. Risacher, "Factors affecting electrode-gel-skin interface impedance in electrical impedance tomography", *Med. Biol. Eng. Comput.*, vol. 34, no. 6, pp. 397-408, 1996.
- [6] I. Nicander and S. Ollmar, "Electrical impedance measurements at different skin sites related to seasonal variations", *Skin Res. Technol.*, vol. 6, no. 2, pp. 81-86, 2000.
- [7] E.T. McAdams and J. Jossinet, "DC nonlinearity of the solid electrode-electrolyte interface Impedance", *Inn Tech. Biol. Med.*, vol. 12, no. 3, pp. 329-343, 1991.
- [8] E. T. McAdams and J. Jossinet, "The importance of electrode-skin impedance in high resolution electrocardiography", *Automedica.*, vol. 13, pp. 187-208, 1991.
- [9] L. A. Geddes and L. E. Baker, "Relationship between input impedance and electrode area", *Med. Biol. Eng.*, vol. 4, no. 5, pp. 439-449, 1966.
- [10] L.A. Geddes and L. E. Baker, eds., "Principles of applied biomedical instrumentation", Wiley-Interscience, New York, 1989.
- [11] J. C. Lawler, M. J. Davis, and E. C. Griffith, "Electrical characteristics of the skin", *J. Invest. Dermato L.*, vol. 34, pp. 301-308, 1960.
- [12] S. Grimnes, "Impedance measurement of individual skin surface electrodes", *Med. Biol. Eng. Comput.*, vol. 21, no. 11, pp. 750-755, 1983.
- [13] D. P. Burbank and J. G. Webster, "Reducing skin potential motion artifacts by skin abrasion", *Med. Biol. Eng. Comput.*, vol. 16, no. 1, pp. 31-38, 1978.
- [14] M. Steffen, A. Aleksandrowicz, and S. Leonhardt, "Mobile noncontact monitoring of heart and lung activity", *IEEE Trans. Biomed. Circuits Syst.*, vol. 1, no. 4, pp. 250-257, Dec. 2007.

- [15] E. Richard and A. D.C. Chan, “Non-obtrusive electrocardiogram system for the Smart Rollator”, IEEE International Symposium on Medical Measurements and Applications, Budapest, Hungary, pp. 95-99, 2012.
- [16] E. Sardini, M. Serpelloni, and M. Ometto, “Multi-parameters wireless shirt for physiological monitoring”, Symposium on Medical Measurements and Applications Proceedings, Bari, 316-321, 2011.
- [17] J. Lee, H. Lee, and D. Kang, “Textile electrode of jacquard woven fabrics for biosignal measurement”, *The Journal of the Textile Institute*, vol. 101, no. 8, 2010.
- [18] T. Ragheb and L. A. Geddes, “The polarization impedance of common electrode metals operated at low current density”, *Ann. Biomed. Eng.*, vol. 19, no. 2, pp. 151–163, 1991.
- [19] D. Godin, P. A. Parker, and R. N. Scott, “Noise characteristics of stainless steel surface electrodes”, *Med. Biol. Eng. Comput.*, vol. 29, no. 11, pp. 585 – 590. 1991.
- [20] E. McAdams, “Biomedical electrodes for biopotential monitoring and electrostimulation”, in Bio-Medical CMOS ICs, H. J. Yoo and C. Hoof, Eds. Boston, MA, Springer US, pp. 31-124, 2011.
- [21] M.Pacelli, G.Loriga., N.Taccini, and R.Paradiso, “Sensing fabrics for monitoring physiological and biomechanical variables: E-textile solutions”, Proceedings of the 3rd IEEE-EMBS, International Summer School and Symposium on Medical Devices and Biosensors, MIT, Boston, USA, pp.1-4, Sept.4-6, 2006.
- [22] P. Tallgren, S. Vanhatalo, K. Kaila, and J. Voipio, “Evaluation of commercially available electrodes and gels for recording of slow EEG potentials”, *Clin. Neurophysiol.*, vol.116, no. 4, pp. 799-806, 2004.
- [23] H. W. Tam, and J. G. Webster, “Minimizing electrode motion artifact by skin abrasion”, *Biomedical Engineering, IEEE Trans. Biomed. Eng.*, vol. 24, no.2, pp. 134-139, March 1977.
- [24] T. Yamamoto, and Y. Yamamoto, “Electrical properties of the epidermal stratum corneum”, *Med. Bio. Eng.*, vol. 14, no. 2, pp. 151-158, 1976.
- [25] B. R. Eggins, “Skin contact electrodes for medical applications”, *Analyst*, vol. 188, no. 4, pp. 439-442, 1993.
- [26] R. Ehret, W. Baumann, M. Brischwein, A. Schwinde, K. Stegbauer, and B. Wolf, “Monitoring of cellular behaviour by impedance measurements on interdigitated electrode structures”, *Biosens Bioelectron.*, vol. 12, no. 1, pp. 29-41, 1997.
- [27] E. McAdams, “Bioelectrodes”, In J. G. Webster (ed.), Encyclopedia of Medical Devices and Instrumentation, 2nd ed., vol. 1, Wiley, New York, pp. 120-166, 2006.

- [28] F. Fine Olivarius, H. C. Wulf, P. Therkildsen, T. Poulsen, J. Crosby, and M. Norval “Urocanic acid isomers: relation to body site, pigmentation, stratum corneum thickness and photosensitivity”, *Arch. Dermatol. Res.*, vol. 289, no.9, pp.501-505, 1997.
- [29] T.B. Fitzpatrick, A.Z. Eisen, K. Wolff, I.M. Freedberg, and K.F. Austen (eds): “Dermatology in General Medicine”, 3rd ed, 2 vol, McGraw-Hill, New York, 1987.
- [30] R. H. Champion, J. L. Burton, and F.J.G. Ebling, (eds): “Textbook of Dermatology”, 5th ed, 4 vol., Blackwell, Oxford, 1992.
- [31] P. Griss, P. Enoksson, H. Tolvanen-Laakso, P. Merilainen, S. Ollmar, and G. Stemme, “Spiked biopotential electrodes”, in *Proc. 13th Annu. Int. Conf. MEMS*, pp.323–328, 2000.
- [32] A. Searle and J. Kirkup, “A direct comparison of wet, dry and insulating bioelectric recording electrodes,” *Physiol. Meas.*, vol. 21, no.2, pp. 271–283, 2000.
- [33] C. Tronstad, G. K. Johnsen, S. Grimnes, and Ø. G. Martinsen, “A study on electrode gels for skin conductance measurements,” *Physiol Meas.*, vol. 31, no. 10, p.p. 1395-1410, 2010.
- [34] E. Huigen, A. Peper, and C. A. Grimbergen, “Investigation into the origin of the noise of surface electrodes”, *Med. Biol. Eng. Comput.*, vol. 40, no.3, pp. 332-338, 2002.
- [35] L. M. A. Nolan, J. Corish,, and O. I.Corrigan, “Electrical properties of human stratum comeum and transdermal drug transport”, *J. Chem. Soc. Faraday Trans.* , vol. 89, no.15, pp 2839- 2845, 1993.
- [36] K. Ki-won K, C. Han-yoon, S. Myeong-heon, Y. Hyung-ro, and J. In-cheol, “Compensation on impedance of the stratum corneum”, *J. of Electrical Engineering & Technology.*, vol. 3, no.3, pp. 444-449, 2008.
- [37] N. O'Connell and B. Tursky, “Silver-silver chloride sponge electrodes for skin potential recording”, *Am. J. Psychol.*, vol. 73, no. 3, pp. 302-304, 1960.
- [38] N. Sha, L. P. Kenney, B. W. Heller, A.T. Barker, D. Howard, and W. Wang, “The effect of the impedance of a thin hydrogel electrode on sensation during functional electrical stimulation”, *Med. Eng. Phys.*, vol. 30, no. 6, pp. 739-46, 2008.
- [39] A. Gruetzmann, S. Hansen, and J. Müller, “Novel dry electrodes for ECG monitoring”, *Physiol. Meas.*, vol.28, no. 11, pp.1375-90, 2007.
- [40] V. Medina, J. M. Clochesy, and A. Omery, “Comparison of electrode site preparation techniques”, *Heart Lung: J. Crit. Care*, vol.18, no.5, pp.456-460, 1989.
- [41] Edelberg R. “Relation of electrical properties of skin to structure and physiologic state”, *J. Invest. Dermatol.*, vol.69, no.3, pp.324-327, 1977.

- [42] R. V. Hill, J. C. Jansen, and J. L. Fling, “Electrical impedance plethysmography: a critical analysis”, *J. Applied Physiol.*, vol. 22, no. 1, pp. 161-168, 1967.
- [43] D. K. Swanson, “Pressure-induced changes in skin through electrode impedance”, M. Sc. Thesis, Univ. Wisconsin, 1972.
- [44] R. Dozio, A. Baba, C. Assambo, and M. J. Burke, “Time based measurement of the impedance of the skin-electrode interface for dry electrode ECG recording”, *Proc. Ann. Intl. Conf. IEEE EMBS*, pp. 5001-5004, 2007.
- [45] A. Baba and M. J. Burke, “Measurement of the electrical properties of ungelled ECG electrodes”, *Intl. J. Biol. Biomed. Eng.*, vol. 2, no. 3, pp. 89 - 97, 2008.
- [46] E. Warburg, “About the behaviour of so-called “impolarizable electrodes” in the present of alternating current”, *Ann. Phys. Chem.*, vol. 67, pp. 493. 1899.
- [47] F. S. Feates, D. J. G. Ives, and J. H. Pryor, “Alternating current bridge for measurement of electrolytic Conductance”, *J. Electrochem. Soc.*, vol. 103, no.10, pp. 580-585, 1956.
- [48] L. A. Geddes and M. E. Valentinuzzi, “Temporal changes in electrode impedance while recording the electrocardiogram with “dry” electrodes”, *Ann. Biomed. Eng.*, vol. 1, no 3, pp. 356–367, 1973.
- [49] C. Gabriel, A. Peyman, and E. H. Grant, “Electrical conductivity of tissue at frequencies below 1 MHz.”, *Phys. Med. Biol.*, vol. 54, no. 16, pp. 4863–78, 2009.
- [50] D. Halliday, and R. Resnick, “Fundamentals of Physics”, 2nd ed., John Wiley & Sons, Inc., New York, pp. 452–453, 1970.
- [51] Tekscan Inc. FlexiForce A201 Standard Force & Load Sensors. “FlexiForce user Manual”, available at: <http://www.tekscan.com>. Boston, MA, USA, 2009.
- [52] A. J. Hinton and B. Sayers, “Advanced Instrumentation for solid state applications”, Solartron Analytical, Farnborough, UK, 1998.
- [53] Solartron analytical. (1995). 1250 Frequency Response Analyzer Manual [Online]. Available: <http://www.solartronanalytical.com/>.
- [54] Solartron analytical. (2009). 1294 A Impedance Manual [Online]. Available: <http://www.solartronanalytical.com/>.
- [55] R. N. Schmidt, F. J. Lisy, G. G. Skebe, and T. S. Prince, “Dry physiological recording electrode”, US Patent # 6785569, 2004.
- [56] D. P. Das and J. G. Webster, “Defibrillation recovery curves for different electrode materials,” *IEEE Trans. Biomed. Eng.*, vol. BME-27, pp. 230–233, Apr. 1980.

- [57] L.A. Geddes and R. Roeder, "Measurement of the direct-current (Faradic) resistance of the electrode-electrolyte interface for commonly used electrode materials", *Ann. Biomed. Eng.*, vol. 29, no. 2, pp.181-6, 2001.
- [58] E. T. Mcadams, P. Henry, and J. Anderson, "Optimal electrolytic chloriding of silver ink electrodes for use in electrical impedance tomography", *Clin. Phys. Physiol. Meas.*, 13, 1992.
- [59] E. S. Kappenman, and S. J. Luck., "The effects of electrode impedance on data quality and statistical significance in ERP recordings", *Psychophysiology*, vol. 47, no. 5, pp. 888-904, 2010.
- [60] M. Devanath and B. V. K. Tilak, "Structure of electrical double layer at metal-solution interface", *Chem. Rev.*, vol. 65, no. 6, pp. 635, 1965.
- [61] M. Trimmel, E. Groll-Knapp, and M. Haider, "Different storage methods for biopotential skin electrodes (sintermetallic Ag/AgCl) and their influence on the bias potential", *Eur. J. Appl. Physiol.*, vol. 50, no.1, pp.105–116, 1982.
- [62] A. Karilainen, S. Hansen, and J. Muller, "Dry and capacitive electrodes for long-term ECG-monitoring", 8th Annual Workshop on Semiconductor Advances, vol. 8, no.17, pp. 155-161, 2005.
- [63] R. M. David, and W. M. Portnoy, "Insulated electrocardiogram electrodes", *Med. Biol. Eng.*, vol.10, no.6, pp. 742-745, 1972.
- [64] T. C. Ferree, P. L. Luu, G. S. Russell, and D. M. Tucker, "Scalp electrode impedance infection risk and EEG data quality", *Clin. Neurophysiol.*, vol.112, no. 3, pp. 536-544, 2001.
- [65] N. A. Alba, R. J. Sclabassi, S. Mingui, and X. T. Cui, "Novel hydrogel-based preparation-free EEG electrode", *Neural Systems and Rehabilitation Engineering, IEEE Transactions on* , vol.18, no.4, pp.415-423, 2010.
- [66] L. A. Geddes, "Electrodes and the measurement of bioelectric events", New York, Wiley-Interscience, 1972.
- [67] S. A. Hoenig , P. L. Gildenberg, and K. Murthy, "Generation of permanent, dry, electric contacts by tattooing carbon into skin tissue", *IEEE Trans Biomed. Eng*, vol. 25, no. 4, pp.380-382, 1978.
- [68] C. D. Oster, "Improving ECG trace quality", *Biomed. Instrum. Technol.*, vol. 34, no.3, pp. 219-222, 2000.
- [69] Ø. G. Martinsen, S. Grimnes, and E. Haug, "Measuring depth depends on frequency in electrical skin impedance measurements", *Skin Res. Technol.*, vol. 5, pp. 179 – 181, 1999.
- [70] E. J. Clar, D. P. Her, and C. G. Sturelle, "Skin impedance and moisturization", *J. Soc. Cosmet. Chem.*, vol. 26, pp. 337- 353, 1975.

- [71] Y. Yamamoto, T. Yamamoto, and T. Ozawa, “Characteristics of skin admittance for dry electrodes and the measurement of skin moisturisation”, *Med. Biol. Eng. Comput* , vol. 24 , pp. 71 – 77, 1986.
- [72] T. J. Faes, H. A. van der Meij, J. C. de Munck, and R. M. Heethaar, “The electric resistivity of human tissues (100 Hz-10 MHz): a meta-analysis of review studies”, *Physiol. Meas.*, vol. 20, no. 4, pp. R1- R10, 1999.
- [73] A. Albulbul, and A. D. C. Chan, “Electrode-skin impedance changes due to an externally applied force”, IEEE Intl. Symp. MeMeA, Budapest, Hungary, pp. 18-19, May 2012.
- [74] Z. Mei, L M. Grummer-Strawn, A. Pietrobelli, A. Goulding, M. I. Goran, and W. H. Dietz “Validity of body mass index compared with other body-composition screening indexes for the assessment of body fatness in children and adolescents”, *Am. J. Clin. Nutr.* vol.75, no.6, pp. 978–985, 2002.